# Ego-centred models of social networks: the social atom

by

Ignacio Tamarit Ramírez

in partial fulfillment of the requirements for the degree of Doctor in

Ingeniería Matemática

Universidad Carlos III de Madrid

Advisor:
Angel Sánchez Sánchez

Tutor:
Angel Sánchez Sánchez

Leganés, May 30, 2019

*a mi madre*

# Agradecimientos

Supongo que siempre es complicado escribir los agradecimientos de una tesis, pero cuando la tesis va de cómo las personas organizamos nuestras relaciones personales, no sé … como que siento una especie de presión extra. Me voy a dejar a gente importante fuera, seguro, así que con carácter preventivo, si estás leyendo esto, gracias.

Me resulta fácil, sin embargo, saber por dónde empezar. Además de verdad. Anxo, gracias por confiar en un músico despreocupado que terminaba una licenciatura en física, de forma un poco tardía, y por amor al arte. No puedo expresar con palabras todo lo que he aprendido contigo y lo que me has ayudado a crecer como persona (¡y lo que me queda!). Gracias por guiarme en este apasionante mundo de la investigación que, pase lo que pase, siempre será una parte importante de mi vida. No solo te debo haber descubierto una parte de mí mismo, sino también el haber conocido a tanta gente que, como tú, ya forma parte de mi vida, y a la que también le tengo mucho que agradecer.

José, no sé si esto es un buen trabajo o no (yo creo que sí), pero si no ha llegado el momento de que empecemos a… no sé cuándo va a ser. Ahora en serio, gracias de verdad por tener la puerta siempre abierta. Nos queda mucha música por delante.

Robin, it has been a sincere pleasure, and a true honour, to meet you. The scientific imprint that I carry thanks to our conversations is priceless, but I am specially glad to have had the opportunity to meet the man behind the "big name"—and also of having developed a taste for Whisky. Not bad.

Amy, Abu (and family), you didn't offer me shelter, you offered me a full, open-hearted home. Thank you, really. And thanks also to Mary, Cole, Jackie, Pablo, and all the people I had the chance to meet there. Oxford is not as cold as they say, and that is thanks to you.

Thanks also to all the people from IBSEN, from whom I have learnt so, so much.

Parecerá mentira, pero una de las razones por las que decidí meterme en esto de la ciencia fue por la gente con la que iba a compartir despacho. No es broma, ese era mi sitio, y lo era gracias a vosotros. Pablo, solamente por tu amistad ya ha merecido la pena todo esto. Gracias por recordarme siempre lo nítido que puede sonar el silencio, y por enseñarme a respirar—y de ciencia ni te cuento. E Ignacio, qué mente más brillante, qué corazón más grande, qué cachondo mental. Me has enseñado lo que significa de verdad tener valores, se dice pronto. Sé que estarás bien, lo mereces, aunque sea *somewhere over the rainbow*. Aquí tienes un amigo. Y Clemente (Tito), que coincidimos poco, pero que marcaste profundamente mi forma de entender la ciencia (entre risa y risa).

Y debe ser una cosa de ese despacho y de su entorno, porque no he dejado de conocer a gente extraordinaria. María, cuyo valor y pasión ante la vida son toda una fuente de inspiración; Alberto (*dottore*), siempre cercano no importa lo lejos que esté (¡ni lo rápido que corra!); Francy, que desafía las leyes de la física metiendo tanto talento y tanto cariño en tan poco espacio; Pablo (Lozano), con el que comparto la misma *visión* de las cosas (lástima que no pueda adjuntar un GIF); Pau, que acaba de llegar (como quien dice) y ya pasa todos los tests con claridad; Vicky, talento en estado puro, con quien sé que comparto amante (la música, no penséis mal); Saúl, pura sensibilidad en el cuerpo de un leonés macizorro (*macizorrus leonensis*); y Pilar, que rebosa ingenio, creatividad y, lo quiera o no, ternura (el que está por venir no sabe la suerte que ha tenido). No es el despacho. Sois vosotros (y vosotras). Gracias, quien diga que la ciencia es fría es que no os conoce.

Bueno, a vosotros y a la máquina de café, por renuirme en torno a tanta gente del departamento con los que he aprendido casi por ósmosis (Froilán, Antonio, estáis en este saco. Tendré que llevar unas pastitas para agradecéroslo). Y en especial a la gente del GISC, que no es un grupo de investigación, es una familia.

Y ahora es cuando echo la vista atrás y sé que me dejaré a gente. Pero a algunos seguro que no. Carlos, Juan, Vero, Jaime, soy lo que soy gracias a vosotros, no importa la distancia, no importa el tiempo, siempre estáis ahí, escuchando todo aquello que ni siquiera puedo decir. Y Gabriel, gracias por todos esos momentos de honestidad intelectual, de apertura a lo desconocido, y de música, por supuesto de música, que no falte—y gracias también a tu padre, Eduardo, no solo por traerte al mundo, sino porque si soy físico es en buena parte gracias a su inspiración. Juan, Nieves (Olmo, y demás familia) para vosotros va un agradecimiento también especial. Literalemente, esta tesis no sería lo que es si no hubiera sido por vosotros. Pero la tiraría ahora mismo a la basura con tal de seguir siendo parte de vuestra familia.

Abro una sección especial para los músicos—y otras gentes de poco fiar. Manuel (Pardo), gracias a ti soy músico. Eternamente agradecido. Adrián, estos agradecimientos no son sólo por lo terriblemente buena persona que eres, sino porque me regalaste Praga y me metiste el gusanillo de la investigación, eso es un amigo. Y Kike, que nos conocemos menos, pero también me has demostrado una mirada profunda, y ser un gran apoyo cuando las *crisis* acechan. Pablo, Elena, desde la distancia os llevo muy dentro, y si no hubiera aprendido a superar dificultades a vuestro lado no estaría escribiendo estas palabras. Y a Yoel, por cruzar ciertas fronteras por mí, para que pueda ver lo que hay detrás, sin arriesgarme a no poder volver—y a Victor, estés donde estés, por exactamente la misma razón. Y Karsten (*matacobras*), he aprendido más de tí de lo que te puedes imaginar, no sólo te doy las gracias, también te llevas un golpe en la nuca. Gracias a toda la gente de Musikene, el conservatorio Padre Antonio Soler, y el conservatorio de Getafe. Me habéis ensenãdo mucho más que música. Y por supuesto, Marco (Socías) y Miguel (Trápaga), por enseñarme que siempre se puede ir un poquito más lejos.

Mi familia es extensa y diversa. Pero madre no hay más que una. Mucha gente me ha enseñado cómo investigar, pero a *ser* investigador me enseñaste tú. Por los millones de *porqués* a los que diste respuesta, y sobre todo por mostrarme que los verdaderamente maravillosos son aquellos no la tienen. Por enseñarme a tener los pies en la tierra y la cabeza (y el corazón) en las nubes. Por todo eso, pero sobre todo porque te quiero. Esta tesis es para ti.

Y gracias a ti, papá (y a Laura), guardo tantas conversaciones, tantas reflexiones, he aprendido tanto, que el científico que hay en mí debería citarte en todos sus artículos. Y Smith (alias Miguel Soto) del que he aprendido cosas que no sé ni cómo explicar, pero que sin duda me han hecho ser mejor persona. Y Miguel, mi hermano. Y Oliver, Ainhoa, e Iván, mis hermanos. Y Álvaro, y Alicia, mis hermanos. A todos, aunque solo sea por tener la oportunidad de deciros que os quiero. Gracias.

Marta. No sé ni por dónde empezar a agradecerte todo lo que te tengo que agradecer. Eres la única que ha estado todo el tiempo conmigo desde el comienzo de esta etapa que ahora termina—y los dos sabemos que no siempre ha sido fácil. Eres mi familia. Aprendo con mirarte, con respirar a tu lado, y solo deseo que el tiempo me permita seguir poder agradeciéndotelo. Por ser como eres, por aguantarme, y por seguir junto a mí. Por dar refugio en tu corazón a toda la belleza que no cabe en este mundo. Gracias. (Y gracias también a toda tu familia, que también es la mía. Y a la cuadrilla, *of course*, que nunca podrá ser la mía, pero que con los *raticos* que pasamos ya me conformo).

Hay mucha gente a la que le estoy agradecido por un motivo u otro: tíos, tías, abuelos, primos, primas,sobrinos, sobrinas, Alicia, Eduardo, Sanet, Ardiel, Alberto (Calvo), mis compaeros/as guitarristas, toda la gente del colegio (cuyo nombre no puedo decir), Silvestre, Alejandro, Pol, Sara, …, y demás compañeros y compañeras de viaje. Pero es que no quiero superar el récord del Dr. Catalán, así que os remito a todos (y todas) al primer párrafo. ¡GRACIAS!

Ignacio Tamarit Ramírez
March 7, 2019

This thesis would not have been possible without the support of Fundación BBVA through its 2016 call project ”Los números de Dunbar y la estructura de las sociedades digitales: modelización y simulación (DUNDIG)”, and we are very thankful for it. Support for early stages of this work through projects IBSEN (European Commission, H2020 FET Open RIA 662725) and VARIANCE (Ministerio de Economía y Competitividad/FEDER, project no. FIS2015-64349-P) is also acknowledged.

# Published and submitted content

Chapter 2 (including Appendix A) is composed entirely by the results published in:

- **Tamarit, Ignacio**, José A. Cuesta, Robin IM Dunbar, and Angel Sánchez. *Cognitive resource allocation determines the organization of personal networks.* Proceedings of the National Academy of Sciences 115, no. 33 (2018): 8316-8321. DOI: 10.1073/pnas.1719233115.

The author of this thesis is the first author of this publication. The material from this source included in this thesis is not singled out with typographic means and references.

Some preliminary results from Chapter 3 are published in:

- **Tamarit, Ignacio**, José A. Cuesta, Robin IM Dunbar, and Angel Sánchez. *Cognitive resource allocation determines the organization of personal networks.* Proceedings of the National Academy of Sciences 115, no. 33 (2018): 8316-8321. DOI: 10.1073/pnas.1719233115.

The author of this thesis is the first author of this publication. The material from this source included in this thesis is not singled out with typographic means and references.

The results presented in Chapter 4 are partly contained in a pre-print available at the personal web page of the supervisor of this thesis Angel Sánchez:

- **Tamarit, Ignacio**, María Pereda, José A. Cuesta, Robin IM Dunbar, and Angel Sánchez. *The structure of negative social relationships*. URL: `http://anxosanchez.eu/wordpress/wp-content/uploads/2018/12/structure-negative-social_v3.pdf`

The author of this thesis is the first author of this publication. The material from this source included in this thesis is not singled out with typographic means and references.

The results presented in Chapter 5 are partly contained in a pre-print available at the personal web page of the supervisor of this thesis Angel Sánchez:

- **Tamarit, Ignacio**, María Pereda, José A. Cuesta, Robin IM Dunbar, and Angel Sánchez. *The structure of negative social relationships*. URL: `http://anxosanchez.eu/wordpress/wp-content/uploads/2018/12/structure-negative-social_v3.pdf`

The author of this thesis is the first author of this publication. The material from this source included in this thesis is not singled out with typographic means and references.

# Summary

This thesis set out to contribute to the realm of social physics, with a particular focus on human social networks. Our approach, however, is somewhat different from what is typical in disciplines such as complex systems or statistical physics. Rather than simplifying the features of the constituents of our system (people), and stressing their rules of interaction, we focus on better understanding those very same constituents, modelling them as *social atoms*. Our rationale is that a better understanding of such an *atom* may shed light on how (and why) it interacts with other atoms to form social collectives.

Given its robustness and the evolutionary roots of its premises, we use the Social Brain Hypothesis as our departure point. This theory states that the evolutionary drive behind the development of large brains in humans was the need to process social information and that the limited capacity of our brains imposes a limit to the number of relationships we can manage—the so-called "Dunbar's number", roughly 150. Moreover, evidence keeps revealing that these relationships are further organised in a series of hierarchically inclusive layers with decreasing emotional intensity, whose sizes exhibit a more or less constant scaling. Notwithstanding the empirical evidence, neither the presence of scaling in the organisation of personal networks nor its connection with limited cognitive skills had been explained so far.

In Chapter 2 we present a mathematical model that solves this puzzle. The assumptions of the model are quite simple, and well founded on empirical evidence. Firstly, the number of relationships we maintain tends to be stable on average. Secondly, these relationships are costly, and our

resources are limited. With these two premises, our results show that the hierarchical organisation emerges naturally from the principle of maximum entropy. Not only that, but we also predict a hitherto unnoticed regime of organisation whose existence we prove using several datasets from communities of immigrants.

The former model considers that relationships can only belong to a discrete set of categories (layers). In Chapter 3 we extend it so that relationships are classified in a continuum. This modification allows us to test the model with data from very different sources such as online communications, face-to-face contacts, and phone calls. Our results show that the two regimes of organisation found in the previous model persist in this variant, and reveal the underlying existence of a (universal) scaling parameter which does not depend on any particular number of layers.

To incorporate these ideas into socio-centric models, we build on the so-called Structural Balance Theory. This theory, underpinned by psychological motivations, posits that the structure of social networks of positive and negative relationships are highly interdependent. However, the theory has received little empirical validation, and negative social relationships are poorly understood—both from an ego-centric and a socio-centric perspective. For that reason, we turn to developing an experimental software in order to gather data within a school.

In Chapters 4 and 5 we present results from these experiments. In Chapter 4 we analyse the socio-centric networks using machine learning techniques and find that the structure of positive and negative networks is indeed very much connected. Besides, we study the two types of networks separately, showing that they exhibit quite distinct features and that gender effects in negative social networks are weak and asymmetrical for boys and girls. In Chapter 5, on the other hand, we focus on the structure of negative personal networks. Remarkably, using data from two different experimental settings, we show that the structure of personal networks of negative relationships mirrors that of the positive ones and exhibits a similar scaling—albeit their size is significantly smaller.

Chapter 6 summarises our results and presents future (and current) lines of investigation. Among them, we outline a model of a *social fluid* that uses the insights gained with this thesis to build a model of social collectives as ensembles of personal networks. This model is compatible, at the

micro-level, with the observations of the social brain hypothesis, and, at the macro-level, with the premises of the structural balance theory.

# Contents

# 1

# Introduction

"Words are a pretty fuzzy substitute for mathematical equations."

*Onum Barr*
Foundation and Empire, Isaac Asimov (1952)

The 19th century witnessed some of the most exciting scientific debates in history. On the one hand, Darwin and his evolutionary theory challenged the very conception of what it meant to be human—were we nothing but evolved primates? On the other hand, a series of social scientists, led by Compte and Quetelet, launched the shocking idea that human behaviour could be governed by universal laws such as those of physics (Lazarsfeld, 1961; Ball, 2002)—we did not even have free will!? The former led to a revolution in the biological sciences, the latter to the birth of a new discipline: social physics.

Quantification in the social sciences (that started in the 17th century with the *political arithmeticians* (Lazarsfeld, 1961)) had reached a point of maturity that allowed it to start rubbing shoulders with that of the natural sciences. The main reason was that important regularities (mostly Gaussian curves) had been detected in human behaviour. These regularities,

unveiled by the laws of probability (and what we now know as statistics), allowed the scientist of the time to speculate with the possibility that human affairs were subject to fundamental laws (Ball, 2002).

In a perhaps unexpected twist of events, the ideas behind social physics lay at the foundation of statistical mechanics—and not otherwise. By the second half of the 19th century, Maxwell and Boltzmann, fathers of statistical mechanics, were inspired by the use of probabilistic methods in the social sciences to abandon a completely deterministic picture of nature and embrace the rules of probability (Ball, 2002)—and the law of large numbers. Boltzmann himself compares molecules to individuals[1]:

"The molecules are like so many individuals, having the most various states of motion, and the properties of gases only remain unaltered because the number of these molecules which on the average have a given state of motion is constant."

These ideas undoubtedly inspired Asimov to conceive, by 1940s, his notion of a *psychohistory*, a mathematical theory of human processes that, when applied to a sufficiently large number of individuals (as in a *Galactic Empire*), would be able to predict, with tremendous precision, the fate of society (Asimov, 1951). But this was only science-fiction. The development of social physics in the first half of the 20th century was a daunting task.

Bernard and Killworth (1979) reviewed the state-of-the-art of this discipline in a paper with an eloquent title: *"Why are there no social physics?"*. The authors point out two main causes for this lack of success. Firstly, that all we can observe from social systems are details, not mean behaviours, which makes complicated to infer the laws underpinning them[2]. Secondly, that we only have access to *snapshots*, not steady-states, of a dynamic system—with an unknown time-scale. Notwithstanding the difficulties,

[1]The quote is extracted from (Ball, 2002), that attributes it to a paper (in German) by Boltzmann: L. Boltzmann, *Weitere Studien über das Wärmegleichegewicht unter Gasmoleküulen*, in: F. Hasenöhrl (Ed.), Wissenschaftliche Abhandlungen, Vol. 1, Leipzig, 1909, p. 317.

[2] Interestingly, the great physicist Richard Feynman makes a very similar point when explaining how complicated it is to infer the laws of nature. He compares it with learning the rules of chess only having access, from time to time, to see some valid positions in a chessboard: defjam99b, "Feynman :: Rules of Chess", Youtube video, 2:48, published on 21 Feb. 2007, `https://www.youtube.com/watch?v=o1dgrvlWML4`

they firmly defend the need to pursue a true social physics, characterised by quantitative models able to make predictions (not obvious from the formulation of the model) and be tested against the empirical evidence.

Research from the late 20th and early 21st centuries foreshadow a promising future for social physics. Scientists have (somewhat) embraced interdisciplinarity, the science of complex systems has experienced notorious advances, and there is increasing availability of data. As a consequence, several successful models have been proposed[3] and the field of social physics (together with computational social sciences) is in vogue (Castellano et al., 2009; Lazer et al., 2009; Conte et al., 2012; Stauffer, 2013; Holovatch et al., 2017).

This is the framework where this work belongs. In particular, we will focus on studying the composition of personal networks[4] (micro-system) and their connection to social networks (macro-system). Our approach, nonetheless, is slightly different from what disciplines such as complex systems or statistical physics tend to take. Instead of assuming a hyper-simplified version of the constituents of our system (people) and focusing on their rules of interaction[5], we will focus precisely on better understanding the individual behaviour of those constituents, the *social atoms*.

Our rationale is that a better understanding of this *atom* may shed light on how (and why) it interacts with other atoms to form social collectives. Additionally, as we shall see in the next section, the way we humans organise our social relationships is deeply connected to the size of our brains, and exhibits pervasive (yet not well understood) regularities. Therefore, it is a hardly mutable feature that must be taken into account if we want to build robust collective models from first principles.

[3] In a way, statistical physics is paying back its debt with social physics, see for example (Castellano et al., 2009).

[4] We acknowledge that our use of some terms might not be entirely consistent with other disciplines, and apologise in advance if that confuses the reader. Unless otherwise specified, we may use the names *ego-centric* and *personal* networks indistinctly throughout the text. Either case, we refer to how a focal individual (that we shall call *ego*) is connected to other individuals, independently of how these other individuals relate to each other.

[5] This is precisely the basic principle of the book entitled *The social atom* (Buchanan, 2008), one of the reasons why we chose the same term in this thesis.

## 1.1 The Social Brain Hypothesis

The intelligence of primates surpasses that of other mammals (Roth and Dicke, 2012). Great apes and eventually humans rest at the top of the list of the most intelligent animals in the world—along with dolphins[6]. Intelligence is a clear advantage in competitive, hostile environments but it also comes at a cost. In order to develop complex cognitive skills the brain must increase its size, and the brain is a very costly organ. For example, even though our brain represents only about 2% of our body weight, it consumes nearly 20% of the calories we intake (Aiello and Wheeler, 1995). Therefore, there must be a strong evolutionary drive fostering the development of such a demanding organ[7].

Traditionally, there has been a consensus that our brain evolved to process information of ecological significance (Dunbar, 1998); this is called the 'Ecological Hypothesis'. The ability to process such information would enable us, for example, to create mental maps of territory or to find food in complex environments, which are definite advantages. In the 1970s Humphrey (1976) proposed an alternative theory. In his view, it is the complexity of social living that requires higher intellectual abilities, and what ultimately provides primates with a competitive leverage—it is worth noting that dolphins also display complex social behaviours. Benefits derived from these faculties include better protection against predators or caring of the offspring. As it was the case of the Ecological Hypothesis, the ability to cohabit and coordinate with conspecifics also requires the processing of complex information, hence the larger brains.

Along these lines, Whiten and Byrne (1988) build their 'Machiavellian Intelligence Hypothesis'. Under this hypothesis, the ultimate drive behind brain development lies in the contentious facet of social relation-

[6]Dolphins are well known to have extraordinary intelligence. Here is an entertaining, educational video summarising some of their outstanding skills: TED-ed, "How smart are dolphins? - Lori Marino", Youtube video, 4:50, published on 31 Aug. 2015, `https://www.youtube.com/watch?time_continue=108&v=05PpTqtGhGU`.

[7]The webpage of the *Smithsonian National Museum of Natural History* offers a fantastic overview of brain development in humans; "Bigger Brains: Complex Brains for a Complex World", *The Smithosonian Institution's Human Origins Program*, last accessed 13 December 2018, `http://humanorigins.si.edu/human-characteristics/brains`.

ships. The principal argument is that abilities such as hiding intentions or plotting strategies would favour primates in gaining social power, thus granting their (genetic) survival. The theory is inspired, among others, by the experimental work of Frans de Waal at the Arnhem Zoo and published in his book 'Chimpanzee politics' (Waal, 1982). For years, Waal and his team collected data on the behaviour of a colony of chimpanzees residing in the zoo. At first sight, the behaviour of a colony of chimpanzees might seem boring and predictable—they merely lay around, eat, and eventually have sex or a fight. But the situation changes drastically when one takes a closer look. What Waal and colleagues observed was a very complex social environment, a world full of alliances, betrayals, strategic behaviour, and power struggles often related to sex. Such is the sophistication of these behaviours that Waal (1982) himself does not hesitate to write that "entire passages of Machiavelli seem to be directly applicable to chimpanzee behaviour."

Dunbar (1992) culminates these ideas by relating the size of different groups of primates directly to the size of their neocortex—the region of the brain that concentrates the highest cognitive faculties. The primary objective of this work was to quantitatively compare the two prevailing theories: the social and the ecological. Both theories tried to explain brain development as a requisite to process information, but differed on what type of information provided higher gains. To compare the two of them, Dunbar (1992) used a collection of data on 38 genera of non-human primates. Among these data is the size of different areas of the brain, mean group size, expansion of their territories, and dietary habits. The main result of his analysis is that only the social hypothesis is compatible with the observations. In particular, he finds a highly significant log-linear relationship ($r^2 = 0.76, p < 0.001$) between the relative size of the neocortex to the rest of the brain (neocortex ratio, $C_R$) and the mean group size ($\mathcal{N}$):

$$\log_{10}(\mathcal{N}) = 0.093 + 3.389 \log_{10}(C_R) \tag{1.1}$$

Furthermore, his results suggest that a) "Large groups are probably created by the hierarchical clustering of smaller cliques" and b) "the cognitive limitations lie in the quality of the relationships involved in the structuring of these cliques" (Dunbar, 1992). As we shall see, these ideas about hierar-

chization and quality (intensity) of relationships are thoroughly developed in later works.

### 1.1.1 Dunbar's number

Shortly after the publication of his 1992 paper, Dunbar (1993) extrapolates the results found for non-human primates to the case of humans. Applying equation 1.1 to humans (with a neocortex ratio of $C_R = 4.1$) predicts a group size of 147.8 with a 95% confidence interval of $(100.2, 231.1)$ —it is customary to round this figure up to 150 for simplicity.

The same study (Dunbar, 1993) confirms the prediction by comparing it with typical sizes of modern and historical hunter-gatherer societies and sizes of independent units in modern armies. Subsequently, many studies have supported this result with data from face-to-face interactions (Hill and Dunbar, 2003; Roberts et al., 2009), online social networks (Gonçalves et al., 2011; Haerter et al., 2012; Dunbar et al., 2015), or (cross-cultural) telephone records (Mac Carron et al., 2016; Wang et al., 2016). Similarly, recent studies endorse not only the validity of the prediction but the predominance of social versus ecological factors in the stability of social groups (Casari and Tagliapietra, 2018). The robustness of this phenomenon and the popularity of the theory have propitiated the number 150 to be currently known as 'Dunbar's number', and entails the consolidation of the so-called 'Social Brain Hypothesis' (SBH) — which supersedes other social hypothesis[8].

### 1.1.2 Hierarchical structure

In principle, the prediction above applies to social groups whose stability depends on broad personal knowledge and frequent face-to-face interactions. However, Dunbar (1993) examined different types of social units and found that all of them seem to have distinctive sizes. These could be either smaller substructures, such as overnight camps $(30 - 50)$, or more massive superstructures, such as tribal groups $(1000 - 2000)$. Dunbar (1998)

[8] Yet some authors may refer to it indistinctly as the 'Machiavellian Hypothesis' (Gavrilets and Vose, 2006), and even Dunbar himself may cite (Whiten and Byrne, 1988) when describing the SBH—see (Zhou et al., 2005) for an example.

elaborates on this observation and associate them characteristic numbers: 5 (support cliques), 12 – 15 (sympathy groups), 35 – 50 (bands, overnight camps), 150 (active network size), 500 (mega-bands), and 2,000 (tribes). According to Dunbar (1998), these groups represent "points of stability or clustering in the degrees of familiarity within the broad range of human relationships, from the most intimate to the most tenuous". So it is the quality (i.e. the degree of intensity or intimacy) of the relationships what determines the different groupings.

The interpretation of these groups as clusters in the degree of familiarity was validated shortly afterwards in an experimental study (Hill and Dunbar, 2003) based on the sending of Christmas cards in the United Kingdom—a deep-rooted tradition that is still in force. The study found that the size of the active network of the participants was $153.5 \pm 84.5$ (verifying the prediction of 150) and that it was structured into clusters of relationships conforming to their emotional intensity[9]. The sizes of these clusters were consistent with the sizes of human collectives found in previous studies ($5, 12 - 15, 35 - 50$)—organised from the most intense to the weakest relationships. The authors consequently conclude that "emotional closeness may be the key parameter underlying the hierarchical differentiation of social networks" (Hill and Dunbar, 2003).

It is important to note that the group sizes characterised in previous works referred to human collectives of historical societies. Hill and Dunbar (2003), on the other hand, analyse the intensity of relationships of individuals belonging to modern Western societies. The authors suggest "that the cognitive constraints on network size may apply universally to all modern humans" (Hill and Dunbar, 2003), thus making a conceptual leap from collectives to individuals—regardless of the size of the population to which they belong.

The hierarchical nature of the diverse human groupings (or, equivalently, of the relationships that an individual maintains within his or her social network) was analysed in detail by Zhou et al. (2005). To do so, they gathered data on the sizes of personal networks reported in the literature. The studies selected record data from different countries and obtained with different methodologies. More than 60 samples and the data from (Hill and Dunbar, 2003) were re-analysed employing more sophisticated techniques.

[9]Reported by the participants on a scale 1-10

In this manner, they identified "a discrete hierarchy of group sizes with a preferred scaling ratio close to three" so that "humans spontaneously form groups of preferred sizes organised in a geometric series approximating 3 – 5, 49 – 15, 30 – 45, etc." (Zhou et al., 2005). More specifically, they found a scaling of 3.2 with a significance of 0.993[10].

The robustness of the analysis and its high degree of statistical significance led Zhou et al. (2005) to conclude that the scaling ratio must be a universal aspect of human personal networks: "it may be that the absolute values of the group sizes are less important than the ratios between consecutive group sizes". In this way, the smallest group (support clique) would function as a seed from which the following levels (or layers) arise by applying the scaling[11]. The same type of analysis has been replicated in independent studies with similar results. Concretely, Hamilton et al. (2007) analysed the structure of 1189 groups belonging to 339 hunter-gatherer societies and found the same auto-similar structure with a mean scaling of 3.60 (3.23 – 4.02, 95% bootstrapped confidence limits).

### 1.1.3 Personal relationships in the digital world

During the last decade, the irruption of the Internet and the online social networks have favoured the availability of extensive data about our social relationships. Although digital platforms have undoubtedly increased our connectivity, the number of active relationships we maintain in them, their intensity, and their substructure, follow the same patterns found in face-to-face interactions (Dunbar et al., 2015). A number of examples in the literature demonstrate the existence of this phenomenon. Evidence come from large datasets from Facebook (Arnaboldi et al., 2013), Twitter (Gonçalves et al., 2011; Arnaboldi et al., 2013), telephone records (Mac Carron et al., 2016) and even from an online game (Pardus[12]) that recreates a virtual, futuristic society (Fuchs et al., 2014). Additionally, these studies unveiled the existence of a new group with size 1.5. These are the individuals with

[10] They do not report confidence intervals.

[11] Interestingly, studies have shown that human conversational groups tend to split when they are larger than about four people (Dunbar et al., 1995), what would naturally yield core groups with the usual size of a support clique.

[12] *Pardus – Massive Multiplayer Online Browser Game*, last accessed 13 December 2018, `https://www.pardus.at/`.

whom we would have maximum intensity relationships (such as romantic partners or best friends), above the level of a support clique—note that the size of this group respects the scaling of $\sim 3$ to the rest.

While the scaling factor found in the different studies exhibits some variability (always between 2 and 4), the empirical evidence keeps revealing the same type of hierarchical organisation. Interestingly, recent studies show that this structure (with constant scaling $\sim 2.5$) is also present in groups of non-human primates (Dunbar et al., 2018). Hence, what these studies suggest is that the layered structure is a universal feature strongly rooted in our psychology (Fuchs et al., 2014).

### 1.1.4 Costs and benefits

The different layers display marked differences regarding emotional closeness, but also in time devoted to relationships. Of all the time we dedicate to our social life, approximately 40% is dedicated to people in our most intimate circle (support clique), 20% to close relationships (sympathy group), and the remaining 40% to the rest of relationships (Sutcliffe et al., 2012)—progressively devoting less to those more distant. Moreover, as expected, the time we devote to our social relationships correlates strongly with their proximity and stability (Oswald et al., 2004; Roberts et al., 2009; Pollet et al., 2013). Once again, similar results apply to relationships mediated by technology (Miritello et al., 2013; Saramäki et al., 2014).

But, why do we invest time and resources in relationships? What benefits do we get from them? In general terms, our network supports us (Friedman and Taylor, 2012), controls the information we receive (Zhang et al., 2007), conditions our academic or work performance (Sparrowe et al., 2001), and may even be crucial to our health (Valente, 2010). All of this is dependent on the intensity of the relationships. For instance, while closer relationships provide us with more significant support in situations of need (Burton-Chellew and Dunbar, 2014), less intense relationships are especially relevant when it comes to getting information from distant regions of our network and finding job opportunities (Granovetter, 1977). Likewise, our tendency to show altruistic behaviour towards others decreases

with the intensity of the relationship[13] (Curry et al., 2013), probably as a consequence of our confidence that such actions will be reciprocated in the future (Burton-Chellew and Dunbar, 2014). In summary, the different layers seemingly correspond to different equilibria between the investment needed to maintain them and the benefits derived from them.

### 1.1.5 Individual differences in network composition

It is important to note that the observed regularities are found on average; thus, there can be considerable variability between one person and another. In the last few years, several studies have deepened in the characterisation of such differences in network size and composition. Stiller and Dunbar (2007) showed that individual differences in network size could be potentially explained by specific mental skills such us 'mentalising' (the ability to read and understand the mental states of other individuals) and memory[14]. Furthermore, studies combining neuroimaging techniques and cognitively demanding tasks were able to show that individual differences in the volume of the orbitofrontal cortex (a specific region of the neocortex) explained differences in mentalising skills, and those, in turn, were able to explain differences in network size (Powell et al., 2012). The same brain regions have been shown to play a crucial role in emotional processing and various forms of empathy—see (Lewis et al., 2011) and references therein for details. These findings provide fine-grained support to the SBH by connecting neurological features, cognitive skills, and network size at the individual's level.

Numerous other factors influence the composition of personal networks. Extraverts, for example, tend to have larger social networks than introverts. Nonetheless, the emotional proximity of their relationships is lower on average (Pollet et al., 2011) in agreement with the existence of a fixed amount of 'social capital' that extraverts would choose to spread more thinly—see also (Miritello et al., 2013). Additionally, personal networks are typically

[13]There exists, however, a 'kinship premium effect'. Within each layer, altruistic behaviour is always higher towards kin than towards non-kin.

[14]Funnily, chimpanzees can even outperform humans in some similar tasks: New Scientist , "Chimps outperform humans at memory task, Youtube video, 0:52, published on 3 Dic. 2007, `https://www.youtube.com/watch?v=nTgeLEWr614&feature=youtu.be`.

homophilous for gender, ethnicity, age, religion, education, and social values (Dunbar, 2018). All these factors mould an individual's social behaviour, which happens to be very stable. In this regard, Saramäki et al. (2014) found that we humans have very robust communication patterns, a sort of 'signature' that is distinctive to each of us and that remains unchanged even though the people with whom we relate vary over time.

### 1.1.6 Discussion

In a nutshell, the big picture drawn by the SBH over the years is that we humans typically deal with a set of about 150 relationships (friends and family) which are organised in a series of inclusive layers of increasing size but decreasing emotional intensity. Approximately, the sizes of these inclusive layers follow a sequence with a fixed scaling ratio close to three: $(1.5), 5, 15, 50$, and $150$[15]. These groups are known as Dunbar's circles[16] and reflect marked differences in trust, tendency towards altruistic behaviour, time invested, and emotional closeness.

Such a widespread theory[17] could not be exempt from some critical positions, and some authors keep defending the ecological hypothesis rather than the social (DeCasien et al., 2017). The interested reader is referred to (Dunbar and Shultz, 2017) for a review of the different ecological and social explanations proposed to the date. Recently, Acedo-Carmona and Gomila (2016) wrote an entire paper devoted to critically review Dunbar's social brain hypothesis. Regarding the empirical evidence, Acedo-Carmona and Gomila (2016) declare that: "much of the evidence amassed

[15] As already mentioned, the sequence can be extended $(500, 1500, \cdots)$ as long as the relationships do not require active maintenance. For example, using surveys on a large sample (+2000), Lubbers et al. (2019) found that Spaniards have an average of 536 acquaintances.

[16] In fact, the view of personal networks as concentric circles around the ego has a long tradition in the psychology literature, see for example (Kahn and Antonucci, 1980). Interestingly, a similar view was employed by the very founder of social network analysis (in the 1930s) Jacob Moreno in what he calls *social atom* (Moreno, 1947).

[17] Its popularity has caused it to be often misused to refer various, often vague, ideas and hypothesis (Dunbar and Shultz, 2017). It is therefore relatively easy to find "straw man arguments" trying to disprove it. For example: Brad McCarty, "Maintaining Relationships: The Fallacy of Dunbars Number, *FullContact*, last accessed 13 December 2018, `https://www.fullcontact.com/blog/maintaining-relationships/`.

over the years is still valid, but some of the claims derived from it turn out to be too simplistic". In particular, they believe that the search for social universals should focus on the motivation that leads us to form robust social bonds. Also, that "the pursuit of 'magic numbers' (5 – 15 – 50 – 150) in effective social configurations overlooks the vast diversity of human social life" (Acedo-Carmona and Gomila, 2016). In our opinion, based on the literature, the SBH does deal with these issues, but, even more importantly, the accumulated empirical evidence (which is not called into question but disregarded as 'magic numbers') is independent of possible explanations for it.

The SBH is an active research area with relevant open questions. Despite the overwhelming empirical evidence, the origin of a layered discretisation with constant scaling is unknown. Zhou et al. (2005) already noted this: "the fundamental question, then, is to determine the origin of this discrete hierarchy. At present, there is no obvious reason why a ratio of three should be important." This assertion was still valid at the time we began our work.

Another open question is to determine the relationship between the composition of personal networks and the different configurations of social collectives—an aspect that is also highlighted by Acedo-Carmona and Gomila (2016). In this sense, our work intends to lay the foundations of a theory that describes social groups as ensembles of personal networks which are compatible with the observations of the SBH. In other words, we will propose how social collectives can be formed out of a well-defined social atom. Before that, it is imperative that we review some of the theories that have been introduced in the literature to explain the formation of social networks.

## 1.2 Models of social networks: a brief review

The analysis and modelling of social networks is a vast field with a marked interdisciplinary character. Disciplines such as Statistical Physics and Computer Science (Toivonen et al., 2009), Economics (Goyal, 2012; Vega-Redondo, 2007; Jackson, 2010), Statistics (Snijders, 2011), or Sociology (Wasserman and Faust, 1994; Carrington et al., 2005) have devoted quite some effort to create plausible models of social networks. However, it is

beyond the scope of this thesis to do a comprehensive review of such a vast stream of literature. We rather focus on a more humble goal, namely to offer a global perspective of the different lines of research and techniques used in literature, with a special focus on the literature of complex systems, sociology, and the models that take into account the premises of the SBH.

### 1.2.1 Social networks as complex systems

From the complex systems (physics-oriented) literature, there is a somewhat recent review on social networks by Toivonen et al. (2009). In their paper, Toivonen et al. (2009) review, classify, and compare a total of nine different network models, and organise them in two principal categories: "*network evolution models*" (NEMs) and "*nodal attribute models*" (NAMs). The defining feature of NEMs is that the addition or removal of new links is based on structural (local) properties of the network. On the contrary, the link formation in NAMs depends exclusively on attributes of the nodes and not on the network structure—they are, to some extent, based on the concept of *homophily* (McPherson et al., 2001).

Besides the types of models mentioned above, the field of complex systems has produced other kinds of models, for example, what we shall call *structural network models* (SNMs) (Watts et al., 2002; Ravasz and Barabási, 2003; Jo et al., 2018). Their defining feature is (broadly speaking) that they focus on structural properties of the networks (such as the existence of communities) instead of the micro-mechanisms behind those properties. A general feature of the models reviewed in (Toivonen et al., 2009) is their emphasis on how local mechanisms of network formation can lead to producing a global, realistic structure.

Toivonen et al. (2009) point to two main mechanisms behind the NEMs they analyse: *triadic closure* and *global attachment*. The former consists of any local rule that increases the probability for two actors to be connected if they have *friends* in common. This mechanism is implemented to reproduce the high transitivity (clustering) observed in real social networks—that is, if $i$ is connected to $j$, and $j$ is connected to $k$, then it is very likely that $i$ is also connected to $k$. Indeed, many other models introduce to some extent a similar rule in a more direct (Murase et al., 2014; Klimek et al., 2016) or indirect manner (Ilany and Akcay, 2016; Antonioni et al., 2014).

In the case of the NAMs, however, the transitivity is usually implicit, either because homophily is itself a transitive property (as in social/physical distance models (Boguná et al., 2004; Murase et al., 2014)) or because it is introduced otherwise in the probability of two actors getting acquainted (Jin et al., 2001).

The *global attachment* rule is introduced to reproduce the "small world" property of social networks (Watts and Strogatz, 1998), namely that the distance between any two actors in a social network is surprisingly small (Milgram, 1967)—the so-called six degrees of separation. The way of implementing it may differ from one model to another, but it mostly consists of including a non-zero probability for random connections or rewirings (Klimek et al., 2016; Murase et al., 2014).

In dynamical models, links are constantly being added to the networks, and a third mechanism is needed to avoid the formation of complete graphs. According to Toivonen et al. (2009), there are two main techniques to prevent this from happening: *link deletion* and *node deletion*. The *link deletion* mechanism implies that each link has a given probability of being deleted at each time step while introducing *node deletion* results in all links of a node being deleted (for instance *as if* the node had dead (Ilany and Akcay, 2016)).

As we have seen, mechanisms like triadic closure, homophily (or distance of any kind), global rewirings and node (or link) deletion could be regarded as standard methods in the literature about social networks. However, some other interesting approaches have been proposed. That is the case of (Ilany and Akcay, 2016), where the emergence of social structure is explained through a process of *social inheritance*—although they focus on the social networks of other animals, not humans. Their model assumes simple neutral demography and focuses on the process of inheritance of social connections from parents, that is, the likelihood of a newborn $A$ connecting with another individual $B$ depends on the relationship between $A$'s *mother* and $B$.

Another technique that is becoming popular in recent years is the use of multiplex networks. For example, in (Murase et al., 2014) the society is modelled as a multilayered structure, where the layers represent different contexts and the probability of making a new connection (undirected and weighted) is higher if two nodes are geographically close—so it is related

to models based on a (metric) *distance*, see also (Barthélemy, 2011; Snijders, 2011). The overlapping structure of communities and the *Grannovetterian* (Granovetter, 1977) structure of social networks (i.e. communities of nodes strongly interconnected that connect through *weak* links to the rest of the network) are some of the features well replicated by their model. A more recent example can be found in (Klimek et al., 2016). In that work, society is understood as a dynamic, co-evolving[18] multiplex network, and the model is used to explore the community sizes distributions of different layers. Both (Murase et al., 2014) and (Klimek et al., 2016) combine features from NAMs and NEMs, including triadic closure, global attachment and homophily.

Toivonen et al. (2009) included in their review two models from the field of exponential random graphs (ERGMs) (Holland and Leinhardt, 1981) which are defined by a probability distribution of graphs. Even though these type of models may be considered to fall under the category of statistical models (Snijders, 2011), they are intimately related to (statistical) physics. Indeed, they offer the best prediction of network properties subject to constraints (via the maximum entropy principle) as the Boltzmann distribution does with macroscopic observables (such as pressure or temperature) subject to restrictions (such as the conservation of the total energy in a closed system) (Park and Newman, 2004). Other than ERGMs, the field of Statistics has produced a considerable amount of models and techniques applied to social networks—see (Snijders, 2011) for a comprehensive review.

Another powerful stream of models of network formation comes from the field of Economics (Goyal, 2012; Vega-Redondo, 2007; Jackson, 2010). The distinctive feature of this approach is that the creation of links is based on costs and benefits, and game-theoretic techniques are used. The focus of these models is usually to study the efficiency, stability and equilibria of networks conditioned to some strategic interaction, and tend to opt for analytical methods. This tendency often leads to somewhat simple network configurations (such as stars or complete graphs) not representative of more general and complex social structures. For that reason, we shall not discuss them in more detail. However, it is a very active field, and it

[18]This coevolution refers to coupled dynamics in both the intra-inter layer structure and the internal states of the nodes

is beyond discussion the importance of cost-benefit considerations in the formation of real social networks—see also section 1.1.4.

### 1.2.2 Sociological models: Structural Balance Theory

Let us now turn our focus to Sociology and other related fields such as Social Psychology and Anthropology. Indeed, ever since the seminal work by psychiatrist Jacob Moreno (Moreno, 1934; Newman, 2018), these fields have led the development of social networks models and their analysis (Wasserman and Faust, 1994). Concretely, we will discuss one of the most influential theories in the realm of network analysis: the *Structural Balance Theory* (SBT) (Heider, 1946; Cartwright and Harary, 1956), that as we will see, is related to some of the result of this thesis.

The theory was first proposed by (Heider, 1946) and generalised, mathematically[19], by Cartwright and Harary (1956). It relies on the existence of two fundamental types of relations, *positive* and *negative*, that characterise our relationships with other people—or with impersonal entities. Importantly, for any of these positive/negative relations there exists an exact opposite; examples are like/dislike, love/hate, and so forth. So, sticking to Heider's notation, we will refer to these relations as $L$ (positive/like) and $\sim L$ (negative/dislike).

Heider (1946) analysed the consistency of the relation between two people, $P$ and $O$, and their relation with an entity (or another person), $X$. Let us illustrate this with one example. Imagine that $P$ and $O$ have a good relationship ($L$). However, while $P$ really loves bullfighting ($X$), $O$ is a convinced activist for animal rights—hence, she hates ($\sim L$) bullfighting. They had just never talked about it until one day the topic comes out in a conversation. What happens then? In Heider's view, there is no balance, and this would create a sort of *tension*[20] that would either change the relationship between $P$ and $O$ or their respective attitudes towards bullfighting.

[19]Let us notice that even though he was a psychologist, and not a mathematician, the original paper by Heider (1946) was already written with a somewhat mathematical formulation.

[20]This tension can be understood as a sort of *cognitive dissonance* (Festinger, 1957).

In his own words: "If no balanced state exists, then forces[21] towards this state will arise" (Heider, 1946).

Cartwright and Harary (1956) used a graph-theoretical (network) approach to generalise Heider's ideas to social (signed, directed) networks. For the simplest case of a (undirected) triplet P-O-X (think now of X as another person), the result is that it is balanced if and only if the *product*[22] of the signs of their (three) relations is positive. Notice that the triplet P-O-X is a cycle of length three. To generalise Heider's notion of balance to more general graphs, they defined that a graph is balanced if (and only if) all of its cycles are positive—semi cycles if the graph is directed. They also proved some interesting theorems. For this thesis, the most relevant states that a signed, undirected graph "is balanced if and only if its points can be separated into two mutually exclusive subsets such that each positive line joins two points of the same subset and each negative line joins points from different subsets" (Cartwright and Harary, 1956). Therefore, it predicts an entirely polarised social structure.

To review the consequences and further developments of the SBT could very much be the topic of an entire thesis. The (somewhat strong) result that networks should be polarised in two groups (Cartwright and Harary, 1956) in order to achieve balance was later on generalised via the concept of *clusterabilty* (Wasserman and Faust, 1994), so that more than two groups (with only positive relationships within) were permissible. Even the critical concept of *transitivity* originates in Heider's theory (Wasserman and Faust, 1994). However, the theory has received little empirical validation (Feng et al., 2018). One important reason is that antipathetic relationships have received much less attention than sympathetic ones, and are not yet well understood (Card, 2010; Feng et al., 2018).

Nevertheless, the analysis of antipathetic relationships is nowadays receiving far more attention and, regarding the theory of social balance, we can find very recent mixed shreds of evidence concerning its validity (Card, 2010; Huitsing et al., 2012; Feng et al., 2018; Kirkley et al., 2019). As

[21] It is worth noticing the use of the term *force* here—see also section 6.2.3

[22] With the usual algebraic rules: $(+)(+) = (+)$, $(-)(-) = (+)$, and $(+)(-) = (+)$.

a consequence, other theories such as the *Status Theory* (ST) (Leskovec et al., 2010b) have been proposed[23], yielding slightly different predictions.

### 1.2.3 Models connected to the SBH

Given the amount of empirical evidence supporting the SBH, there are relatively few studies that take its ideas (somewhat) explicitly into account to recreate the structure of social networks[24]. We have found only two models that include the idea of limited cognitive capacity. The first one is from Jin et al. (2001). Their model relies on three basic principles that are easily understood from a social point of view: "(1) meetings take place between pairs of individuals at a rate that is high if a pair has one or more mutual friends and low otherwise; (2) acquaintances between pairs of individuals who rarely meet decay over time; (3) there is an upper limit on the number of friendships an individual can maintain" (Jin et al., 2001). The first one is a type of triadic closure, but the second and the third introduce interesting features qualitatively shared with the SBH. The decay of friendships and kin relationships over time has been, for example, experimentally studied in (Roberts and Dunbar, 2011a) and the upper limit on the number of bonds is nothing but a reflection of a limited cognitive capacity (Dunbar, 1993).

Another more recent model by Antonioni et al. (2014) considers that actors have a limited amount of *social energy* that they can spend on maintaining their social relationships, in clear consonance with the SBH. The model also includes a geometric distance between actors and a mechanism for triadic closure, called *synergy*, consisting of reducing the cost of a link if the involved actors have common friends. In both references (Jin et al., 2001; Antonioni et al., 2014) the models can reproduce high clustering and community structure, and the intuitive ideas behind them are especially suitable to our interests. However, none of them introduce (or explore the emergence of) the hierarchical layered structure found in empirical studies—see section 1.1.2.

[23]This theory also relies on the idea that networks of positive and negative relations are highly interdependent, but it interprets positive (out) links as signalling lower status, and negative (out) links as indicators of a higher (perceived) status.

[24]We refer here to models that aim to recreate social structure. Notice that concepts related to the SBH have been used with other modelling purposes in the literature, see for example (Gonçalves et al., 2011; Omodei et al., 2017).

From the perspective of what we called SNMs (structural network models), one recent reference is worth noticing. Harré and Prokopenko (2016) introduced a model "able to combine a specific socio-cognitive mechanism with the discrete scale invariance observed in ethnographic studies" (Harré and Prokopenko, 2016)—with explicit mention to the SBH. In our opinion, however, their proposal is a mathematically sound *description* of a hierarchically layered social network but does not provide further insights into the causes or consequences of that structure. We recall that once SNMs assume as facts some observed properties of the networks, its primary utility should be to replicate realistic social networks and to provide tools for further applications. Nevertheless, their work is the only model we have found that focuses explicitly on the premises of the SBH to model a global social structure.

### 1.2.4 Discussion

Our goal in this section was to set up a solid background before designing our models. The literature review, although not comprehensive, provided us with at least a hint of the vast amount of publications relating to social networks and the main ideas behind them. As we have seen, the models from the physics-oriented fields seem to be the ones that stress more the importance of finding plausible mechanisms. However, they typically introduce ad-hoc (plausible, nonetheless) mechanisms with the specific intention of recreating a particular property such as community structure, high clustering, degree correlations, small world, and so forth[25].

We believe that a more consistent approach, based on first principles, is needed, allowing us to advance our understanding of social structures cumulatively—so that the different laws and mechanisms that are found have to be preserved in future models, just as they are in physics. Most importantly, such models must yield testable predictions (Bernard and Killworth, 1979). In our opinion, the SBH is an excellent starting point as it provides a solid evolutionary and experimental foundation for how we humans manage our social relationships. Following this guideline, another

[25]Surprisingly, none of the models we have reviewed aims to reproduce the surprisingly low levels of reciprocity typically found in experimental studies. See for example (Almaatouq et al., 2016; Huitsing et al., 2012) and Chapter 4.

line of research that we consider particularly inspiring is the SBT, since it is based on aspects inherent to human psychology, and therefore hardly mutable. Interestingly, it is unclear how both theories relate to each other. Even though the SBH has its roots in a *machiavellian* view of human relationships, little is known about the organisation of negative personal networks, and whether or not they follow a similar pattern of organisation has not been determined.

As we have seen, the more realistic a social network model, the more complicated it becomes. Hence, an *ideal* model of social networks would likely consist of a directed, weighted, multilayer, time-dependent graph, with several mechanisms regarding link formation and deletion. Although possible, we must not forget that models are useful as long as they simplify reality while capturing some of its essential features. Perhaps, the network approach to the social structure must be superseded by another type of models. We intend to establish the basis that permits us to model human groupings as collectivities of individuals (atoms) who are subject to follow precise rules, based on first principles inherited from the evolutionary nature of our brains (and our sociality), and psychological *forces*. Let us now describe, more precisely, what the goals of this thesis are.

## 1.3 Summary and objectives

The SBH states that our brains became large as a result of the need to process social information (Dunbar, 1998). However, their size and capacity are finite, which imposes a limit on the number of relationships we can handle (Dunbar, 1993)—150, Dunbar's number. Connected to this theory, a gargantuan amount of empirical evidence shows that, not only do we have an upper limit to the number of relationships we can manage, but also that these relationships are further organised, according to their intensity, in a series of hierarchically inclusive layers with a characteristic scaling ratio close to three (Hill and Dunbar, 2003; Roberts et al., 2009; Haerter et al., 2012; Gonçalves et al., 2011; Dunbar, 2014; Sutcliffe et al., 2012; Dunbar, 2014; Hill and Dunbar, 2003; Dunbar et al., 2015; Zhou et al., 2005). Notwithstanding the empirical evidence, neither the hierarchical organisation nor its connection with cognitive constraints has been explained so far.

In Chapter 2 we will present a mathematical model that solves this puzzle. The model is based on the facts that we have a limited cognitive capacity, and that maintaining relationships is costly. Even though this model is presented taking into account the discrete nature of the layers in which we typically organise relationships, in Chapter 3 we will show that it can be naturally extended to a continuum of layers, revealing that the patterns behind the SBH are indeed more general.

To advance in our understanding of the structure of human collectives, we must then incorporate these ideas in an adequate socio-centric model. To that end, we rely on the ideas from the SBT (Heider, 1946; Cartwright and Harary, 1956), precisely because psychological motivations also underpin them. This is crucial to our interests, since, ultimately, we intend to be able to explain human collectives (or at least their main characteristics) from immutable factors that define our social behaviour—thus the concept of the social atom. Nevertheless, the networks (both personal and socio-centric) of negative relationships are yet poorly understood, and we faced the need to undertake our own experimental research.

In Chapters 4 and 5 we will present results from these experiments, in which we collected data on positive and negative relationships within a school. In Chapter 4 we will analyse the main features of these networks, and use machine learning techniques to explore the interplay between the positive and negative ones. Chapter 5, on the other hand, will focus on the structure of negative personal networks and its connection with the SBH.

Finally, Chapter 6 will serve as a summary of our results and will introduce some of the lines of research that open as a consequence of this work. Importantly, we will outline a model that collects the insights of this thesis and depicts social collectives as ensembles of personal networks, providing a proof-of-concept of the ideas here presented.

# 2

# The social atom

> "The bonds between ourselves and another person exists only in our minds. Memory as it grows fainter loosens them, and notwithstanding the illusion by which we want to be duped and which, out of love, friendship, politeness, deference, duty, we dupe other people, we exist alone. Man is the creature who cannot escape from himself, who knows other people only in himself, and when he asserts the contrary, he is lying."
>
> *Marcel Proust*
> In Search of Lost Time Vol. VI: The Sweet Cheat Gone (1925)

In this chapter we develop a mathematical model of the building blocks of social systems (*social atoms*) that should serve to connect the individual and collective perspectives of human societies. Indeed, whatever the (global) social structure is, it must comply with the (local) organisation of the ego-networks—just as any physical object must be consistent with its atomic composition. As we will show below, our model not only accounts for the layered structure described in section 1.1, but also predicts the ex-

istence of a hitherto unnoticed, different regime. Indeed, we will see that depending on the relation between cost and available relationships, an inverted structure may arise in which layers with larger emotional content are also larger in size.

## 2.1 Model description

In a population of $N$ individuals, relationships (links) can be established out of a set of $r$ different categories (that we will later refer to as "layers") according to the strength of the links. This is the problem that we want to model, but in its bare bones, this amounts to distributing a certain number of balls (links) in urns (layers)—in effect, a multinomial distribution. Of itself, this distribution yields no structure whatsoever, but it is a reasonable prior to assume as the default. In this setting, the probability that there are $\ell_k$ balls in urn $k \in \{1, 2, \ldots, r\}$ is

$$P_0(\boldsymbol{\ell}|N) = \frac{(N-1)!(r+1)^{-N+1}}{\ell_1!\ell_2!\cdots\ell_r!(N-1-\ell_1-\ell_2-\cdots-\ell_r)!}, \tag{2.1}$$

where $\boldsymbol{\ell} = (\ell_1, \ell_2, \ldots, \ell_r)$.

Let us now assume that there is a cost $s_k$ associated to each ball placed in urn $k$. Urns are initially indistinguishable, so without loss of generality we can sort them by decreasing costs, $s_{max} > s_2 > \cdots > s_{min}$. We now look for a probability distribution that is constrained to have a fixed average number of balls $\mathcal{L}$ and a fixed average amount of resources $\mathcal{S}$ to afford its costs, that is,

$$\sum_{k=1}^{r} \mathbb{E}(\ell_k) = \mathcal{L}, \qquad \sum_{k=1}^{r} s_k \mathbb{E}(\ell_k) = \mathcal{S}. \tag{2.2}$$

### 2.1.1 Maximum entropy distribution

In order to add this information to our prior (Eq. 2.1), the procedure to follow is the maximum entropy principle (Jaynes, 2003; Sivia and Skilling, 2006), as it is the only way to guarantee a posterior distribution that is compatible with the prior, compatible with the additional information, and

unbiased (Jaynes, 2003; Caticha and Giffin, 2006). In other words, the posterior $P(\boldsymbol{\ell}|\mathcal{S},\mathcal{L},N)$ is obtained through maximisation of

$$\mathscr{S}[P] = \sum_{\boldsymbol{\ell}} \left\{ -\log\left[\frac{P(\boldsymbol{\ell}|\mathcal{S},\mathcal{L},N)}{P_0(\boldsymbol{\ell}|N)}\right] - \hat{\tau} - \hat{\gamma}\sum_{k=1}^{r}\ell_k - \hat{\mu}\sum_{k=1}^{r}s_k\ell_k \right\} P(\boldsymbol{\ell}|\mathcal{S},\mathcal{L},N), \tag{2.3}$$

where $\hat{\tau}$, $\hat{\gamma}$ and $\hat{\mu}$ are Lagrange multipliers associated, respectively, to the normalisation of $P(\boldsymbol{\ell}|\mathcal{S},\mathcal{L},N)$ and to the two constraints (2.2). The Lagrange multipliers must be determined a posteriori by enforcing $P(\boldsymbol{\ell}|\mathcal{S},\mathcal{L},N)$ to satisfy those same constraints. The posterior distribution obtained through this method is

$$P(\boldsymbol{\ell}|\mathcal{S},\mathcal{L},N) = Z(\hat{\gamma},\hat{\mu},N)^{-1}\binom{N-1}{\boldsymbol{\ell}}\exp\left\{\sum_{k=1}^{r}(-\hat{\gamma}-\hat{\mu}s_k)\ell_k\right\}, \tag{2.4}$$

$$Z(\hat{\gamma},\hat{\mu},N) = \sum_{\boldsymbol{\ell}}\binom{N-1}{\boldsymbol{\ell}}\exp\left\{\sum_{k=1}^{r}(-\hat{\gamma}-\hat{\mu}s_k)\ell_k\right\}. \tag{2.5}$$

In terms of the 'partition function' $Z(\hat{\gamma},\hat{\mu},N)$, the two constraints (2.2) become

$$-\frac{\partial}{\partial\hat{\gamma}}\log Z(\hat{\gamma},\hat{\mu},N) = \mathcal{L}, \qquad -\frac{\partial}{\partial\hat{\mu}}\log Z(\hat{\gamma},\hat{\mu},N) = \mathcal{S}. \tag{2.6}$$

Besides, if we extend this partition function with new variables $\boldsymbol{\beta} = (\beta_1,\ldots,\beta_r)$ as

$$Z(\hat{\gamma},\hat{\mu},N,\boldsymbol{\beta}) = \sum_{\boldsymbol{\ell}}\binom{N-1}{\boldsymbol{\ell}}\exp\left\{\sum_{k=1}^{r}(-\hat{\gamma}-\hat{\mu}s_k-\beta_k)\ell_k\right\}, \tag{2.7}$$

we can obtain $\mathbb{E}(\ell_k)$ through

$$\mathbb{E}(\ell_k) = -\frac{\partial}{\partial\beta_k}\log Z(\hat{\gamma},\hat{\mu},N,\boldsymbol{\beta})\bigg|_{\boldsymbol{\beta}=\mathbf{0}}. \tag{2.8}$$

These expressions to compute $\mathcal{L}$, $\mathcal{S}$, and $\mathbb{E}(\ell_k)$ are particularly simple once we realise that

$$Z(\hat{\gamma},\hat{\mu},N,\boldsymbol{\beta}) = \sum_{\boldsymbol{\ell}}\binom{N-1}{\boldsymbol{\ell}}\prod_{k=1}^{r}\left(e^{-\hat{\gamma}-\hat{\mu}s_k-\beta_k}\right)^{\ell_k} = \left(1+\sum_{k=1}^{r}e^{-\hat{\gamma}-\hat{\mu}s_k-\beta_k}\right)^{N-1}, \tag{2.9}$$

for then

$$\mathcal{L} = \frac{(N-1)\sum_k e^{-\hat{\gamma}-\hat{\mu}s_k}}{1+\sum_k e^{-\hat{\gamma}-\hat{\mu}s_k}}, \qquad \mathcal{S} = \frac{(N-1)\sum_k s_{min} e^{-\hat{\gamma}-\hat{\mu}s_k}}{1+\sum_k e^{-\hat{\gamma}-\hat{\mu}s_k}}, \tag{2.10}$$

and

$$\mathbb{E}(\ell_k) = \frac{(N-1)e^{-\hat{\gamma}-\hat{\mu}s_k}}{1+\sum_k e^{-\hat{\gamma}-\hat{\mu}s_k}}. \tag{2.11}$$

Dividing $S$ and $\mathbb{E}(\ell_k)$ by $\mathcal{L}$ we obtain

$$\frac{\mathcal{S}}{\mathcal{L}} = \frac{\sum_k s_{min} e^{-\hat{\mu}s_k}}{\sum_k e^{-\hat{\mu}s_k}}, \qquad \frac{\mathbb{E}(\ell_k)}{\mathcal{L}} = \frac{e^{-\hat{\mu}s_k}}{\sum_k e^{-\hat{\mu}s_k}}. \tag{2.12}$$

The first of these two equations allows us to determine $\hat{\mu}$ as a function of $\mathcal{S}/\mathcal{L}$, and then we can use this value to obtain $\hat{\gamma}$ from the first of Eqs. (2.10) as

$$e^{-\hat{\gamma}} = \frac{\mathcal{L}}{(N-1-\mathcal{L})\sum_k e^{-\hat{\mu}s_k}}. \tag{2.13}$$

As a matter of fact, we can use identity (2.13) to simplify the posterior distribution (2.4). To begin with,

$$\begin{aligned} Z(\hat{\gamma},\hat{\mu},N) &= \left(1+e^{-\hat{\gamma}}\sum_{k=1}^{r} e^{-\hat{\mu}s_k}\right)^{N-1} \\ &= \left(1+\frac{\mathcal{L}}{N-1-\mathcal{L}}\right)^{N-1} = \left(1-\frac{\mathcal{L}}{N-1}\right)^{-N+1}. \end{aligned} \tag{2.14}$$

Thus, denoting $L \equiv \sum_k \ell_k$,

$$\begin{aligned} P(\boldsymbol{\ell}|\mathcal{S},\mathcal{L},N) &= \left(1-\frac{\mathcal{L}}{N-1}\right)^{N-1}\binom{N-1}{\boldsymbol{\ell}} e^{-\hat{\gamma}L} e^{-\hat{\mu}\sum_k s_k\ell_k} \\ &= \left(1-\frac{\mathcal{L}}{N-1}\right)^{N-1-L}\binom{N-1}{\boldsymbol{\ell}}\left(\frac{\mathcal{L}}{N-1}\right)^{L}\frac{e^{-\hat{\mu}\sum_k s_k\ell_k}}{\left(\sum_k e^{-\hat{\mu}s_k}\right)^{L}}, \end{aligned} \tag{2.15}$$

and using

$$\binom{N-1}{\boldsymbol{\ell}} = \binom{N-1}{L}\binom{L}{\boldsymbol{\ell}}. \tag{2.16}$$

we arrive at the desired, simplified posterior distribution

$$P(\boldsymbol{\ell}|\mathcal{S},\mathcal{L},N) = \mathscr{B}(L,\mathcal{L}/N,N)\binom{L}{\boldsymbol{\ell}}\frac{e^{-\hat{\mu}\sum_k s_k\ell_k}}{\left(\sum_k e^{-\hat{\mu}s_k}\right)^L}, \tag{2.17}$$

with $\mathscr{B}(x,p,n) = \binom{n}{x}p^x(1-p)^{n-x}$ the binomial distribution, and where the constraint $L = \sum_k \ell_k \leqslant N-1$ is to be understood in $P(\boldsymbol{\ell}|\mathcal{S},L,N)$.

Lastly, let us remark that this result is similar if we consider small populations. If $N$ is so small that everyone knows everybody else, then $\mathcal{L} \to N-1$. In this limit $\mathscr{B}(L,\mathcal{L}/(N-1),N-1) \to \delta_{L,N-1}$, therefore

$$\lim_{\mathcal{L}\to N-1} P(\boldsymbol{\ell}|\mathcal{S},\mathcal{L},N) = \binom{N-1}{\boldsymbol{\ell}}\frac{e^{-\hat{\mu}\sum_k s_k\ell_k}}{\left(\sum_k e^{-\hat{\mu}s_k}\right)^{N-1}}, \qquad \sum_{k=1}^{r}\ell_k = N-1. \tag{2.18}$$

### 2.1.2 Application to ego-networks

Notice that the model presented is fully general and applies to any situation in which a certain number of items of any sort have to be assigned to some categories with different costs —in fact, equation 2.17 describes a distribution that measures the likelihood of different allocations of balls to urns with different costs. However, based on what we described in section 1.1, its connection with the organisation of links within ego-networks is rather natural.

Although relationships change over time (they strengthen or weaken, new ones are created, and some old ones fade (Saramäki et al., 2014)), each individual handles a certain average number of links $\mathcal{L}$ at any one time (Sutcliffe et al., 2012). These relationships are further organised into different layers (urns, $\ell_k$) according to the emotional strength (or *closeness*) of the links (see for example (Dunbar, 2018; Kawachi and Berkman, 2001) and references therein). Additionally, studies of both offline and online social networks indicate that time invested in interacting with individual alters seems to determine the emotional strength of the relationship (the higher the investment, the closer the relationship) (Oswald et al., 2004; Sutcliffe et al., 2012), and is thus largely responsible for their layered structure (Sutcliffe et al., 2012; Hill and Dunbar, 2003; Dunbar et al., 2015; Mac Carron et al., 2016; Roberts and Dunbar, 2015; Dunbar, 2018;

Hall, 2018). These investments reflect the costs, $s_k$, that individuals have to make to create functional relationships. If we further assume a limited (cognitive) capacity $\mathcal{S}$ of individuals to handle relationships (Hill and Dunbar, 2003; Powell et al., 2012), we have a problem to which the previous model applies. In what follows, we will analyse which kind of testable predictions can be inferred from the organisation of links in an ego-network implied by the model.

### 2.1.3 Results

We explore the emergence of structure using the equation (2.11) for the expected number of links in each layer. The ratio of this quantity between consecutive layers is

$$\frac{\mathbb{E}(\ell_{k+1})}{\mathbb{E}(\ell_k)} = e^{\hat{\mu}|\Delta s_k|}, \tag{2.19}$$

where $|\Delta s_k| = |s_{k+1} - s_k| > 0$ is the cost difference between them. Equation 2.19 identifies two distinct regimes according to whether $\hat{\mu} > 0$ or $\hat{\mu} < 0$:

- If $\hat{\mu} > 0$, then $\mathbb{E}(\ell_{k+1}) > \mathbb{E}(\ell_k)$, and the most expensive layers will be less populated than the less expensive ones. We will call this the *standard* regime.
- If $\hat{\mu} < 0$, then $\mathbb{E}(\ell_{k+1}) < \mathbb{E}(\ell_k)$, and the most expensive layer will be the most populated one. We will call this the *inverse* regime.

Let us now consider the special case in which the cost decreases linearly with the layer, $s_k = s_{max} - (s_{max} - s_{min})(k-1)/(r-1)$, with $s_{max} > s_{min} > 0$. In that case

$$\Omega(\hat{\mu}) = \sum_{k=1}^{r} e^{-\hat{\mu}s_k} = e^{-\hat{\mu}s_{max}} \sum_{k=0}^{r-1} \left(e^{\hat{\mu}(s_{max}-s_{min})/(r-1)}\right)^k = \tag{2.20}$$

$$= e^{-\hat{\mu}s_{max}} \frac{e^{\hat{\mu}(s_{max}-s_{min})r/(r-1)} - 1}{e^{\hat{\mu}(s_{max}-s_{min})/(r-1)} - 1}, \tag{2.21}$$

and

$$\sigma \equiv \frac{\mathcal{S}}{\mathcal{L}} = -\frac{\partial}{\partial \hat{\mu}} \log \Omega(\hat{\mu}) = s_{max} + \frac{s_{max} - s_{min}}{r-1} \left( \frac{e^{\mu}}{e^{\mu} - 1} - \frac{r e^{r\mu}}{e^{r\mu} - 1} \right), \tag{2.22}$$

where we define $\mu \equiv \hat{\mu}(s_{max} - s_{min})/(r-1)$ for convenience[1]. Then

$$\frac{s_{max} - \sigma}{s_{max} - s_{min}} = f(\mu) \equiv e^{\mu} \frac{(r-1)e^{r\mu} - re^{(r-1)\mu} + 1}{(r-1)(e^{r\mu} - 1)(e^{\mu} - 1)}. \tag{2.23}$$

Function $f(\mu)$ monotonically increases from its smallest value $\lim_{\mu \to -\infty} f(\mu) = 0$ (corresponding to $\sigma = s_{max}$) up to $\lim_{\mu \to \infty} f(\mu) = 1$ (corresponding to $\sigma = s_{min}$). As $s_{min} < \sigma < s_{max}$, $\mu$ can take any value $-\infty < \mu < \infty$. Since

$$\lim_{\mu \to 0} f(\mu) = \frac{1}{2}, \tag{2.24}$$

whenever $s_{min} < \sigma < (s_{max} + s_{min})/2$ we have that $\mu > 0$. On the other hand, if $(s_{max} + s_{min})/2 < \sigma < s_{max}$ then we have that $\mu < 0$ (see Fig. 2.1).

Hence, which regime an individual belongs to depends on $\sigma$ (the ratio $\mathcal{S}/\mathcal{L}$) and this in turn depends on the total number of social relationships that an individual has. If $\mathcal{L}$ is large this structure will be standard. This is what has been observed in most studies analysing the organisation of ego-networks (see section 1.1), and it is what seems reasonable to expect: the less costly a relationship is the more of them you can have. If, on the contrary, $\mathcal{L}$ is small, the structure is inverted. In other words, the more time or cognitive capacity that an individual has, the more he/she is able to devote to strengthening all his/her relationships.

Following the customary use in the anthropological literature, we define circle $k$ as including all links from layers $1, 2, \ldots, k$. Thus, we use the term circle as a proxy for proximity, so that egos have closer (more costly) relationships with alters in the inner circles than those in the outer circles. The expected fraction of links in layer $k$ is given by

$$\epsilon_k \equiv \frac{\mathbb{E}(\ell_k)}{L} = \frac{e^{k\mu} - e^{(k-1)\mu}}{e^{r\mu} - 1}, \tag{2.25}$$

so the fraction of links in circle $k$ is then

$$\chi_k = \sum_{j=1}^{k} \epsilon_k = \frac{1}{e^{r\mu} - 1} \sum_{j=1}^{k} (e^{j\mu} - e^{(j-1)\mu}) = \frac{e^{k\mu} - 1}{e^{r\mu} - 1}. \tag{2.26}$$

In the standard regime ($\mu > 0$) $\chi_k \approx e^{(k-r)\mu}$, and we recover the constant

[1] Notice that the choice $|\Delta s_k| = 1$ implies that $\hat{\mu} = \mu$, so in (Tamarit et al., 2018) we used both interchangeably.

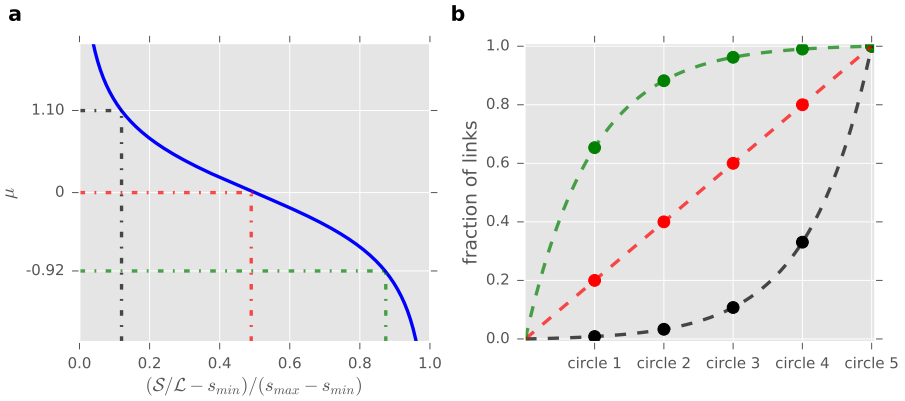


**Figure 2.1: The two regimes as a function of the mean cognitive cost allocatable per link**. **a,** Dependency of the parameter $\mu$ with the ratio $\mathcal{S}/\mathcal{L}$. The blue line represents the typical dependency of the parameter with the mean cognitive cost $\mathcal{S}/\mathcal{L}$ that an individual can spend in maintaining a link. As a reference, it has been computed with (2.23) for $r = 5$ circles and $\Delta s_k = 1$, but it is representative of the expected behaviour. Given a fixed cognitive capacity $\mathcal{S}$, increasing $\mathcal{L}$ implies moving to the left in the graph. The particular value of $\mathcal{S}/\mathcal{L}$ determines the value of $\mu$. Dotted lines represent example cases (fixed $\mathcal{S}$); in green, an individual with "few" alters (inverse regime; $\mu = -0.92$), in red, the limit case (change of regime; $\mu = 0$), and, in black, an individual with "many" alters (standard regime; $\mu = 1.10$). **b,** Expected regimes as a function of $\mu$, presented through the fraction of links in every circle. The colors follow the specifications given in (**a**). That is, the black line represents the standard regime, the red the limit case, and the green one the inverse regime. Solid dots represent the expected fraction of links in each circle for the different examples.

scaling ratio $\chi_{k+1}/\chi_k \approx e^{\mu}$ between consecutive circles that has been extensively reported in the literature (Hill and Dunbar, 2003; Dunbar et al., 2015). However, in the inverse regime ($\mu < 0$) $\chi_k$ quickly approaches 1 as $k$ increases, implying that most links are within the innermost circle. Therefore, a second, as yet unnoticed, regime is predicted in which the structure is reversed—the more demanding the layers, the more populated they are.

This regime is expected to arise when the ratio $\mathcal{S}/\mathcal{L}$ is particularly large. That would be the case, for instance, of individuals living in small

populations or within limited social environments. Assuming that the capacity of those individuals is similar to the capacity of individuals elsewhere, the reduced number of possible relationships should be translated into an inversion of their circles, making apparent the inverse regime predicted by the model. This phenomenon can in fact be observed in data collected during an oceanic scientific expedition (Bernard and Killworth, 1973) and, perhaps, within a community of immigrants (Granovetter, 1977)—but it seems that neither of these studies were aware of this.

## 2.2 Empirical validation

We test our model (see Fig. 2.2 for an schematic representation) on five communities. One is a community of college students (where we expect the standard regime to predominate) and the other four are communities of immigrants (where we expect the inverse regime to be more common because they are likely to lack opportunities to make friendships outside their respective communities). Note that we use the term *community* here in a broad sense, as a group of people living in the same place or having a particular characteristic in common. Importantly, our model is defined at the individual level, and the background information (such as the community an individual belongs to) is merely used to conjecture what regime should prevail in each case. Before we analyse any data, let us describe how the model is fitted[2].

### 2.2.1 Bayesian estimate of the parameter

The data we will analyse come from surveys in which the participants rate their relationships on a Likert scale with different levels. We use these answers as a proxy for the intensities of the links and build a vector ($\boldsymbol{\ell} = (\ell_1, \ell_2, \ldots, \ell_r)$) for each participant accordingly —$\ell_1$ being the number of strongest relationships and $\ell_r$ the number of weakest ones. The likelihood

[2]All numerical analysis are carried out in `Python` with the packages `scipy.optimize` and `scipy.integrate` (see the documentation for details). The code and the data used in the paper are available at `https://github.com/1gnaci0/Cognitive`

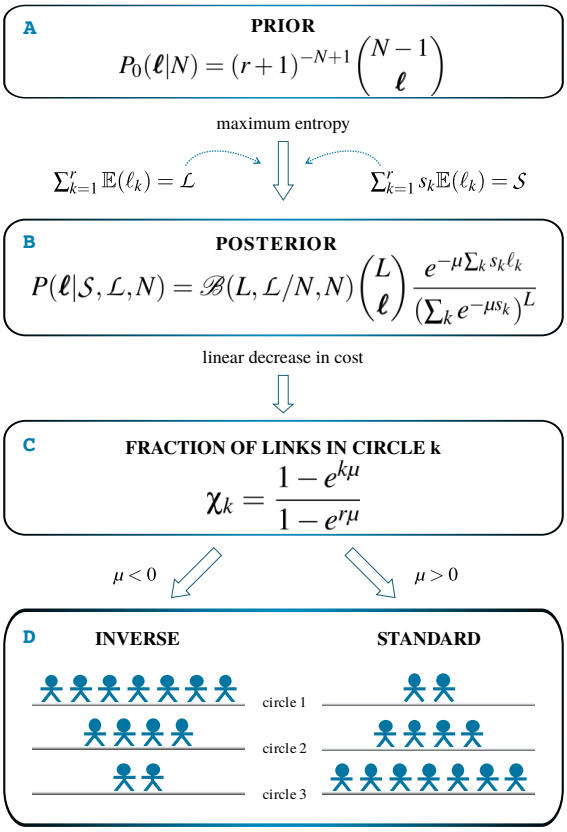


**Figure 2.2: Schematic representation of the model. A,** There are $r$ social layers and individuals distribute their links among them. Without further assumptions, and given that there are $N$ individuals in the population, the *prior* distribution of links in layers (given by the vector $\boldsymbol{\ell} = (\ell_1, \ldots, \ell_r)$) is a random choice. **B,** Maintaining a link in a layer $k$ has a cost $s_k$. This cost limits the number of relationships that can be formed. Assuming that an individual maintains on average $\mathcal{L}$ links incurring an average cost $\mathcal{S}$, we can use the *maximum entropy principle* to incorporate that information into a *posterior distribution*. The parameter $\mu$ is a function of $\mathcal{S}/\mathcal{L}$. **C,** We consider the special case in which the cost decreases linearly with the layer. This simplification allows us to find an exact expression for the fraction of links in a given circle $k$, with a single parameter ($\mu$). **D,** Depending on the value of the parameter $\mu$, two distinct regimes arise: *standard* and *inverse*. This constitutes a prediction of our model.

for $\boldsymbol{\ell}$ (hence also for $L = \sum_k \ell_k$) is given by

$$P(\boldsymbol{\ell}|\mathcal{L},\mu,N) = \mathscr{B}(L,\mathcal{L}/(N-1),N-1)\left(\frac{e^{\mu}-1}{e^{\mu r}-1}\right)^{L}\binom{L}{\boldsymbol{\ell}}\exp\left\{\mu\sum_{k=0}^{r-1}k\ell_{k+1}\right\}. \tag{2.27}$$

Our goal is to determine $P(\mathcal{L},\mu|\boldsymbol{\ell},N)$ using Bayesian inference. To this aim we choose a neutral uniform prior for the parameters $\mu$ and $\mathcal{L}$. Thus,

$$P(\mathcal{L},\mu|\boldsymbol{\ell},N) = \frac{N}{\binom{L}{\boldsymbol{\ell}}\Xi(\boldsymbol{\ell})}P(\boldsymbol{\ell}|\mathcal{L},\mu,N), \tag{2.28}$$

with

$$\Xi(\boldsymbol{\ell}) = \binom{L}{\boldsymbol{\ell}}^{-1}\int_0^{N-1}d\mathcal{L}\int_{-\infty}^{\infty}d\mu\,P(\boldsymbol{\ell}|\mathcal{L},\mu,N). \tag{2.29}$$

The factor $N$ in the numerator of (2.28) arises from

$$\int_0^{N-1}\mathscr{B}(L,\mathcal{L}/(N-1),N-1)\,d\mathcal{L} = \frac{1}{N}. \tag{2.30}$$

Now, if we denote

$$F_t(R) \equiv \int_0^t\left(\frac{1-e^{-\mu}}{1-e^{-\mu r}}\right)^{L}e^{-\mu R}\,d\mu, \tag{2.31}$$

then

$$\begin{aligned}\Xi(\boldsymbol{\ell}) &= \int_{-\infty}^{\infty}\left(\frac{e^{\mu}-1}{e^{\mu r}-1}\right)^{L}e^{\mu L_1}\,d\mu\\ &= \int_0^{\infty}\left(\frac{e^{\mu}-1}{e^{\mu r}-1}\right)^{L}e^{\mu L_1}\,d\mu + \int_0^{\infty}\left(\frac{1-e^{-\mu}}{1-e^{-\mu r}}\right)^{L}e^{-\mu L_1}\,d\mu\\ &= F_\infty(L_2) + F_\infty(L_1),\end{aligned} \tag{2.32}$$

where

$$L_1 \equiv \sum_{k=0}^{r-1}k\ell_{k+1}, \qquad L_2 \equiv L(r-1) - L_1 = \sum_{k=0}^{r-1}k\ell_{r-k}. \tag{2.33}$$

Summarising, $P(\mathcal{L},\mu|\boldsymbol{\ell},N) = P(\mathcal{L}|\boldsymbol{\ell},N)P(\mu|\boldsymbol{\ell})$, where

$$P(\mathcal{L}|\boldsymbol{\ell},N) = N\mathscr{B}(L,\mathcal{L}/(N-1),N-1), \tag{2.34}$$

$$P(\mu|\boldsymbol{\ell}) = \Xi(\boldsymbol{\ell})^{-1}\left(\frac{e^{\mu}-1}{e^{\mu r}-1}\right)^{L} e^{\mu L_1}. \tag{2.35}$$

The maximum likelihood estimate for $\mathcal{L}$ is obviously $\mathcal{L} = L$. That for $\mu$ can be obtained differentiating

$$\log P(\mu|\ell) = \mu L_1 + L\log(e^{\mu}-1) - L\log(e^{\mu r}-1) - \log\Xi(\boldsymbol{\ell}), \tag{2.36}$$

which leads to

$$\frac{L_1}{L} = \sum_{k=1}^{r-1} k\frac{\ell_{k+1}}{L} = \frac{e^{\mu}}{e^{\mu}-1} - \frac{re^{r\mu}}{e^{r\mu}-1} = (r-1)f(e^{\mu}). \tag{2.37}$$

This equation is identical to (2.23) if we use $\boldsymbol{\ell}$ as estimates for $\mathbb{E}(\boldsymbol{\ell})$. For the results presented in this chapter, we estimate $\mu$ by solving equation 2.37 — we use the function `fsolve` (`Python`) with tolerance $10^{-6}$ for the relative error between two consecutive iterates.

Finally, the $1-2\delta$ confidence interval for $\mu$, given $\boldsymbol{\ell}$, is obtained through the cumulative distribution

$$G(t|\boldsymbol{\ell}) = \int_{-\infty}^{t} P(\mu|\boldsymbol{\ell})\,d\mu. \tag{2.38}$$

The extremes of the confidence interval $[t_1,t_2]$ are obtained by solving $G(t_1|\boldsymbol{\ell}) = \delta$, $G(t_2|\boldsymbol{\ell}) = 1-\delta$. Notice that $G(t|\boldsymbol{\ell})$ can be obtained as

$$G(t|\boldsymbol{\ell}) = \begin{cases} \dfrac{F_\infty(L_1) - F_{-t}(L_1)}{F_\infty(L_1)+F_\infty(L_2)}, & t<0, \\ \dfrac{F_\infty(L_1)+F_t(L_2)}{F_\infty(L_1)+F_\infty(L_2)}, & t\geqslant 0. \end{cases} \tag{2.39}$$

The results presented in this chapter consider $\delta = 0.025$ (95% confidence interval). To compute these integrals for finite values of $t$ we use the function `quad` (`Python`). For $t\to\infty$ we evaluate them using a Gauss-Laguerre quadrature with 150 points. Overflows in (2.31) due to the exponentials are avoided by evaluating the logarithm of the integrand, and

the singularity at $\mu = 0$ is avoided by Taylor expanding $e^{-\mu r}$ and $e^{-\mu}$ up to third order. Likewise, the singularity at $\mu = 0$ of (2.26) is avoided by using the Taylor expansion $\chi_k \approx k/r + (k/2r)(e^{\mu} - 1)(k - r)$ for $|e^{\mu} - 1| \leq 10^{-6}$. The extremes of the confidence interval $[t_1, t_2]$ are then obtained by solving $G(t_1|\boldsymbol{\ell}) = \delta$ and $G(t_2|\boldsymbol{\ell}) = 1 - \delta$ —we use again the function `fsolve` with tolerance $10^{-6}$.

### 2.2.2 Standard regime

We begin analysing data from a group of students from a major Middle Eastern university (Almaatouq et al., 2016). In this survey, 84 students (60% female and 40% male) volunteered to participate. Each participant was presented with a list of the other 83 participants, and was asked about his/her relationship with each one of them. The question we are interested in was stated as follows: "How close are you to this person?" And the options were: "0- I do not know this person"; "1- I recognize this person but we never talked"; "2- Acquaintance (we talk or hang out sometimes)"; "3- Friend"; "4- Close Friend"; "5- One of my best friends". For each participant we store the number of answers of each type in an array ($\boldsymbol{\ell} = (\ell_1, \ell_2, \ldots, \ell_6)$), so that $\ell_{6-k}$ is the number of type $k$ answers. These numbers are our representation of the layers. For the analysis we present here we excluded the cases scored with either 0 (no relation whatsoever) or 1 [3]. The latter are excluded for two reasons: (a) recognising someone but having never talked with them hardly counts as a meaningful relationship; (b) there surely are other people outside this sample that the surveyed subjects recognise but never talked to, but are not part of the survey[4] (limited to the 84 students).

The results are summarised in Fig. 2.3. Most individuals ($\sim 98\%$) have a value of $\mu > 0$, meaning that their circles show the standard structure (Fig. 2.3b), as expected. These values of $\mu$ (Fig. 2.3a) are grouped around a central value $\mu = 0.978$, corresponding to a scaling ratio of $x \equiv e^{\mu} = 2.66$

[3] Also, the model presents singularities when all the relationships happen to be in either the first layer (then $f(\mu) = 0$, which holds for $\mu \to -\infty$) or the last layer (then $f(\mu) = 1$, which holds for $\mu \to +\infty$). The data from this survey includes one individual (id 80) with this sort of structure, so we excluded this datum from our analysis.

[4] For completeness, in Appendix A.2 we show a complete set of figures considering also these answers. The results are similar.

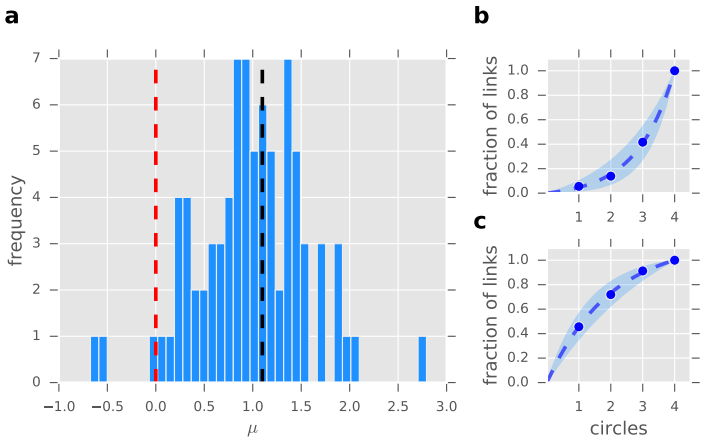


**Figure 2.3: Summary of the results for the community of students. a,** Distribution of the parameter estimates for the community of students ($n = 83$). The black, dashed line indicates the typically observed scaling ratio $e^{\mu} = 3$ ($\mu = 1.099$). The red, dashed line marks the change of regime $\mu = 0$. In the analysis of the community of students we did not take into account the scores 0 and 1. We also excluded one individual who had no alters in the considered layers (see section 2.2.2). **b,** Representative fitting for an individual exhibiting the standard regime, with layers $\boldsymbol{\ell} = (2, 3, 10, 21)$ and estimated parameter $\mu = 0.846$. Solid dots represent experimental data, blue dashed lines represent the graph of equation (2.26) with the corresponding estimated parameter, and shaded regions show the 95% confidence interval for that estimate (see section 2.2.1). **c,** Representative fitting for an individual exhibiting the inverse regime, with layers $\boldsymbol{\ell} = (26, 15, 11, 5)$ and estimated parameter $\mu = -0.503$. Solid dots, blue dashed lines, and shaded regions have the same interpretation as in **b**. A comprehensive set of figures, including fittings for every subject, is available in Appendix A.2.

(3.13 if we average the $x$'s instead), in agreement with previous studies (Hill and Dunbar, 2003; Dunbar et al., 2015; Zhou et al., 2005; Mac Carron et al., 2016). However, the data also allow us to detect a small proportion ($\sim 2\%$) of individuals whose networks lie within the inverse regime (Fig. 2.3c).

### 2.2.3 Inverse regime

In order to elicit the inverse regime we focus on four different communities of immigrants.The first derives from a sociological study conducted in 2008 in Roses (Mestres et al., 2012), a small town of about 20 000 inhabitants in Girona (Catalonia, Spain). This study sampled ($n = 25$) personal networks within a community of approximately 80 Bulgarian immigrants. The remaining three derive from a different study carried out in Barcelona (Catalonia, Spain) (Molina et al., 2015; Molina and Pelissier, 2010). In this case, the focal groups were communities of Chinese (sampled $n = 21$), Sikh ($n = 24$), and Filipino immigrants ($n = 25$), each numbering some thousands of individuals. As we shall see below, even though the total size of these communities is much larger than in the case of the Bulgarians, their idiosyncrasy and the way they are formed strongly endorse the idea that their individuals also count on limited options to create relationships.

The data were collected in a similar way between November 2008 and April 2009 in all four immigrant studies, using the open source software *EgoNet*[5]. In the case of the Bulgarians, the following name generator was used (Mestres et al., 2012): "Tell us about 30 people who you know on a first name basis, with whom you have had contact in at least the last two years and who you could contact again if necessary. It is important that all categories of contacts (family, friends, workmates [...]) be represented". For the remaining three communities, the name generator was (Molina et al., 2015; Molina and Pelissier, 2010): "Tell us 30 people you know by name, and vice versa. It can be everyone. Try to mention people important for you, but also other people not so close but whom you meet frequently. Try to use pseudonyms, but be sure you can recognize them later." In both cases each participant rated the perceived closeness of their relationship with each alter. The options were: "1- Not close at all"; "2- Not very close"; "3- Quite close"; "4- Close"; "5- Very close". With this information we create an array as before. This kind of generators tends to elicit strong links at the beginning, but the list is long enough to gather information from other types of relationships, including weak links

[5] "EgoNet", *Sourceforge*, last accessed 21 December 2018 `https://sourceforge.net/projects/egonet/`

(Molina and Pelissier, 2010). Thus, this methodology would be able to capture either the standard or the inverse regimes.

Although there are differences among the sampled groups, all of them belong to well differentiated communities within their respective social environments, which tend to use and preserve their native languages and traditions, and form a support network for their members. Indeed, one of the main mechanisms for the formation of these communities is that the individuals already settled in the hosting location serve as links for those yet to come. This process facilitates the integration of the newcomers in the host country in terms of professional and housing opportunities, among others (see (Mestres et al., 2012; Molina et al., 2015; Molina and Pelissier, 2010)). All these facts suggest that these communities form independent, smallscale social environments within their places of residence—hence perfect candidates for the context in which an inverse regime might hold.

Figure 2.4 summarises our results for these communities. Remarkably, 75% of the networks analysed lie within the inverse regime with $\mu < 0$, confirming our hypothesis. Furthermore, the remaining 25% present values of $\mu$ very close to 0, significantly lower than in the case of the community of students (compare Figs. 2.3 and 2.4).

The case of the Bulgarians (Figs. 2.4A and 2.4a) is particularly striking since this percentage goes up to 96% of the networks. As noted before, this sample was taken from a community of only about 80 individuals, a small population by any standards. Indeed, the researchers of the original study (Mestres et al., 2012) concluded that the context of Roses allowed the community to form a denser and more homogeneous ethnic network than in larger towns (i.e. Barcelona).

The Sikhs (Figs. 2.4B and 2.4b) and the Chinese (Fig. 2.4C and 2.4c) show similar percentages, 88% and 86% respectively, whereas for the Filipino community (Figs. 2.4D and 2.4d) this number is significantly lower (68%). These differences might be a consequence of a number of sociological and cultural factors that we shall not discuss here (see (Mestres et al., 2012; Molina et al., 2015; Molina and Pelissier, 2010) and Appendix A.1 for details). In either case, our results suggest that the subjective number of available contacts is in fact smaller than average in all the communities, resulting in a predominance of inverted personal networks. It is important to stress that the type of structure that was predicted, hierarchical inclusive

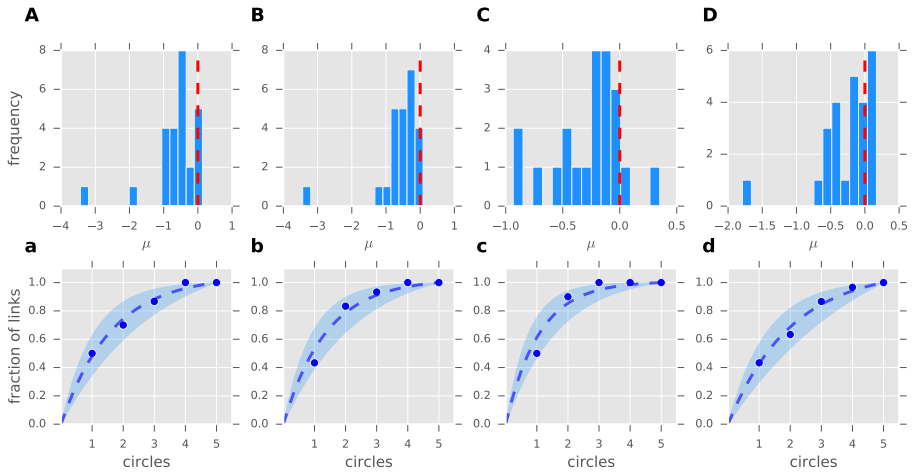


**Figure 2.4: Summary of the results for the communities of immigrants.** Upper panels show the distributions of the parameter estimates for the communities of immigrants. The red, dashed lines mark the change of regime (i.e. $\mu = 0$). **A,** Distribution of the parameter estimates for the community of Bulgarians ($n = 25$). **B,** Distribution of the parameter estimates for the community of Sikhs ($n = 24$). **C,** Distribution of the parameter estimates for the community of Chinese ($n = 21$). **D,** Distribution of the parameter estimates for the community of Filipino ($n = 25$). Lower panels show representative examples of fittings for individuals in each community. Solid dots represent experimental data, blue dashed lines represent the graph of $(2.26)$ with the corresponding estimated parameter, and shaded regions show the 95% confidence interval for that estimate (see section 2.2.1). **a,** Example of fitting for an individual in the community of Bulgarians with layers $\boldsymbol{\ell} = (15,6,5,4,0)$ and $\mu = -0.616$. **b,** Example of fitting for an individual in the community of Sikhs with layers $\boldsymbol{\ell} = (13,12,3,2,0)$ and $\mu = -0.727$. **c,** Example of fitting for an individual in the community of Chinese with layers $\boldsymbol{\ell} = (15,12,3,0,0)$ and $\mu = -0.934$. **d,** Example of fitting for an individual in the community of Filipino with layers $\boldsymbol{\ell} = (13,6,7,3,1)$ and $\mu = -0.496$. A comprehensive set of figures, including fittings for every subject, is available in Appendix A.2.

layers of increasing intensity with increasing size, had been so far only anecdotally suggested in the literature (Bernard and Killworth, 1973; Granovetter, 1977).

## 2.3 Discussion

One possible criticism of these results is that they may be an artifact of the way the questions are posed in the surveys—people are usually asked to classify their relationships in predefined categories. However, as we described in Section 1.1, other approaches used in the literature yield much the same pattern in different types of data sets: online social networks such as those based on Twitter or Facebook as well as those based on phone calls (Dunbar et al., 2015; Mac Carron et al., 2016) show exactly the same layered organisation as we find in self-rated questionnaire-based ratings (Hill and Dunbar, 2003; Sutcliffe et al., 2012; Zhou et al., 2005).

Another possible criticism could be that the data we used in our empirical validation was obtained using different methodologies. Nevertheless, there are examples in the literature that suggest that the influence of the different protocols is not significant. Studies with larger source populations (i.e. more choices available) (Powell et al., 2012; Dunbar and Spoors, 1995) have shown that, even when using an open-ended method, individuals only list about 10-30 people, and the structure found was still the standard regime. This is because imposing a cut-off on a standard network does not change it into an inverse structure: this is clear from Fig. 2.3b where a cut-off at, say, layer 2 or 3 would not change the form of the distribution into that shown in Fig. 2.3c (see also the examples given by (Saramäki et al., 2014)). Notice that the name generator used with the groups of immigrants had a limit of 30 names, and we nonetheless found both standard and inverse regimes. Additionally, the data reported in the shipboard survey mentioned above (Bernard and Killworth, 1973), where individuals living in a boat were asked about their relationships with other members of the expedition (a protocol similar to that employed with the community of students that we use in this paper), suggest average sizes of 14.6 and 26.7 individuals for the first and second circles respectively, much as would be expected for an inverse regime. The inverse regime is precisely what we would have expected to emerge in this setting. Therefore, although further studies should investigate the impact of different protocols, there is no a priori reason to suppose that either methodology would bias the results in any particular direction.

Notice that all distributions (see Fig. 2.3a and the upper panels in Fig. 2.4) show a large dispersion, implying that the structure of circles is quite personal (and depends, among other things, on the individual's number of links). This confirms an earlier empirical finding suggesting that individuals allocate their social effort in quite different and consistent ways, such that each is characterised by a kind of "social signature" (Saramäki et al., 2014). In fact, taking both results together, the parameter of our model may serve as a quantitative characterization of such a fingerprint—we explore this phenomenon in more detail in the next chapter.

It may be surprising that there are individuals whose ego-networks show an organisation opposite to what is typical in their contexts. There are several reasons why this might be so, all of which derive from the fact that the potential size of the ego-network is constrained. As such, these are predictions of the model that could be tested. One is that an individual's cognitive capacity (the ability to manage many relationships, which is a function of an individual's brain size (Powell et al., 2012; Kanai et al., 2012; Kwak et al., 2018) or intellectual ability (Dunbar, 2015) or the time costs of investment in ties (Oswald et al., 2004; Pollet et al., 2013)) are limited or because the available population is small (for geographical or, as in the case our immigrant samples, social reasons). As we saw in section 1.1, network size might also vary with personality differences. Introverts, for example, typically have significantly smaller ego-centric social networks than extraverts (Pollet et al., 2011). In such cases, introverts have smaller but emotionally more intense relationships on average than extraverts, or those with large networks, who seem to spread their available cognitive capital more thinly (Pollet et al., 2011; Roberts et al., 2009). This seems to be due to a constraint on available social time that applies across all individuals (Miritello et al., 2013).

Additionally, our model predicts how the increasing availability of online social networks may affect the way we handle our relationships. Since these technologies reduce the effective cost of maintaining some relationships, it should be easier for individuals to establish larger networks and this should promote the standard regime. However, if online relationships are cheaper to maintain because they obviate the costly business of physically meeting up with an alter (Pollet et al., 2013), it follows that any increase in online network size will be associated with a reduction in average

tie strength. This would incentivise weak relationships, which might well be another reason why the inverse regime has remained largely unnoticed until now—see next Chapter.

Lastly, from a socio-centric perspective, our model suggests a way to identify whether an interconnected set of individuals (i.e. a community in the technical network analysis sense) is "small" or not, namely according to the regime of their ego networks. Consider as a reference a layered structure $\boldsymbol{\ell} = (5, 10, 35, 100)$ (giving the typical structure of circles: 5, 15, 50, 150), and an arbitrary linear decrease in the costs. In such setting we find that the change of regime happens at a network size of 88, and that there is a maximum network size of 220 (a value close to the maximum observed network size of $\sim 250$ (Hill and Dunbar, 2003; Pollet et al., 2011)). We also find that communities with sizes less than or equal to 55 members will have most of their contacts in the inner circle (thus, forming an absolutely cohesive group). This latter finding is of particular interest, because groupings of $\sim 50$ occur frequently in small scale traditional societies: this is the typical size of huntergatherer bands (overnight camp groups), a grouping of special functional importance in terms of foraging and protection against predators (Lehmann et al., 2014). It also represents the primary functional social grouping in personal social networks, being the set of alters to whom an Ego devotes most of his social time and effort (Sutcliffe et al., 2012; Roberts et al., 2009). More interestingly, perhaps, communities built up on a mixture of the two regimes might exhibit quite different properties from the socio-centric point of view. They might also gell less well and hence be less stable. Exploring these differences may shed light, for instance, into our understanding of the internal structure of human societies and the reasons why natural communities fission when they do (Dunbar and Sosis, 2018).

## 2.4 Conclusions

We introduce a simple model of how individuals manage their relationships which depends only on the individual and his/her environment and not on the links among his/her alters (see Fig. 2.2 for an schematic representation of the model). Individuals are the ultimate constituents of any social system, so the mathematical description we provide is a suitable rep-

resentation of a social atom. The model naturally reproduces the layered structure of personal social networks in which each successive layer includes disproportionately more alters, and reveals an unexpected finding, namely, that in a proportion of cases an inverse structure emerged in which more alters are found in the inner layers. These inverse structure networks are associated with smaller than usual networks, and seen to imply that individuals have a (more or less) fixed quantity of cognitive capital (indexed as time available for investing in alters) which they can either spread thinly among many alters or thickly among fewer alters.

More importantly, perhaps, our model unveils the nature of the pervasive scaling between consecutive layers that we described in section 1.1. We can now affirm, mathematically, that: when individuals handle a fixed number of relationships (on average) (Hill and Dunbar, 2003; Saramäki et al., 2014; Wang et al., 2016), which are not equally costly (Oswald et al., 2004; Sutcliffe et al., 2012), and they have a constrained capacity (on average) to manage them (Dunbar, 1993; Miritello et al., 2013), then the most likely organisation of these relationships (dictated by the maximum entropy principle) exhibits a constant scaling (Zhou et al., 2005; Hamilton et al., 2007; Dunbar et al., 2015)—given the particular ratio $\mathcal{S}/\mathcal{L}$ for humans. Our results strongly support the SBH by mathematically connecting two of its most contrasted empirical facts, namely 'Dunbar's number' ($\mathcal{L}$, which arises from cognitive constraints) and the hierarchical organisation of personal networks.

# 3

# A continuous interpretation of the social atom

To infinity and beyond!

*Buzz Lightyear*
Toy Story (1995)

The model we introduced in Chapter 2 represented relationships as discrete categories according to their intensity. In physics, atoms have a similar discretisation in the energy levels (layers in the social version) at which electrons (alters) can orbit around nuclei (egos). This is due to the very nature of energy, which can only be exchanged through discrete packages called quanta. In the case of the social atom, however, this was just a modelling decision. In this chapter we build on the discrete version of the model and create a variant in which ties are classified in a continuum; the layers are no longer needed. The two structural regimes obtained when there are discrete layers also arise in this version which, importantly, relies on the same principles.

## 3.1 Model description

In section 2.1, relationships could only belong to a set of $r$ discrete categories (layers) that were defined based on their intensity. This approach is particularly convenient when such intensity is measured in Likert scales, as it is often the case when data is obtained via questionnaires—see section 2.2. However, there are alternative ways of measuring tie strength which do not rely on a discrete scale. Good examples are frequency of contact (Roberts et al., 2009), time spent together (Mastrandrea et al., 2015), or number of messages (information) exchanged (Saramäki et al., 2014; Dunbar et al., 2015). Even though some of these quantities could be technically regarded as discrete, the fact that they consist of hugely many possibilities makes this viewpoint rather unpractical. More importantly, these measures do not have clear maxima and minima to play the role of the first and last layers, respectively. This calls for a generalisation of the model to make it capable of dealing with a continuum of tie strengths.

Our goal is to build a model similar to the one we introduced in Chapter 2 but in which the intensity of the relationships is captured by any (positive) real number instead of a discrete set of layers. Generally speaking, an excellent way to obtain such a continuous model is to develop a discrete version first and then, at the right time, take the appropriate limits (Jaynes, 2003; Sivia and Skilling, 2006). Consequently, our starting point will be the posterior distribution found in section 2.1 (equation 2.17 ),

$$P(\boldsymbol{\ell}|\mathcal{S},\mathcal{L},N) = \mathscr{B}(L,\mathcal{L}/N,N)\binom{L}{\boldsymbol{\ell}}\frac{e^{-\hat{\mu}\sum_k s_k\ell_k}}{\left(\sum_k e^{-\hat{\mu}s_k}\right)^L},$$

which, assuming that costs vary linearly, could be written as (equation 2.27)

$$P(\boldsymbol{\ell}|\mathcal{L},\mu,N) = \mathscr{B}(L,\mathcal{L}/(N-1),N-1)\left(\frac{e^{\mu}-1}{e^{\mu r}-1}\right)^L\binom{L}{\boldsymbol{\ell}}e^{\mu L_1},$$

with $\mu \equiv \hat{\mu}(s_{max}-s_{min})/(r-1)$, $L=\sum_{k=1}^{r}\ell_k$, and $L_1=\sum_{k=0}^{r-1}k\ell_{k+1}$.

We can modify this model into one with a continuum of layers by considering $r\to\infty$, so that the relationships are now labelled by a continuous index $t\equiv(k-1)/(r-1)\in[0,1]$. Notice that $t=0$ corresponds to $s_{max}$ and

$t = 1$ to $s_{min}$, so the parameter $t$ can be interpreted as a measure of distance to the ego. The transformation $r\ell_k \sim \ell(t)$ changes $\ell_k$ into a density of links $\ell(t)\,dt$. Hence,

$$L \to \lim_{r\to\infty} \sum_{k=1}^{r} \ell_k = \int_0^1 \ell(t)\,dt \equiv \tilde{L}, \tag{3.1}$$

and

$$\mu L_1 \to \mu \lim_{r\to\infty} \sum_{k=0}^{r-1} k\ell_{k+1} = \eta \int_0^1 t\ell(t)\,dt \equiv \eta\tilde{L}_1. \tag{3.2}$$

where $\eta \equiv \mu(r-1)$. Moreover, when the number of layers $r$ is large, the probability that two individuals coexist in the same layer goes to zero, so $\ell_k$ would be either 0 or 1 for all $k$. Noticing this we can write $\binom{L}{\boldsymbol{\ell}} = L!$.

Although the above approach is entirely valid, taking the limit on eq. 2.27 results in a cumbersome expression—more technically, in a distribution of path integrals. The way to overcome this complication is to take the limit elsewhere (Jaynes, 2003). Actually, our main objective is to find an expression for the expected value of the number of alters with whom an ego has a relationship of intensity $t$ (the equivalent in the continuum to equations 2.25 and 2.26), and a way to properly fit the model to experimental data, $\ell(t)$. As we show below, we can achieve this goal without having to deal with a continuous version of equation 2.27.

### 3.1.1 A continuum of circles

When considering a discrete number of layers we found that the expected fraction of links in layer $k$ was given by eq. 2.25

$$\epsilon_k = \frac{e^{k\mu} - e^{(k-1)\mu}}{e^{r\mu} - 1},$$

and, consequently, the fraction of links in circle $k$ (eq. 2.26) was

$$\chi_k = \frac{e^{k\mu} - 1}{e^{r\mu} - 1}.$$

Taking the limit $r \to \infty$ transforms these expresions into

$$\epsilon_k \to \epsilon(t)\,dt = \frac{\eta e^{\eta t}}{e^{\eta} - 1}\,dt, \tag{3.3}$$

and

$$\chi_k \to \chi(t) = \frac{e^{\eta t} - 1}{e^{\eta} - 1}, \tag{3.4}$$

respectively.

As it can be readily noticed, these expressions are the continuous equivalent to those in the discrete case. In particular, $\chi(t)$ (eq. 3.4) is the cumulative distribution of the fraction of links with whom an ego has a relationship with proximity less or equal than $t$, that is, a continuous interpretation of the circles. In order to analyse its scaling properties, we compute the logarithmic derivative

$$\frac{\dot{\chi}(t)}{\chi(t)} = \frac{\eta e^{\eta t}}{e^{\eta t} - 1}, \tag{3.5}$$

which asymptotically behaves as

$$\frac{\dot{\chi}(t)}{\chi(t)} \approx \eta \quad (\eta \to \infty), \tag{3.6}$$

$$\frac{\dot{\chi}(t)}{\chi(t)} \approx 0 \quad (\eta \to -\infty). \tag{3.7}$$

Therefore, for large, positive values of $\eta$ we obtain that $\chi(t+dt)/\chi(t) \approx e^{\eta\, dt}$. Recall that in the discrete version of the model we found that $\chi_{k+1}/\chi_k \approx e^{\mu}$, for large, positive values of $\mu$—see section 2.1.3. To compare these two results, notice that if we now discretise the continuum version we have that $dt \approx 1/(r-1)$ (the distance between consecutive layers), so that $e^{\eta\, dt} \approx e^{\eta/(r-1)} \equiv e^{\mu}$. Hence, the results are equivalent, but, contrary to what happened in the discrete case, this scaling does not depend on any particular choice of $r$—a clear advantage of its continuous counterpart. However, since $\eta$ is only defined for $r \to \infty$ the particular values of $\mu$ and $\eta$ are not directly comparable. A (very) rough estimate of how both parameter compare can be achieved by considering $1 + \eta d\, t \approx e^{\mu}$, which leads to $\eta \approx (r-1)(e^{\mu} - 1)$. Since the typical scaling found in discrete settings with $r = 4$ is about $e^{\mu} \approx 3$ (see section 1.1 and (Dunbar et al., 2015)), then we should expect $\eta \approx 6$ in continous settings—or at least something in that order of magnitude.

On the other hand, when the parameter takes large, negative values, we have that $\dot{\chi}(t) \approx 0$. Since $\chi(t)$ is a cumulative distribution this result implies that $\chi(t) \approx \chi(0) = 1$, so all relationships happen to have maximum

intensity—or, equivalently, maximum closeness to the ego. Hence, the two regimes persist although there are no longer any layers, and the parameter $\eta$ has a similar interpretation as $\mu$ had in the discrete case. Indeed, in section 2.1.3 we showed that the parameter $\mu$ and the ratio $\sigma = \mathcal{S}/\mathcal{L}$ were connected through equation (2.23)

$$\frac{s_{max} - \sigma}{s_{max} - s_{min}} = e^{\mu} \frac{(r-1)e^{r\mu} - re^{(r-1)\mu} + 1}{(r-1)(e^{r\mu} - 1)(e^{\mu} - 1)} \equiv f(\mu).$$

Now, in the continuum limit, this expression becomes

$$\frac{s_{\max} - \sigma}{s_{\max} - s_{\min}} = \frac{e^{\eta}}{e^{\eta} - 1} - \frac{1}{\eta} \equiv g(\eta), \tag{3.8}$$

and connects $\eta$ and $\sigma$ similarly. Notice that,

$$\lim_{\eta \to -\infty} g(\eta) = 0, \qquad \lim_{\eta \to 0} g(\eta) = \frac{1}{2}, \qquad \lim_{\eta \to +\infty} g(\eta) = 1,$$

and $g'(\eta) > 0$ (for all $\eta \in \mathbb{R}$), so equation (3.8) has a unique solution for $s_{\min} \leqslant \sigma \leqslant s_{\max}$. Small values of $\sigma$ lead to solutions with $\eta > 0$ and correspond to the standard regime, whereas, when $\sigma$ is large, the solutions are $\eta < 0$ and correspond to the inverse one.

## 3.2 Data analysis

As we showed in the previous section, it is possible to build a model based on the same principles as the one introduced in Chapter 1, but able to fit continuous data. In this section we illustrate this by using data from phone calls (Saramäki et al., 2014), face-to-face contacts (Isella et al., 2011), and interactions between Facebook users (Arnaboldi et al., 2012). Before that, let us describe in detail how the fits are made[1].

### 3.2.1 Bayesian estimate of the parameter in the continuum case

Similarly to what we did in section 2.2.1, our goal is to determine $P(\mathcal{L}, \eta | \ell(t), N)$ using Bayesian inference. We follow the same strategy as

[1] All numerical analyses are carried out in `Python` with the packages `scipy.optimize` and `scipy.integrate` (see the documentation for details).

before and start off from the expressions we obtained in the discrete case (eq. 2.35), where $P(\mathcal{L},\mu|\boldsymbol{\ell},N) = P(\mathcal{L}|\boldsymbol{\ell},N)P(\mu|\boldsymbol{\ell})$ with

$$P(\mathcal{L}|\boldsymbol{\ell},N) = N\mathscr{B}(L,\mathcal{L}/(N-1),N-1),$$
$$P(\mu|\boldsymbol{\ell}) \propto \left(\frac{e^{\mu}-1}{e^{\mu r}-1}\right)^{L} e^{\mu L_1}.$$

In the limit $r \to \infty$, we can use the expressions 3.1 and 3.2 to obtain the new distribution

$$P(\mathcal{L},\eta|\tilde{L},\tilde{L}_1,N) = \frac{N}{N-1}\mathscr{B}(\tilde{L},\mathcal{L}/(N-1),N-1)P(\eta|\tilde{L},\tilde{L}_1), \tag{3.9}$$

where

$$P(\eta|\tilde{L},\tilde{L}_1) = \Omega(\tilde{L},\tilde{L}_1)^{-1}\left(\frac{\eta}{e^{\eta}-1}\right)^{\tilde{L}} e^{\eta\tilde{L}_1}, \tag{3.10}$$

and

$$\Omega(\tilde{L},\tilde{L}_1) \equiv \int_{-\infty}^{\infty}\left(\frac{\eta}{e^{\eta}-1}\right)^{\tilde{L}} e^{\eta\tilde{L}_1}\,d\eta. \tag{3.11}$$

The equation 3.10 represents a well-defined, tractable distribution that enables us to find the value of $\eta$ given some data—thus, fully characterising eqs 3.3 and 3.4. Therefore, as anticipated, we do not need to deal with a continuous version of eq. 2.27 at all. Additionally, in the notation of this posterior distribution we have made clear the fact that conditioning is not on $\ell(t)$ itself, but simply on the two integrals

$$\tilde{L} = \int_0^1 \ell(t), \quad \tilde{L}_1 = \int_0^1 t\ell(t)\,dt. \tag{3.12}$$

The maximum likelihood estimate for $\mathcal{L}$ is given by $\mathcal{L} = \tilde{L}$, and differentiating

$$\log P(\eta|\tilde{L},\tilde{L}_1) = \tilde{L}\left[\log\eta - \log(e^{\eta}-1) + \eta\frac{\tilde{L}_1}{\tilde{L}}\right] - \log\Omega(\tilde{L},\tilde{L}_1) \tag{3.13}$$

with respect to $\eta$ we obtain the corresponding one for $\eta$

$$\frac{\tilde{L}_1}{\tilde{L}} = \frac{e^{\eta}}{e^{\eta}-1} - \frac{1}{\eta}, \tag{3.14}$$

which, compared to eq. (3.8), provides the interpretation

$$g(\eta) = \frac{s_{\max} - \sigma}{s_{\max} - s_{\min}} = \frac{\tilde{L}_1}{\tilde{L}}. \tag{3.15}$$

The above equation 3.15 enables us to estimate the value of the parameter given empirical data. However, let us remark that the values of $s_{max}$ and $s_{min}$ must be now determined using information external to the problem, an issue that was not present when we considered a discrete set of layers—see Chapter 2, section 2.1. Recall that $s_{max}$ defines the maximum possible intensity of a relationship, whereas $s_{min}$ defines the minimum intensity necessary to consider that there is a relationship whatsoever. That is, these values establish the scale with which to measure the strength of relationships. When we considered a discrete setting, fixing the number of layers $r$ and assuming that the intensities (costs) vary linearly was enough to have such a scale—the price to be paid was the dependence of the model on the number of layers. However, in a setting with no layers this scale must be imposed via $s_{min}$ and $s_{max}$. Therefore, to fit the continuous variant, we first need to (externally) determine what $s_{max}$ and $s_{min}$ are for each individual. Once this is done, we can use the transformation $t_i = (s_{max} - s_i)/(s_{max} - s_{min})$ ($\in [0, 1]$) to find $\ell(t_i)$, and solve eq. 3.15 numerically to get the maximum likelihood estimate for $\eta$. For the results we introduce in this chapter we use the function `fsolve` (`Python`) (with tolerance $10^{-6}$) to that end—as we did in the previous chapter.

The way to compute the confidence intervals for the parameter estimate is equivalent to what we described in section 2.2.1. If we introduce the function

$$\Phi(R) \equiv \int_0^t \left(\frac{\eta}{1 - e^{-\eta}}\right)^{\tilde{L}} e^{-R\eta}\, d\eta, \tag{3.16}$$

then the $1 - 2\delta$ confidence interval for $\eta$, given $\tilde{L}$ and $\tilde{L}_1$, is obtained through the cumulative distribution

$$\Gamma(t|\tilde{L}, \tilde{L}_1) = \int_{-\infty}^{t} P(\eta|\tilde{L}, \tilde{L}_1)\, d\eta. \tag{3.17}$$

More precisely, the confidence interval is $[t_1, t_2]$, where $\Gamma(t_1|\tilde{L}, \tilde{L}_1) = \delta$, $\Gamma(t_2|\tilde{L}, \tilde{L}_1) = 1 - \delta$, and $\Gamma(t|\tilde{L}, \tilde{L}_1)$ can be obtained as

$$\Gamma(t|\tilde{L}, \tilde{L}_1) = \begin{cases} \dfrac{\Phi_\infty(\tilde{L}_1) - \Phi_{-t}(\tilde{L}_1)}{\Phi_\infty(\tilde{L}_1) + \Phi_\infty(\tilde{L} - \tilde{L}_1)}, & t < 0, \\ \dfrac{\Phi_\infty(\tilde{L}_1) + \Phi_t(\tilde{L} - \tilde{L}_1)}{\Phi_\infty(\tilde{L}_1) + \Phi_\infty(\tilde{L} - \tilde{L}_1)}, & t \geqslant 0. \end{cases} \tag{3.18}$$

All the results we present in this chapter consider $\delta = 0.025$ (95% confidence interval), and are found numerically following the exact same procedure we described at the end of section 2.2.1.

### 3.2.2 Mobile phones dataset

The first dataset that we analyse corresponds to the one used by Saramäki et al. (2014)[2], and contains the phone activity of 24 individuals during 18 months. At the beginning of the study, all participants (12 males, 12 females, ages 17-19) were in their final year of secondary school, so that about six months later they transitioned into either University (18 of them) or labour market. The data from the phones (which were given for free to the participants together with 500 free monthly voice minutes and unlimited text messages) were complemented with three questionnaires, one at the beginning of the study, another one at month 9, and a last one at month 18. With this information, the authors were able to merge phone numbers that belonged to the same person, and, most importantly, to conclude that the number of calls was a reliable estimate of the emotional closeness of the relationships—see (Saramäki et al., 2014) for details.

Saramäki et al. (2014) studied the communication patterns of the participants by dividing the dataset into three time intervals ($T_1, T_2,$ and $T_3$) of six months each. For each time interval, they counted the number of calls from each ego to each alter and subsequently ranked the latter based on this number. Then, the fraction of calls as a function of this rank is used as a representation of the communication pattern of the ego. The main result of their study is that, even though the composition of personal networks varies considerably over time, these patterns are consistent across

[2]The data were originally collected for another study by Roberts and Dunbar (2011b).

the different time windows. They named these patterns *social signatures* and conjectured that they were likely a consequence of a constraint on the available resources (time and cognitive skills) necessary to manage relationships.

To analyse the data we first aggregate them into the same time windows used by Saramäki et al. (2014), so that we end up with a list (per time window) of pairs $(a_i, N_i)$ for each ego, where $a_i$ is a given alter and $N_i$ is the total number of calls made to that alter. As we explained in section 3.2.1, prior to fitting the model we need to determine what $s_{min}$ and $s_{max}$ are for each participant (at each time window). To that end, we first select the minimum and the maximum number of calls each ego made on each month to any alter. Then, the $s_{min}$ for each of the time windows is computed as the sum of the monthly minima and, similarly, the $s_{max}$ is computed as the sum of the maxima. The heuristics behind this decision is simple. If a person could make a maximum of $N_{max}$ phone calls (at a given month) to a given alter, it is reasonable to assume that the maximum number of calls he or she could have made to a single alter during the time window under consideration is given by the sum of the maximum number of monthly calls made in that same time interval to any person—and equivalently for $s_{min}$. Once we fix the values of $s_{min}$ and $s_{max}$, we filter out any interaction below $s_{min}$ and fit the model as explained in section 3.2.1.

Figure 3.1 summarises our results. As we can see in panels A-D, the distributions of the parameter estimates are centred around values in good agreement with the predicted $\eta \approx 6$—see section 3.2.1. Additionally, the model is able to capture individual's nuances (panels a-d), and the fittings are, generally speaking, strikingly good—see Appendix B.1.1 for a comprehensive set of figures, including fittings for every subject at every time window. Furthermore, we find a very high, significant correlation between the estimated parameter for each ego and the number of alters in his or her network ($\tilde{L}$). More precisely: $\eta^{T_1} \sim \tilde{L}^{T_1}$ ($r = 0.84, p < 10^{-6}$), $\eta^{T_2} \sim \tilde{L}^{T_2}$ ($r = 0.52, p < 10^{-3}$), $\eta^{T_3} \sim \tilde{L}^{T3}$ ($r = 0.81, p < 10^{-5}$) and $\eta^{T_1 \cup T_2 \cup T_3} \sim \tilde{L}^{T_1 \cup T_2 \cup T_3}$ ($r = 0.83, p < 10^{-6}$)—Pearson's $r$ coefficients, 2-tailed tests. This fact further endorses the claim that the amount of resource available to form relationships is a seemingly fixed quantity that individuals spread according to the maximum entropy principle (Tamarit et al., 2018).

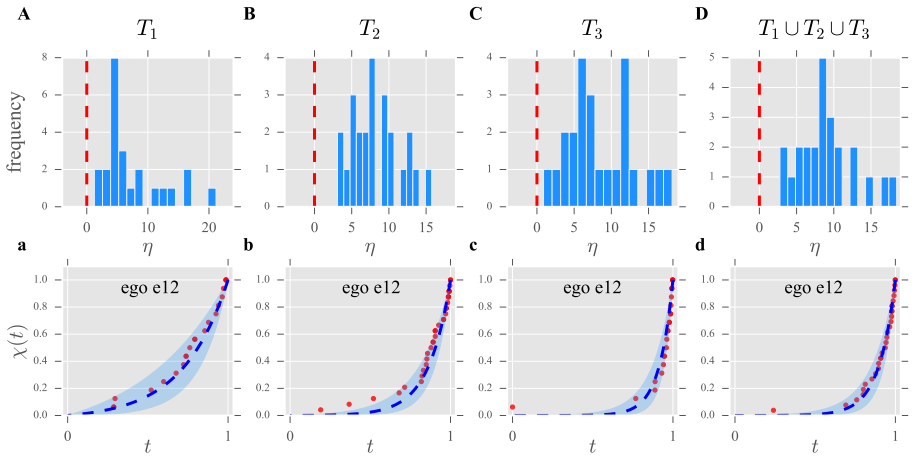


**Figure 3.1: Summary of the results for the mobile phones dataset.** Upper panels show the distributions of the parameter estimates for the different time windows—see section 3.2.2 for details. The red, dashed lines mark the change of regime (i.e. $\eta = 0$). **A,** Distribution of the parameter estimates for the first time window (months 1-6); $mean = 7.52$, $median = 5.32$, $std = 5.07$. **B,** Distribution of the parameter estimates for the second time window (months 6-12); $mean = 8.32$, $median = 8.00$, $std = 3.31$. **C,** Distribution of the parameter estimates for the second time window (months 12-18); $mean = 8.48$, $median = 7.00$, $std = 4.56$. **D,** Distribution of the parameter estimates for the full time window (months 1-18); $mean = 9.07$, $median = 8.75$, $std = 3.92$. Lower panels show the fittings for the same indvidual (ego "e12") at each of the time windows. Solid dots represent experimental data, blue dashed lines represent the graph of (3.4) with the corresponding estimated parameter, and shaded regions show the 95% confidence interval for that estimate (see section 3.2.1). **a,** Example of fitting for an individual ("e12") in the first time window. Estimated $\eta = 3.55$, 95% confidence interval $(1.82, 5.77)$, $\tilde{L} = 21$. **b,** Example of fitting for an individual ("e12") in the second time window. Estimated $\eta = 7.38$, 95% confidence interval $(5.18, 10.34)$, $\tilde{L} = 33$. **c,** Example of fitting for an individual ("e12") in the third time window. Estimated $\eta = 11.79$, 95% confidence interval $(7.87, 17.69)$, $\tilde{L} = 23$. **d,** Example of fitting for an individual ("e12") in the full time window. Estimated $\eta = 9.77$, 95% confidence interval $(6.83, 13.95)$, $\tilde{L} = 30$. A comprehensive set of figures, including fittings for every subject at all time windows, is available in Appendix B.1.1.

Lastly, we analyse if the parameter $\eta$ may serve as a quantitative characterisation of the social signatures—see also the discussion in section 2.3. In their paper, Saramäki et al. (2014) used the Jensen-Shannon divergence (JSD) (Lin, 1991) to measure the shape difference (distance) between signatures. Sticking to their notation, let $d_{ab}^{ij}$ denote the JSD distance between the signature of ego $i$ in time $a$ and ego $j$ in time $b$. They used this measure to compute the variation between the signatures of the same ego ($i$) in consecutive time windows as $d_{12}^{ii} \equiv d_{12}^{self}(i)$ and $d_{23}^{ii} \equiv d_{23}^{self}(i)$. For comparison, they also computed the reference distances $d_{22}^{ref}(i) = \frac{1}{N_{egos}-1}\sum_{j\neq i} d_{22}^{ij}$, and $d_{33}^{ref}(i) = \frac{1}{N_{egos}-1}\sum_{j\neq i} d_{33}^{ij}$ , and found that these reference distances were consistently higher than the ones between signatures of the same ego—see (Saramäki et al., 2014) for details.

We perform a parallel analysis using the relative change between two different values of $\eta$ as a measure of the "distance" between them. That is, keeping the notation used by Saramäki et al. (2014), we have that the self-distances are given by $d_{12}^{self}(i) \equiv \frac{|\eta_1^i - \eta_2^i|}{|\eta_1^i|}$, and $d_{23}^{self}(i) \equiv \frac{|\eta_2^i - \eta_3^i|}{|\eta_2^i|}$, whereas the reference distances are $d_{22}^{ref}(i) = \frac{1}{N_{egos}-1}\sum_{j\neq i} \frac{|\eta_2^i - \eta_2^j|}{|\eta_2^i|}$, and $d_{33}^{ref}(i) = \frac{1}{N_{egos}-1}\sum_{j\neq i} \frac{|\eta_3^i - \eta_3^j|}{|\eta_3^i|}$. Following (Saramäki et al., 2014), we then create a distribution of self-distances $d^{self} = \bigcup_i^{N_{egos}} \{d_{12}^{self}(i), d_{23}^{self}(i)\}$ and another of reference distances $d^{ref} = \bigcup_i^{N_{egos}} \{d_{22}^{ref}(i), d_{33}^{reff}(i)\}$—a total of 48 points per distribution.

In Fig. 3.2 we show the resulting distributions of the self-distances ($d^{self}$) and the reference ones ($d^{ref}$). The distribution $d^{ref}$ is again consistently higher than that of $d^{self}$—which is confirmed by a Mann-Whitney U test yielding $p < 10^{-3}$ (two-sided). Therefore, the different egos tend to have a persistent value of $\eta$ just like they have a persistent social signature. Given that the central premise of our model is that the resources available to create relationships are limited (see section 2.1), this result reinforces the conjecture made by Saramäki et al. (2014), that is, that the existence of social signatures is a consequence of this very constraint.

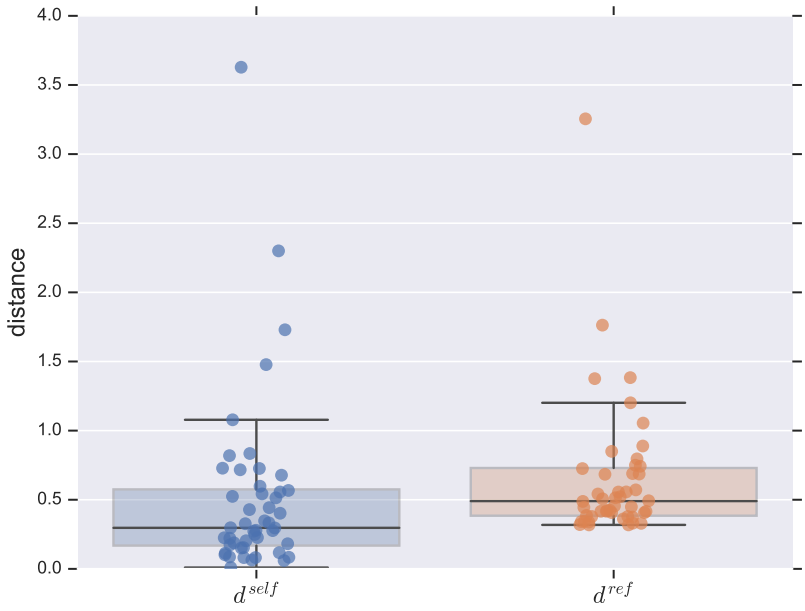


**Figure 3.2: Evidence of the persistence of $\eta$ through time windows.** The boxplot to the left (blue) shows the distribution of distances between the parameter estimates for the same individual at consecutive time intervals ($d^{self}$). The boxplot to the right (orange) shows the distribution of reference distances between the parameter estimate for each individual and the rest of the population ($d^{ref}$). In both cases, the solid dots represent the empirical points—*jittered* for a better visualisation. The distances in $d^{ref}$ are consistently higher than those in $d^{self}$, meaning that the individual's $\eta$ tends to be persistent across time intervals—see section 3.2.2 for details.

### 3.2.3 Face-to-face contacts dataset

In this section we analyse data[3] from face-to-face interactions that took place during a scientific conference[4] held in Turin, Italy, between June

[3]Downloaded from: "DATASET: Hypertext 2009 dynamic contact network", Sociopatterns, last accessed 24 January 2019, `http://www.sociopatterns.org/datasets/hypertext-2009-dynamic-contact-network/`.

[4]"Hypertext 2009: 20th ACM Conference on Hypertext and Hypermedia", last accessed 24 January 2019, `http://www.ht2009.org/`.

29th and July 1st in 2009 (Isella et al., 2011). The data were collected using proximity sensors that voluntary participants ($n = 111$, about 75% of the attendees) had embedded in their conference badges. The sensors recorded interactions over intervals of $20s$ when two or more participants were facing each other at less than about $1.5 - 2m$—see (Alani et al., 2009; Van den Broeck et al., 2010; Cattuto et al., 2010; Isella et al., 2011) for technical details. With this information, we can build the network of interactions for each participants using the time spent together as a proxy of the intensity of the implied relationships.

The high temporal resolution of the data permits us to characterise the values of $s_{min}$ and $s_{max}$ in several ways. One natural option is to aggregate the data over one day (Isella et al., 2011), and use a similar rule to the one we applied in section 3.2.2. That is, use the sum of the maximum time spent with any alter on each day as $s_{max}$, and the sum of the minima as $s_{min}$. However, during a conference, many different time restrictions may apply to the attendees, such as having an agenda of presentations to attend or deliver. As a consequence, the aforementioned heuristic may not apply here, since it is very likely the case that it was not entirely up to the participants with whom to spend their time at a given moment. Furthermore, we do not have any information on the interactions with the 25% of individuals who were at the venue but chose not to participate. These facts impose clear limitations to the conclusions we can draw from applying our model, and they are hardly avoidable. We, therefore, adopt a rather cautious position and do not aggregate the data on daily time windows. Instead, we simply take $s_{max}$ as the maximum time spent (and recorded) with one alter during the whole conference, and $s_{min}$ as the minimum one[5]. Additionally, we exclude all participants who had less than five alters in their networks, ending up with a total of 95 valid cases.

Our results (see Fig. 3.3a) show a long-tailed distribution for the parameter estimates with a clear peak close, once again, to the predicted $\eta \approx 6$, which suggests that the overall behaviour of the contact patterns seems to agree with our model.

[5]For completeness, in Appendix B.1.2 we show the results considering the same approach as in section 3.2.2 regarding $s_{max}$ and $s_{min}$. The individual fittings are slightly worse and the distribution of the parameter estimates is centred around a higher value $\eta \approx 14$.

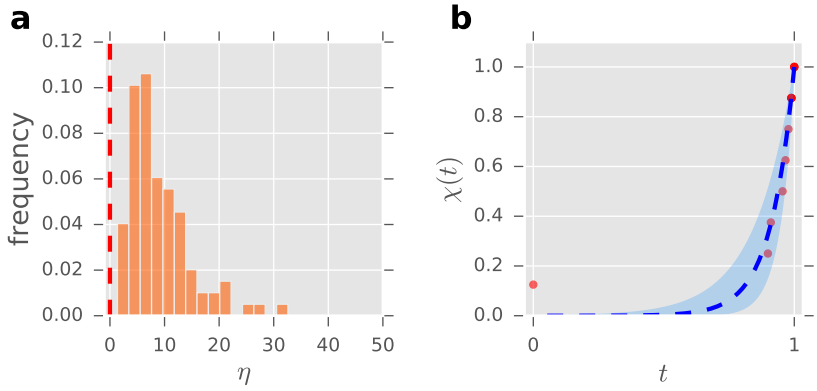


**Figure 3.3: Summary of the results for the face-to-face contacts dataset.** **a,** Distribution of the parameter estimates for the face-to-face contacts dataset ($n = 95$). The red, dashed line marks the change of regime $\eta = 0$; $mean = 9.08$, $median = 7.35$, $mode = 5.54$, $std = 5.86$ **b,** Representative fitting for an individual in the face-to-face contacts dataset (chosen at random from those with a strictly positive $95\%$ confidence interval). Solid dots represent experimental data, blue dashed lines represent the graph of equation (3.4) with the corresponding estimated parameter, and shaded regions show the 95% confidence interval for that estimate (see section 3.2.1). Estimated $\eta = 11.12$, $95\%$ confidence interval $(6.74, 18.34)$, $\tilde{L} = 15$. See Fig. B.6 (Appendix B.1.3) for a sample of 24 other fittings chosen randomly from the entire population.

However, even though some fittings are remarkably good (see Fig. 3.3b), they are mostly not as good as they were in the mobile phones dataset—see Fig. B.6 in Appendix B.1.3. As we explained above, these data are inherently noisy and assessing the intensity of the relationships (or even merely of the interactions) based solely on time spent together during a conference can be misleading. Ideally, we would need this type of data but from individuals in their daily lives, so that the interactions recorded would better correspond to decisions of the individual. Nevertheless, even with the mentioned limitations, the model is still capable to partially capture the patterns of face-to-face interactions.

### 3.2.4 Facebook dataset

If we compare the results from sections 3.2.2 and 3.2.3 (see Figs. 3.1a and 3.3a) we can appreciate how, as the sample size increases, the distribution of the parameter estimates seems to smooth around a well-defined central value of $\eta \approx 6$. If that is the case, it would be a clear indication that the parameter of the model is indeed capturing a real feature of the way individuals manage relationships.

To further explore this possibility, we analyse a larger dataset of interactions in Facebook[6] (Arnaboldi et al., 2012). This dataset was obtained using a crawler on April 2008 and comprises data on roughly 3 million Facebook users and 23 million edges. Importantly, it also contains the number of interactions (photo comments or Wall posts) between users. The data is divided into four different time windows (referred to the time of the crawl): last month, last six months, last year and all—which contains all the interactions among the users since they established their links (Arnaboldi et al., 2012).

To analyse the structure of the personal networks in Facebook, Arnaboldi et al. (2012) filtered the data to retain only active, relevant users from which the relative frequency of contact with all his or her alters could be adequately assessed—see (Arnaboldi et al., 2012) for details. The resulting dataset contains about 90.000 users and 4.5 million links[7]. Applying two different clustering techniques, *k*-means (Wang and Song, 2011), and DBSCAN (Ester et al., 1996), they found that the structure of personal networks of Facebook users consists of a set of 4 concentric, inclusive circles according to the intensity of their links, and that the sizes of these circles exhibited a more or less constant scaling ratio close to 3—thus, resembling what is found in offline social networks (Dunbar et al., 2015).

Since clustering algorithms find an optimal partition of personal networks into four circles with a scaling of approximately 3, our model should yield a distribution of parameters centred around 6. In this case, we use

[6]This data used to be available, under request, at `http://current.cs.ucsb.edu/socialnets/` under the name "Anonymous regional network A". However, as of January 24, 2019, it seems that the web is no longer available. We are very thankful to Prof. Ben Zhao for granting us access to the data.

[7]We are very thankful to Dr Valerio Arnaboldi for sharing with us the final, curated dataset precisely as they used it in their paper.

again that, for each individual, $s_{max}$ is simply given by his or her most intense interaction, and $s_{min}$ by the least intense one—with this decision, we can use the same data as Arnaboldi et al. (2012) without any further pre-processing. Figure 3.4 confirms our hypothesis, showing a smooth distribution with *mean* = 8.25, *median* = 7.17, and *mode* = 5.48. Interestingly, the size of this sample allows us to find, for the first time, individuals exhibiting an inverse regime with $\eta < 0$. More precisely, we find 256 users, about 0.3% of the population, exhibiting this type of structure—in fact, for only 7 of them (0.007%) the 95% confidence interval does not include the zero. In Figs 3.4b and 3.4c, we show representative fittings of individuals in the standard and the inverse regime, respectively. Let us remark that, not only does our model capture the typical structure of personal networks as Arnaboldi et al. (2012) do, but it also unveils that the inverse regime (Tamarit et al., 2018) is equally present in digital communications.

## 3.3 Discussion

In this chapter, we have presented an extension of the model introduced in Chapter 2 that treats the intensity (i.e. the cost) of the links as a continuous variable. Even though this new model does not rely on a specific number of layers, its behaviour is qualitatively identical to its discrete counterpart. Remarkably, our experimental results show that the estimates of this new parameter ($\eta \approx 6$) are consistent with what is typically observed in discrete settings ($\mu \approx 1$). Consequently, one may wonder whether the organisation of personal networks has a discrete (as empirical evidence has suggested) or continuous nature.

Given the abundant empirical evidence for the existence of discrete layers (and the results we will present in Chapter 5), we are inclined to think that, in effect, there is some characteristic discretization[8]. However, this discretisation will hardly be perfect and may be subject to fluctuations. Moreover, even if the (psychological) organisation of the networks were perfectly discrete, it would be difficult for all people within the same layer to receive precisely the same attention (number of calls, contact time, and

[8] Perhaps as a consequence that it may be easier to deal with relationships if we somehow organise them into categories.

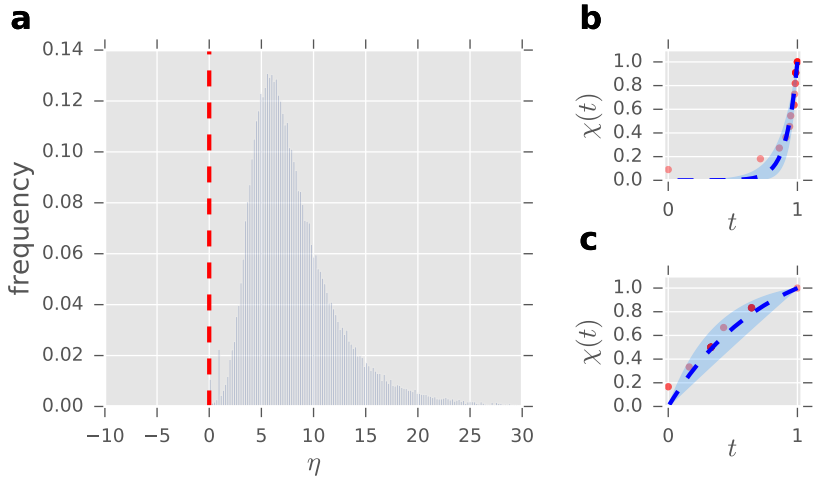


**Figure 3.4: Summary of the results for the Facebook dataset. a,** Distribution of the parameter estimates for the Facebook dataset ($n = 98258$). The red, dashed line marks the change of regime $\eta = 0$; $mean = 8.25$, $median = 7.17$, $mode = 5.48$, $std = 4.91$ **b,** Representative fitting for an individual exhibiting the standard regime (chosen at random from those with a strictly positive $95\%$ confidence interval). Solid dots represent experimental data, blue dashed lines represent the graph of equation (3.4) with the corresponding estimated parameter, and shaded regions show the $95\%$ confidence interval for that estimate (see section 3.2.1). Estimated $\eta = 11.64$, $95\%$ confidence interval $(7.62, 17.79)$, $\tilde{L} = 21$. **c,** Example of fitting for an individual exhibiting the inverse regime (chosen at random from those with a strictly negative $95\%$ confidence interval). Solid dots, blue dashed lines, and shaded regions have the same interpretation as in **b**. Estimated $\eta = -1.34$, $95\%$ confidence interval $(-2.71, -0.08)$, $\tilde{L} = 30$. See Fig. B.7 (Appendix B.1.4) for a sample of 24 other fittings chosen randomly from the entire population.

so on) at all times, which would cause continuous fluctuations. Let us emphasise that under no circumstances are both results incompatible, since our (continuous) model does not assume at any time that the distribution of intensities is continuous, but only that it can be so—which allows us to adjust this type of data. Importantly, the principles underlying both types of structures are indeed the same, namely that relationships are costly and that the resources we can devote to them are limited.

Getting rid of the layers allowed us to find a parameter with a universal character, but the price to pay was that the scale in which the intensity of the relations is measured (i.e. $s_{min}$ and $s_{max}$) had to be inferred with information external to the problem. This creates an additional challenge when fitting the data, and decisions have to be made based on plausible reasons—but there might be other possibilities. This might well be one of the reasons why the individual fittings seem to be somewhat worse than the ones we showed in the previous chapter, and it is an issue that deserves further attention.

It should be noted, however, that the model considers that the effort devoted to relationships is a perfect indicator of their intensity, while the different types of information with which we have measured these efforts (number of calls, face-to-face contact, and number of messages exchanged) are nothing more than proxies. In particular, we may be observing only one of the channels through which relationships are maintained, and including all the data of contacts among people through any means could improve the results. On the other hand, it is more than likely that not all communications made have the same intensity, even if they last the same, which is a significant source of noise for our model. In any case, given the simplicity of the model and the particularities of the data, the fits are remarkably good. Furthermore, the aggregate distribution of the parameter estimates (which might compensate individual errors) exhibits a clear shape centred around the expected value of $\eta \approx 6$, which is a remarkable result.

Lastly, let us note that even in the case that there were no layers at all the continuous model still inherits a somewhat discrete feature, namely $s_{min}$. Indeed, any effort devoted below this threshold would not contribute to creating a relationship at all, as if there was a minimum *quantum of attention* needed to develop a bond.

## 3.4 Conclusions

The model of social atom presented in (Tamarit et al., 2018) can be extended into one that considers the intensity (i.e. the cost) of the links as a continuous, instead of discrete, variable—hence, using no layers. The two regimes found in (Tamarit et al., 2018) hold again in this version of the model, with similar interpretations. For consistency with the results ob-

tained in the discrete variant, the new model predicts a value of its (unique) parameter of $\eta \sim 6$. We confirm this prediction using three different data sets coming from phone records (Saramäki et al., 2014), face-to-face contacts (Isella et al., 2011), and interactions in Facebook (Arnaboldi et al., 2012). As the sample size increases, the distributions of estimated parameters smooth around a well-defined central value of $\eta \approx 6$. The existence of a characteristic value of the parameter at the population level indicates that the model is capturing a universal feature on how humans manage relationships.

Even though populations seem to group around a central value of the parameter, each estimate serves as a sort of social fingerprint that distinguishes the individual's behaviour. This result supports the hypothesis that the very existence of social signatures is a consequence of having to allocate finite resources into different relationships (Saramäki et al., 2014). Lastly, our analyses also confirm the results found in (Arnaboldi et al., 2012), that is, that the structure of online personal networks mirrors those in the off-line world (Dunbar et al., 2015). Importantly, our model does not depend on any sort of clustering technique and, besides reproducing the same global picture found in (Arnaboldi et al., 2012), also captures a small fraction (0.3%) of networks in the inverse regime—which is seen here for the first time in online communications.

# 4

# The interplay between positive and negative relationships: an empirical study

> "It doesn't matter how beautiful your theory is, it doesn't matter how smart you are. If it doesn't agree with experiment, it's wrong."
>
> *Richard Feynman*

In Chapters 2 and 3 we have shown how a mathematical model, based on simple assumptions on the amount of resource available to sustain relationships, was able to reproduce the way we humans organise our social world. However, little has been said about the global structures (i.e. social networks) that arise when these personal networks interconnect with each other. Likewise, so far we have mainly been discussing sympathetic relationships, leaving aside antipathetic ones. In this chapter, we begin to tackle these questions using a novel dataset gathered with our own experiments—and experimental software. Importantly, the characteristics

we found in this study will be most useful as a reference for a possible theory of social structure based on our ”social atom”.

## 4.1 Description of the study

We present results from a sociometric study conducted in a school[1] (Madrid, May 2017) with students from grades 5 to 11—the highest level offered in the school. The total number of students within this range was 322, of whom 321 (195 males) agreed to participate, and 308 ended up participating. The range of ages was $10-19$ with an average of $13.42 \pm 2.12$ (see table 4.1 for a summary of the characteristics of the participants).

To collect the social information, we asked the participants six questions about both their positive and negative[2] relationships within the school. The questions we used were in Spanish (see Appendix C.1), so we provide here a translated version (the abbreviations after each question will be used to refer to it hereafter):

- If you had a serious personal problem, which other schoolmates would you be willing to share it with? (SP)
- If there are schoolmates that you wouldn't want (by any means) they had to leave the school, please mark them. (DL)
- If you could choose with whom to seat at the lunch table (independently of the actual size of the tables), who would you choose? (LT)
- If there are schoolmates with whom you'd rather not do any kind of activity, please mark them. (DN)
- If you had to complete an assignment in the school, who would you like to work with? (Mark 'None' if you'd rather work on your own) (WW)

[1]The study was approved by the Ethics Committee of the *Universidad Carlos III de Madrid* and the school gathered parental consent agreements for all the participants.

[2]Throughout this and the following chapter we call *positive* to sympathetic relationships, and *negative* to antipathetic ones.

- Mark the schoolmates with whom you'd rather not work in a school assignment (regardless of your personal relationship with them). (DW)

To carry out the study we divided the participants into groups (about 25 participants per group) and scheduled a time when their teachers had to bring them to the computer room of the school. Once there, after a brief presentation of the activity by the researcher, they were instructed to enter an online platform (*ConectAula*) that we had previously developed (see Appendix C.2 for details) and answer the survey. The online platform allowed the participants to quickly find and select any other student while keeping their identities anonymous to the researchers. They could nominate as many alters as they wanted in each question and, to facilitate the process, each of the questions was displayed together with a drop-down button organising the possible answers (i.e. all the participants with the exception of the ego herself) with the same structure of grades and groups as in the school (see Appendix C.2 for details). At any given moment, at least one researcher and one teacher were present in the room, and occasionally assisted the students who had troubles understanding a question. This procedure was repeated during three consecutive days (the whole activity took about 30-45 minutes per group to be completed) and enabled us to collect 308 surveys —that is, 96 % of the total population.

## 4.2 Network analysis

The answers provided by the students allow us to recreate the social structure of the school (see Fig. 4.1). For each of the questions, we create a directed network in which there is an edge from node $i$ to node $j$ if student $i$ nominated student $j$ in that particular question. We refer to these networks as: SP (*share problem*), DL (*don't leave*), LT (*lunch table*), WW (*work with*), DW (*don't work*), and DN (*do nothing*). For example, if student $i$ nominated student $j$ as someone with whom he or she would like to seat at the lunch table, then there will be a directed edge from $i$ to $j$ in the network LT.

In addition to the collected networks, we build the new ones: IPN (*intersection of positive networks*, a directed edge from $i$ to $j$ exists if $i$ marked

**Table 4.1: Descriptive statistics of participants**

| Grade | Average age (std. err.) | Group | Participants (male) |
|---|---|---|---|
| 5 | 10.29 (0.46) | A | 22 (14) |
| | | B | 23 (15) |
| 6 | 11.36 (0.47) | A | 22 (11) |
| | | B | 23 (14) |
| 7 | 12.47 (0.62) | A | 23 (12) |
| | | B | 24 (16) |
| 8 | 13.61 (0.63) | A | 23 (13) |
| | | B | 28 (21) |
| 9 | 14.60 (0.69) | A | 27 (15) |
| | | B | 25 (18) |
| 10 | 15.60 (0.64) | A | 25 (13) |
| | | B | 23 (16) |
| 11 | 16.58 (0.87) | A | 8 (1) |
| | | B | 13 (7) |
| | | C | 12 (9) |
| | | | 321 (195) |

*j* in all positive networks), IPN* (similar to IPN but excluding the answers to the question WW), UPN (*union of positive networks*, a directed edge from *i* to *j* exists if *i* marked *j* in at least one positive network), INN (*intersection of negative networks*, a directed edge from *i* to *j* exists if *i* marked *j* in all negative networks), and UNN (*union of negative networks*, a directed edge from *i* to *j* exists if *i* marked *j* in at least one negative network).

Some of the features of these networks are summarised in Table 4.2. In particular, we show the experimental values for the *average degree* (number of links coming in/out a given node), the *average reciprocity* (fraction of links coming out a node that are also coming in), the *assortativity coefficient* (Newman, 2003) (tendency of nodes to create relationships with other nodes of the same gender, class[3], or grade), the number of *weakly/strongly connected components* (sets of nodes that can reach each other via links), and the number of nodes—see Appendix C.3 for a more technical description of the different quantities.

Notice that the number of nodes is slightly smaller in three of them. The reason is that some of the 308 questionnaires gathered had missing

[3]We refer to a class as the grade plus the group. For example: Grade 7, group A.

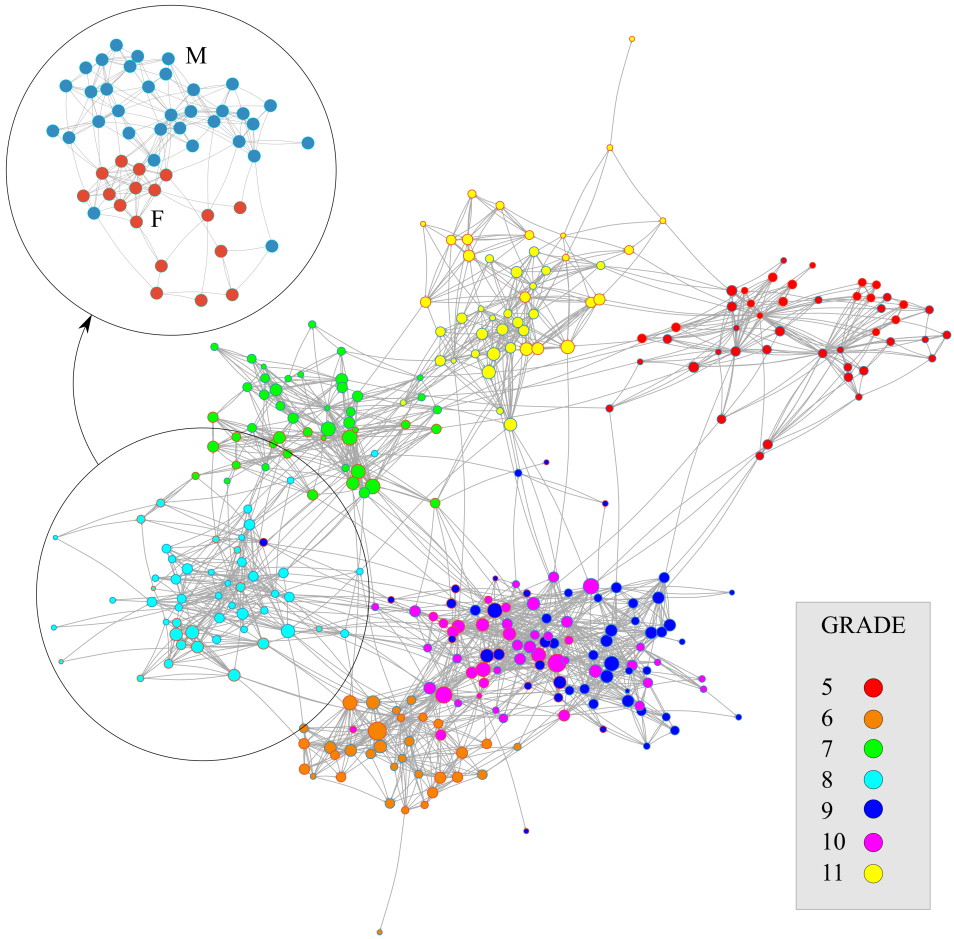


**Figure 4.1: Representation of the SP network.** The nodes are coloured according to the grade they belong to, and their size is proportional to their in-degree. Inset: relationships within the 8th grade with nodes coloured according to their gender (red for girls and blue for boys). The entire visualisation makes apparent the fact that relationships tend to occur between students belonging to the same grade and having the same gender—see also Table 4.2.

information, resulting in a different number of nodes in each of the networks. Many approaches can be adopted to deal with this missing data to minimise its impact in the estimation of network measures (Robins et al.,

2004; Kossinets, 2006; Huisman, 2009). In the worst case scenario, we have complete information of 305 out the 308 who actually answered from the 322 potential participants. Since the fraction of nodes for which we don't have information is negligible ($\sim 5\%$), and they are missing at random, we merely exclude these nodes from our analyses.

Firstly, let us notice that the values shown in Table 4.2 are in good agreement with other studies carried on in similar settings (Almaatouq et al., 2016; Huitsing et al., 2012; Rambaran et al., 2015). Generally speaking, the negative networks show a higher level of fragmentation than the positive ones, as they systematically have a larger number of connected (weakly and strongly) components. Notice in this regard that the only network that shows complete cohesiveness is UNN. Interestingly, the average degree of this network is $\sim 15$, which is precisely the typical size of a *sympathy group*— the second layer in Dunbar's circles (see section 1.1 and (Dunbar, 2018)). We will delve deeper into this fact in the next chapter.

In this chapter, we will focus on investigating the explanatory factors in the formation of the different networks, and on the structural connection that exists between the two types, positive and negative. The levels of assortativity shown in Table 4.2 indicate (see also Fig. 4.1) that all relationships tend to happen between individuals within the same grade (or age)—which is somewhat natural, acknowledging that they share plenty of school-related activities. They also show the presence of a strong gender homophily (McPherson et al., 2001) effect for the positive networks, and a small (but significant) *heterophily* effect for the negative ones. Investigating these phenomena is the focus of the next section.

### 4.2.1 Gender effects

The gender homophily in social relationships, that is, the tendency for positive relationships to occur between individuals of the same sex, is a well documented empirical fact, especially among young people, but persistent also across ages (Stehlé et al., 2013; Roberts et al., 2008; Shrum et al., 1988; Laniado et al., 2016). Antipathetic relationships, however, have been shown to be much less gendered than positive ones (Dijkstra et al., 2007; Card, 2010; Berger and Dijkstra, 2013), and seem to be more affected by other factors such as status dissimilarity (Berger and Dijkstra, 2013). In

**Table 4.2: Summary of network measures**. Summary of network measures (see Appendix C.3 for a brief description of these quantities) for the collected networks (upper table) and the constructed ones (lower table)—see section 4.2. The numbers in parenthesis show the standard errors of the different measures.

| | Avg. degree | | Reciprocity | Assortativity | | | #Connected components | | #Nodes |
|---|---|---|---|---|---|---|---|---|---|
| | in | out | Avg. | Gender | Grade | Class | Weakly | Strongly | N |
| SP (+) | 6.23 (5.39) | 6.23 (3.24) | 0.45 (0.24) | 0.46 (0.02) | 0.84 (0.01) | 0.61 (0.01) | 1 | 17 | 307 |
| DL (+) | 10.96 (9.48) | 10.96 (4.69) | 0.45 (0.21) | 0.23 (0.02) | 0.87 (0.01) | 0.60 (0.01) | 1 | 29 | 308 |
| LT (+) | 8.17 (5.48) | 8.17 (4.04) | 0.47 (0.21) | 0.33 (0.02) | 0.88 (0.01) | 0.64 (0.01) | 1 | 15 | 308 |
| WW (+) | 6.55 (5.52) | 6.55 (3.90) | 0.36 (0.22) | 0.28 (0.02) | 0.91 (0.01) | 0.67 (0.01) | 2 | 27 | 307 |
| DW (-) | 6.83 (8.19) | 6.83 (4.84) | 0.18 (0.16) | -0.09 (0.02) | 0.93 (0.01) | 0.55 (0.01) | 6 | 110 | 308 |
| DN (-) | 5.97 (7.81) | 5.97 (4.67) | 0.19 (0.18) | -0.08 (0.02) | 0.84 (0.01) | 0.46 (0.01) | 6 | 124 | 305 |
| IPN (+) | 2.58 (3.04) | 2.58 (2.04) | 0.33 (0.29) | 0.58 (0.03) | 0.93 (0.01) | 0.71 (0.02) | 20 | 182 | 306 |
| IPN* (+) | 3.70 (3.79) | 3.70 (2.29) | 0.40 (0.28) | 0.55 (0.03) | 0.92 (0.01) | 0.68 (0.01) | 7 | 111 | 307 |
| UPN (+) | 14.92 (9.09) | 14.92 (5.97) | 0.54 (0.16) | 0.21 (0.01) | 0.85 (0.01) | 0.58 (0.01) | 1 | 1 | 308 |
| INN (-) | 3.77 (5.63) | 3.77 (3.38) | 0.13 (0.16) | -0.11 (0.03) | 0.93 (0.01) | 0.55 (0.02) | 22 | 195 | 305 |
| UNN (-) | 9.04 (9.88) | 9.04 (6.04) | 0.23 (0.18) | -0.07 (0.02) | 0.86 (0.01) | 0.49 (0.01) | 1 | 63 | 308 |

this section, we analyse to what extent such effects are present in our data, disentangling the existing differences between the social behaviour of boys and girls.

### Network composition

We begin by analysing differences in group size between girls and boys. To that end, we perform a (two-tailed) Wilcoxon signed-ranks test on each of the networks' degree distributions —see Table 4.3. The results for the out-degrees reveal that girls nominate a significantly higher number of alters ($p < 0.05$) in all the negative networks (DW, DN, INN and UNN) and in IPN, that is, the most restrictive positive one. In the case of the negative networks, our analysis does not support what is observed in a meta-study on antipathetic relationships, where Card (2010) observed quite the opposite, a small but reliable tendency for boys to have more antipathetic relationships. Nevertheless, the effect we detect is rather low and may have no impact on the overall conclusions of this meta-study.

The analysis of the in-degree distributions reveals a significant tendency for boys to receive more nominations in the network DW, so that

**Table 4.3: Average degrees by gender.** The table shows the average in/out degrees of the different networks split by gender. The significance of the differences between boys and girls is assessed using a (two-tailed) Wilcoxon signed-ranks test—see 4.2.1 for details.

| | Average out-degree | | | | Average in-degree | | | |
|---|---|---|---|---|---|---|---|---|
| | Female | Male | Total | Significance | Female | Male | Total | Significance |
| Collected | | | | | | | | |
| SP (+) | 5.98 | 6.39 | 6.23 | 0.945 | 6.77 | 5.89 | 6.23 | 0.084 |
| DL (+) | 9.80 | 11.68 | 10.96 | 0.338 | 10.80 | 11.06 | 10.96 | 0.323 |
| LT (+) | 8.05 | 8.25 | 8.17 | 0.649 | 7.58 | 8.54 | 8.17 | 0.036 |
| WW (+) | 6.87 | 6.35 | 6.55 | 0.296 | 6.93 | 6.31 | 6.55 | 0.198 |
| DW (-) | 7.70 | 6.29 | 6.83 | 0.042* | 6.19 | 7.24 | 6.83 | 0.047* |
| DN (-) | 7.00 | 5.33 | 5.97 | 0.024* | 6.03 | 5.94 | 5.97 | 0.945 |
| Constructed | | | | | | | | |
| IPN (+) | 2.82 | 2.43 | 2.58 | 0.023* | 3.07 | 2.28 | 2.58 | 0.001** |
| IPN* (+) | 3.92 | 3.56 | 3.70 | 0.054 | 4.14 | 3.43 | 3.70 | 0.015* |
| UPN (+) | 13.84 | 15.58 | 14.92 | 0.242 | 14.49 | 15.18 | 14.92 | 0.166 |
| INN (-) | 4.03 | 3.60 | 3.77 | 0.041* | 3.68 | 3.82 | 3.77 | 0.667 |
| UNN (-) | 10.71 | 8.01 | 9.04 | 0.008** | 8.53 | 9.36 | 9.04 | 0.188 |

* $p < 0.05$, ** $p < 0.01$

they are more likely to be avoided in work-related activities[4]. Girls, however, are significantly more nominated in the networks IPN and IPN*, so that they receive strong positive nominations more often. The fact that girls tend to choose and be chosen more often in the most restrictive positive networks supports the claim that girls (women in general) tend to invest more in close relationships with a higher level of intimacy (Vigil, 2007; Dunbar, 2018).

We now analyse the differences in the composition of the personal networks of boys and girls. When examining gender effects, it is essential to make this distinction clear, since there are typically significant asymmetries regarding the social behaviour of both genders (Dijkstra et al., 2007; Vigil, 2007; Dunbar, 2018). Additionally, several factors must be controlled for, such as the relative proportion of girls/boys in the population, or

[4]According to informal conversations with some of the teachers in the school, this is very likely because boys tend to be less organised in work-related activities.

other possible effects present, such as a tendency to have friends/enemies of the same age—as the high values of the *assortativity* by grade (see Table 4.2) indicate in our data. To detect possible asymmetries in gender effects, while controlling for as many factors as possible, we create an ad-hoc null model to compare against the empirical data. For each of the networks, we randomise the edges preserving the source nodes (and all its attributes) but replacing the target nodes at random with others who belong to the same class as they do—excluding the source node (ego) if necessary to avoid self-loops. Then, for each realisation, we count the average number of links from male-to-male, male-to-female, female-to-female, and female-to-male, and create a distribution based on 10000 runs.

The 95% (two-tailed) confidence intervals of these distributions are shown, together with the experimental values, in Fig. 4.2. We can appreciate how both boys and girls exhibit very significant gender homophily effects in all positive relationships, in agreement with previous works (Dijkstra et al., 2007; Vigil, 2007; Dunbar, 2018). The situation with antipathetic relationships is more subtle. As we observed in Table 4.2, there exists a small but significant negative gender homophily (a sort of heterophily) effect in these networks. Nevertheless, as shown in Fig 4.2, this effect is solely due to the nominations made by girls, who tend to nominate more boys than what would be expected by the null model. Boys, however, show complete neutrality in this regard. Let us remark that unravelling this asymmetry was only possible with the aid of a somewhat refined null model.

### Reciprocity

The overall levels of reciprocity shown in Table 4.2 are, although strikingly low, in good agreement with other studies for both positive and negative relationships (Almaatouq et al., 2016; Huitsing et al., 2012). In this section, our goal is to disentangle the possible differences between males and females. Similarly to what we did in section 4.2.1, we need to find a suitable null distribution for the average reciprocity of individuals with sex $A$ towards individuals with sex $B$ —that is, the fraction of links that $A$s would return to $B$s if no gender effect was present. To do that, we first select all the nodes with sex $A$. Then, for each of these nodes, we count the number

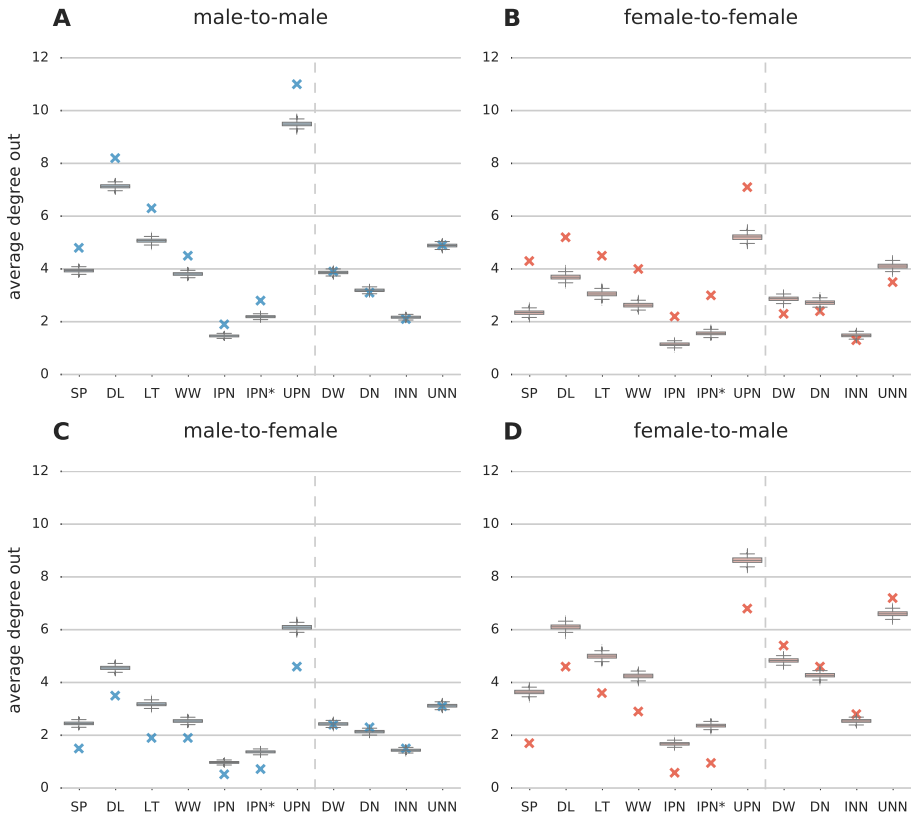


**Figure 4.2: Differences in out-degrees by sex.** Solid crosses represent the observed average values. The boxplots represent the expected distribution (null model) of the average out degrees if edges where chosen independently of the sex of the target node —see section 4.2.1. The vertical, dashed lines separate the regions of positive networks (left) and negative networks (right).

$n_B$ of links received from nodes with sex $B$ and select the same number $n_B$ of links at random (without replacement) from all his/her incoming links. That is, the null model considers that the ego is blind to the gender of his or her incoming ties—notice that all remaining attributes of the alters (such as the class and group they belong to) remain unchanged. Lastly, we just compute the fraction of all these 'new relationships' that are reciprocal

to obtain one value of the desired distribution, and repeat the process for 10000 runs.

Our results show that (Figs. 4.3A and 4.3C) boys reciprocate other boys within the range expected by the null model ($ci = 95\%$), except for a small but significant *over-reciprocation* in the networks DL, LT, WW, and UPN. Notice in particular that there is no gender effect in either the negative networks or the *most intense* positive ones —IPN, IPN*, and, arguably, SP. Moreover, this pattern is opposite to that exhibited for reciprocation towards females (Fig. 4.3C), which shows a significant tendency to *under-reciprocate* positive relationships in DL, LT, WW, and UPN, and no effects for the rest of the networks.

The situation is rather different for the girls —see Figs. 4.3B and 4.3D. In Fig. 4.3B we can observe how the positive relationships between girls tend to be much more reciprocal than what would be expected according to the null model. Again, the situation is the opposite when it comes to reciprocating links coming out from boys (Fig. 4.3D), with stronger *under-reciprocation* effects. Regarding the negative networks, there is a small, but significant, tendency to *under-reciprocate* other girls in WW and UNN, and to *over-reciprocate* the boys in the same networks.

## 4.3 Interplay between positive and negative networks

As we have shown, the negative and positive networks in our study exhibit quite different patterns. However, both types of networks shall be structurally interdependent as suggested by theories such as the *Structural Balance Theory* (SBT) (Heider, 1946; Cartwright and Harary, 1956) or the *Status Theory* (ST) (Leskovec et al., 2010b). Very briefly (see also section 1.2), the former states that triads are *stable* as far as the product of the "signs" of its links is positive, whereas the latter considers that the signs of the links are a consequence of differences in subjective "status" of the nodes—that is, a positive link from node $i$ to node $j$ is signalling that $i$ considers that $j$ has higher status than himself, and a negative link is signalling the opposite. Both theories draw predictions about the "directions" in which a given network might evolve, so cross-sectional studies (like the one we present here) are insufficient to explore their validity (Ram-

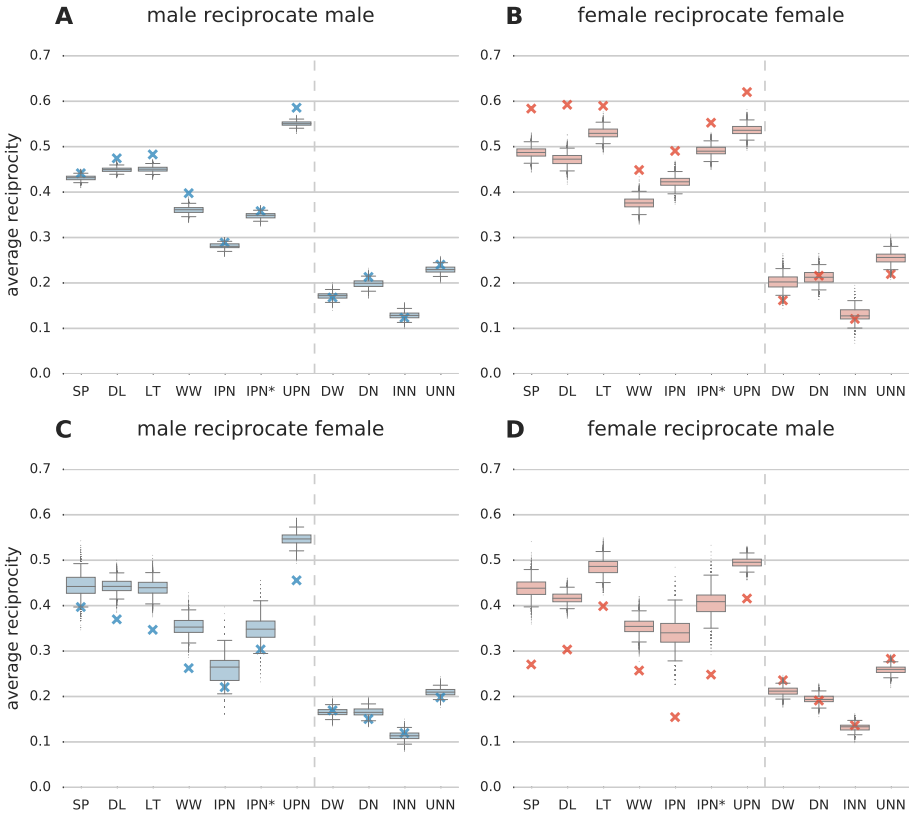


**Figure 4.3: Differences in reciprocity by sex.** Solid crosses represent the average values of reciprocity observed in our data. The boxplots represent the expected distribution (null model) of the average reciprocity if edges where chosen independently of the sex of the target node. The vertical, dashed lines separate the regions of positive networks (left) and negative networks (right).

baran et al., 2015). Nevertheless, according to either theory, each of the network types should contain latent information about the links in the opposite one. We tackle this issue from a machine learning approach with the goal of quantifying the amount of information that each network type contains about the other. Structural information on negative relationships has already been shown to have predictive power on positive ones in on-

line social networks (Leskovec et al., 2010a), but we are not aware of any similar analysis being performed in off-line, face-to-face relationships.

### 4.3.1 Machine Learning approach

The task we want to accomplish is similar to the *link prediction problem* (Liben-Nowell and Kleinberg, 2007) or the *sign prediction problem* (Leskovec et al., 2010b), and can be defined as follows: given any two nodes $i$ and $j$, we want to predict whether a (directed) link from $i$ to $j$ exists or not, based solely on local, structural properties (predictors) of the nodes. We use three different sets of predictors. First, the out-degree of each node ($i$ and $j$) plus the number of individuals that both have nominated in common —we call this set "*out*" for brevity. Second, the in-degree of each node plus the number of individuals that nominate both of them simultaneously ("*in*"). And third, the first and the second altogether ("*in & out*"). Notice that the information we use is simply what would be needed to compute the Jaccard index[5] of the sets of *in* and/or *out* edges of any two nodes. The input information is drawn from each of the networks described in Table 4.2 separately, and the target network (for which we want to predict the existence of links) is either UPN (positive relationships) or UNN (negative relationships)—adding up a to a total of 66 different cases.

To guarantee the robustness of our results we trained six state-of-the-art machine learning classification algorithms: CART (Therneau and Atkinson, 1997), Pruned Trees (Therneau and Atkinson, 1997), Random Forest (Liaw and Wiener, 2002), SVM with radial kernels and SVM with linear kernels (Dimitriadou et al., 2011). Since we consider that being able to predict an existing link is as important as predicting a non-existing one (i.e. type I and type II errors are equally important), we chose *accuracy* (also known as classification rate) as the performance metric for model selection—it accounts for the ratio of correctly classified instances. The estimation of the performance metrics was done using a nested 10-fold cross-validation scheme (Varma and Simon, 2006; Anderssen et al., 2006), whereas a 10-fold cross-validation (Hastie et al., 2001) was used to train the classifiers. To prevent sampling biases during the training, the datasets were balanced so that the two classes (exiting link, non-existing link) were

[5]The Jaccard index of two sets $A$ and $B$ is defined as $J(A,B) = |A \cap B|/|A \cup B|$.

present in the same proportion. We use all the instances of the class with the minimum size (exiting link), and sample at random the same number of cases from the other one (non-existing link)—notice that this implies that the baseline accuracy is 50%. Although Pruned Trees, Random Forest, and SVM with radial kernels yielded the best predictions, with similar performances, all the considered algorithms produced comparable results, confirming the desired robustness.

### 4.3.2 Results

In Fig. 4.4 we show the accuracy of the (best) trained models for each of the classification tasks. The first thing to be noticed is that the performance is strikingly high, reaching accuracy levels of 92% in both UPN and UNN. This is a much higher value than those obtained in other attempts made on off-line positive networks (using information of the same network) (Almaatouq et al., 2016), and similar to those obtained for the simpler task of *sign prediction* on on-line settings (Leskovec et al., 2010a). In all cases, with the only exception of the one using information from UPN to predict UPN itself (see Fig. 4.4A), the "*in*" set was a better predictor than the "*out*" one —and both performed worse than the "*in & out*", as could be expected. This is a quite interesting result since it is showing that there is more information about the relationship between two individuals in the set of people considering them as *friends* (*enemies*) than in the group of people that they regard as *friends* (*enemies*). This points to a sort of assymetry that is not accounted for in neither the SBT (Cartwright and Harary, 1956) nor the ST (Leskovec et al., 2010b). Interestingly, the information about incoming ties is typically available also for non-respondents in sociometric surveys. Hence, our machine learning approach could be prove to be a powerful tool to deal with missing information in these studies, thus minimising the impact that missing information may have on the inferred network metrics.

As could be expected the prediction task is better accomplished when the input information comes from the same type of network (positive/negative) as the one we want to predict—compare Figs. 4.4A and 4.4B column-wise. But, importantly, our results also show that each type of network contains (very) much information about the other one, confirming the hypothesis that their structure is interdependent. More precisely, the

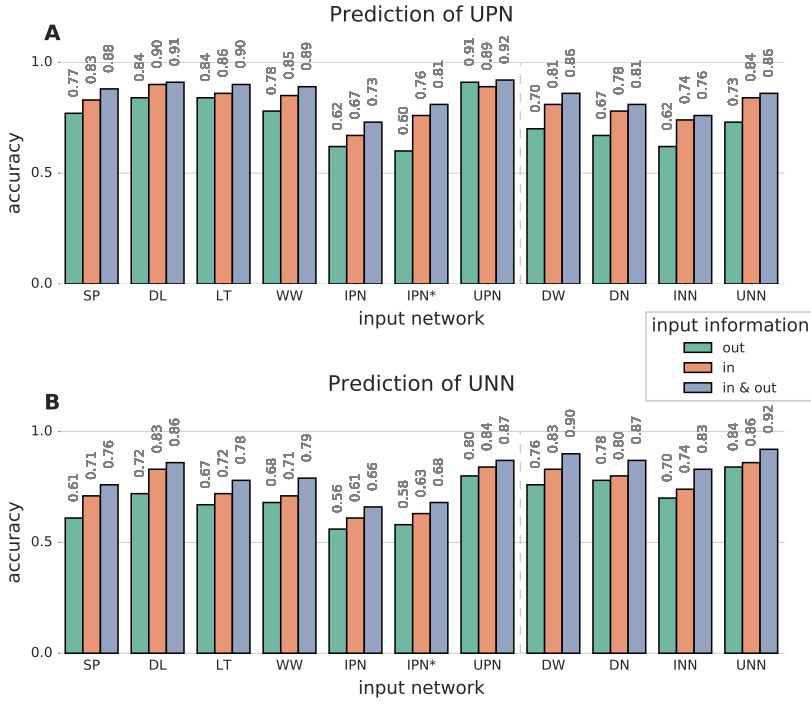


**Figure 4.4: Accuracy in links prediction.** The colour of the bars indicates the type of information (see legend) given to the algorithms for the prediction task (see section 4.3.1). The bars to the left of the dashed, grey lines use information from networks of positive relationships, while the bars to the right use information provided by negative ones. **A,** Prediction of links in the network of positive relationships, UPN. The highest level of accuracy (92%) is found when the input information comes from the same network, UPN. When the information comes from the networks of negative relationships the maximum (86%) is achieved using UNN for the input information. **B,** Prediction of links in the network of negative relationships, UNN. The maximum accuracy (92%) is achieved using the same UNN for the input information. When positive networks are used to predict this negative one, the maximum (87%) is reached using information from UNN.

existence of (positive) links in the network UPN is predicted with an accuracy of 86% when the input information comes from the network UNN.

Conversely, the existence of (negative) links in the network UNN is predicted with an accuracy of 87% when the input information comes from the network UPN. Notice that the results are symmetrical, so that positive networks contain as much information on negative ones as otherwise.

## 4.4 Discussion

In this chapter we have presented results from the first of a series of ongoing (longitudinal) sociometric studies that aim, among other things, to contribute to the growing literature on negative social relationships (Card, 2010). The software we developed to that effect (*Conectaula*, see Appendix C.2 for more info) enabled us to quickly collect high-quality data while preserving the privacy of the participants. Importantly, the participants could select as many other alters as they wanted from the entire pool, so we capture the entire social structure of the school—rather than relationships among people in the same class or grade. Since the data we have used were collected from boys and girls from a school (ages 16-19), our findings and their possible implications must be understood within that context.

Let us remark that the randomisation method we used to unravel the gender effects (see section 4.2.1) has proven to be a compelling technique. While other methods (Freeman, 1978; Shrum et al., 1988; Dijkstra et al., 2007; Roberts et al., 2008) rely on assumptions about the underlying distributions, or the linearity of the relationship between variables, the one we employed here does not use any information that was not initially present in the data. Also, it allows to control for as many factors as possible and can detect asymmetrical effects—a fact that had been vastly overlooked until somewhat recently (Dijkstra et al., 2007). Furthermore, this methodology can be extended naturally to analyse any other type of homophily in social networks (McPherson et al., 2001).

Notice that the information we used to predict the existence of (directed) links comes exclusively from the personal networks of the participants. Indeed, either of the sets employed (*in*, *out*, and *in & out*) consists of nominations that the participants made or received, that is, is solely based on their social relationships. As we have seen (section 4.3), this local information was enough to predict (directed) links with accuracy levels of

92%. Strikingly, the same information produced accuracy levels of about 87% when predicting links in a different network, with opposite *sign*—let us notice that this numbers would very likely be even higher if we had combined information from both types of networks to predict the structure of one of them.

The implications of this result are profound. On the one hand, it confirms the hypothesis that positive and negative networks are not independent, but closely intertwined (Cartwright and Harary, 1956; Leskovec et al., 2010b). On the other hand, it conveys the message that the structure of social networks is very well explained as the interconnection of personal networks—notice in this regard that the algorithms we used had no information about either the gender or the age of the participants. Hence, rather than viewing (local) personal networks as subsets of a social (global) network, social networks shall be best understood as ensembles of personal networks.

Since the accuracy reached is strikingly high the use of these techniques for dealing with missing information in sociometric studies (Robins et al., 2004; Kossinets, 2006; Huisman, 2009) is a promising line of research. This, nonetheless, might also raise ethical questions. Indeed, even though one person decides not to participate in a given study, the set of nominations made towards him or her (*in*) constitutes a powerful predictor of his or her relationships. A similar concern has been raised for online platforms, the so-called *shadow profile hypothesis* (Garcia, 2017). This theory states that it is possible to know very much about non-users of these platforms if we know their acquaintances well enough. Our analysis reveals that this issue should also be considered when dealing with off-line data, such as the ones obtained via surveys.

## 4.5 Conclusions

Our results confirm the existence of relevant gender effects in social networks, both in the composition of the personal networks and on the reciprocity of the relationships (Shrum et al., 1988; Dijkstra et al., 2007; Roberts et al., 2008; Card, 2010; Berger and Dijkstra, 2013; Stehlé et al., 2013; Laniado et al., 2016). On the one hand, networks of sympathetic (positive) relationships exhibit strong homophily effects, which are mostly

symmetrical for boys and girls. On the other hand, negative relationships show much weaker and asymmetrical effects. In our study, the tendency is for girls to have a slightly higher number of antipathetic relationships with boys than what would be expected according to a (sophisticated) null model.

Although gender is a relevant characteristic, the use of machine learning techniques reveals that most of the information that determines the existence of links (and therefore the overall structure of the networks) is contained in the way in which the various personal networks are intertwined. Hence, we propose that social networks shall be best understood as ensembles of personal networks (or social atoms)—instead of considering personal networks as mere subsets of a larger system. The same techniques also reveal that the configurations of the networks of sympathetic and antipathetic relationships are highly interdependent, which confirms the underlying hypothesis of theories such as the *Social Balance Theory* (Cartwright and Harary, 1956) or the *Status Theory* (Leskovec et al., 2010b).

# 5

# The structure of negative personal networks

"Keep your friends close, but your enemies closer."

*Michael Corleone*
The Godfather: Part II (1974)

The structure and composition of affiliative (sympathetic) personal networks has been studied in considerable detail (Dunbar, 2018). In contrast, far less attention has been given to negative relationships (Card, 2010) and the precise composition of negative personal networks is not yet well understood. Interestingly, in Chapter 1 (section 1.1) we saw that the Social Brain Hypothesis grew out of a Machiavelian perspective of human sociality (Humphrey, 1976; Whiten and Byrne, 1988; Dunbar, 1993), so the way we handle antagonistic relationships might also have been key to the development of large brains. If so, the model of social atom we introduced in Chapter 2 should also apply to describe the organisation of negative personal networks.

## 5.1 Analysis of personal networks

In this chapter, we continue analysing data from the study presented in Chapter 4. In particular, we will focus on the structure and composition of personal networks, with emphasis on the antipathetic ones. Further support for our results and conclusions will be provided by additional evidence obtained in a different, specifically designed, study.

### 5.1.1 Degree distributions

The information needed to characterise the composition of an ego network (from the ego point of view) is encoded in his or her out-degree distribution—or *embeddedness*. Indeed, the number of relationships reported by the ego in each of the networks (SP, DL, WW, LT, DN, and DW) encodes how he or she internally organises his or her social world. In Table 5.1 we can see that these numbers exhibit a very clear pattern of correlations. Networks are positively correlated if they belong to relationships of the same type (both positive or both negative) and, interestingly, not correlated otherwise. Hence, there is no connection between the number of reported positive relationships and the number of reported negative ones, suggesting that positive and negative networks are handled separately.

Even though the participants reported an unconnected number of positive and negative relationships, the overall structure of the emergent social networks is highly interdependent (see Chapter 4). From a socio-centric perspective, the best way to characterise an ego is to look at his or her in-degree (or *popularity*), since it reflects how others see him or her. What we observe (see Table 5.1) is that the in-degree distributions are (highly) positively correlated if they belong to the same type and, unlike the out-degree distributions, negatively otherwise. Hence, individuals who are popular in a network of positive relationships tend to be so in all of them, and not 'popular' in negative ones—and vice versa for individuals who are listed frequently in a network of negative relationships. Note that in section 4.3 we saw that information about the in-degree was more relevant than that about the out-degree when trying to predict links, which is consistent with the correlation patterns we find here.

**Table 5.1: Degree correlations.** The upper triangular part of the table shows the Pearson correlation coefficient for each pair of variables. The lower triangular shows the 99% confidence interval for each coefficient, computed using BCa Bootstrap (Bishara and Hittner, 2012; DiCiccio and Efron, 1996). In bold, the values for which the confidence interval does not include the zero.

| | | SP | | DL | | LT | | WW | | DW | | DN | |
|---|---|---|---|---|---|---|---|---|---|---|---|---|---|
| | | out | in | out | in | out | in | out | in | out | in | out | in |
| SP | out | —— | 0.08 | **0.36** | 0.06 | **0.51** | 0.07 | **0.40** | 0.03 | 0.00 | −0.07 | −0.02 | −0.05 |
| | in | (−0.09, 0.26) | —— | 0.07 | **0.68** | 0.05 | **0.66** | 0.00 | **0.69** | −0.02 | **−0.43** | −0.04 | **−0.38** |
| DL | out | **(0.18, 0.53)** | (−0.08, 0.22) | —— | 0.14 | **0.43** | **0.18** | **0.20** | 0.15 | 0.04 | −0.12 | 0.02 | −0.10 |
| | in | (−0.09, 0.20) | **(0.58, 0.76)** | (−0.01, 0.31) | —— | 0.05 | **0.78** | −0.04 | **0.72** | −0.01 | **−0.45** | −0.01 | **−0.44** |
| LT | out | **(0.31, 0.68)** | (−0.10, 0.20) | **(0.26, 0.59)** | (−0.09, 0.19) | —— | 0.08 | **0.42** | 0.05 | 0.01 | −0.10 | 0.10 | −0.05 |
| | in | (−0.09, 0.21) | **(0.56, 0.74)** | **(0.01, 0.37)** | **(0.71, 0.83)** | (−0.08, 0.22) | —— | −0.03 | **0.70** | −0.03 | **−0.43** | −0.03 | **−0.38** |
| WW | out | **(0.20, 0.60)** | (−0.15, 0.14) | **(0.04, 0.38)** | (−0.18, 0.12) | **(0.19, 0.61)** | (−0.16, 0.10) | —— | 0.03 | 0.02 | −0.02 | 0.13 | −0.01 |
| | in | (−0.13, 0.19) | **(0.59, 0.76)** | (−0.01, 0.32) | **(0.63, 0.79)** | (−0.09, 0.19) | **(0.60, 0.77)** | (−0.11, 0.17) | —— | 0.07 | **−0.56** | −0.02 | **−0.47** |
| DW | out | (−0.12, 0.17) | (−0.14, 0.11) | (−0.09, 0.17) | (−0.14, 0.12) | (−0.12, 0.17) | (−0.16, 0.11) | (−0.10, 0.12) | (−0.06, 0.20) | —— | −0.07 | **0.62** | −0.07 |
| | in | (−0.19, 0.08) | (−0.53, −0.32) | (−0.24, 0.03) | (**−0.56**, **−0.32**) | (−0.22, 0.03) | (**−0.54**, **−0.29**) | (−0.15, 0.12) | (**−0.63**, **−0.47**) | (−0.19, 0.06) | —— | 0.06 | **0.85** |
| DN | out | (−0.15, 0.12) | (−0.17, 0.10) | (−0.12, 0.17) | (−0.13, 0.13) | (−0.06, 0.29) | (−0.16, 0.12) | (−0.00, 0.27) | (−0.14, 0.12) | **(0.28, 0.77)** | (−0.09, 0.25) | —— | 0.10 |
| | in | (−0.18, 0.09) | (**−0.49**, **−0.26**) | (−0.23, 0.04) | (**−0.54**, **−0.31**) | (−0.17, 0.07) | (**−0.49**, **−0.26**) | (−0.13, 0.13) | (**−0.56**, **−0.36**) | (−0.19, 0.07) | **(0.81, 0.89)** | (−0.06, 0.36) | —— |

### 5.1.2 Overlapping of networks and social circles

If we focus on the sympathetic networks, we can appreciate how the answers (*out edges*) overlap to a great extent (see Fig. 5.1), meaning that the participants typically nominated the same alter in more than one network. In fact, as we noticed in section 4.2, if we consider the network constructed as the union of all the positive networks (UPN), we see that the average degree becomes 14.92 (see Table 4.2) as opposed to 31.91, which would be the expected value if the networks were entirely disjoint.

Recall (see section 1.1) that number ($\sim 15$) is precisely the typical size of the *sympathy group*, which could be defined as '*all the people whose death tomorrow would cause great distress*'(Buys and Larson, 1979; Dunbar, 2018). Remarkably, as we showed in Table 4.2, this network is the only one with a single strongly connected component (SCC)—see Appendix C.3 for a succinct definition. Therefore, relationships at this level explain how the entire social network achieves cohesiveness.

Since the network UPN includes the *sympathy groups* of the students, we explore whether there is any evidence for the first of the circles, the *support network* (Dunbar, 2018), in our data. This network represents the closest relationships of ego, his or her primary source of emotional support, advice, and assistance in time of need, and has a typical size of $\sim 5$ (Dunbar and Spoors, 1995; Hill and Dunbar, 2003). Among all the questions we asked, the one with the closest meaning is the question about sharing a severe personal problem—SP. The average degree, in this case, is 6.23 (see Table 4.2), which would be in good agreement with the commonly observed value of $\sim 5$.

Let us move to the focus of this chapter, namely negative relationships. In fig 5.1 we can appreciate how the networks DN and DW also overlap to a great extent and do not overlap ($Jaccard = 0.05$) with the positive relationships—which was not unexpected. Additionally, the union of the negative networks (UNN) has degree 9.04 and the *most intense* one (DN) has an average degree of 5.97. A meta-study on antipathetic relationships(Card, 2010) showed that unlimited choice procedures and the use of less intense items assessing dislike (for example, *least like* instead of *enemy*) lead to a higher prevalence of antipathetic relationships. Therefore, it is reasonable to expect that we would have obtained a higher number of

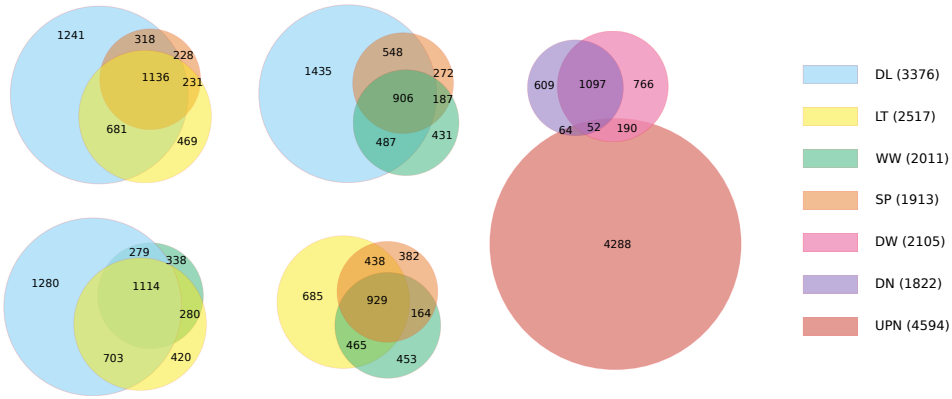


**Figure 5.1: Network overlap (I).** The numbers in each separate region show the number of edges common to the corresponding overlapping networks. The areas are depicted for illustrative purposes and do not reflect the exact sizes of the networks. Colour codes in the right indicate which network appears in each plot.

antagonistic relationships if more questions designed to elicit *weak*, negative relationships had been included. In section 5.3 we present results from a different experiment designed to explore this hypothesis and the finer structure of personal networks of antipathetic relationships.

## 5.2 The atomic organisation of negative relationships

The model we presented in Chapter 2 (and similarly in Chapter 3) predicts that the distribution of the intensities (i.e. in terms of emotional closeness (Dunbar, 2018)) of human relationships may exhibit two distinct patterns, namely, hierarchical inclusive layers with a constant scaling ($\mu > 0$) or a tendency to accumulate very intense relationships leaving aside less significant ones ($\mu < 0$).

This pattern is a consequence of the different *costs* associated with the different types of relationships(Oswald et al., 2004; Takano, 2018) —the closer the relationship, the more costly. Since negative social relationships also come at a cost (time and cognitive wise), the model should be able to capture how we organise them. Unfortunately, the experiment we introduced in Chapter 4 did not include any direct measure of the intensity

of the reported relationships. Hence, to fit the model to these data we first need to assign a weight to each of the links of any given ego.

### 5.2.1 Assignment of costs

In his classic paper, Granovetter (1977) classified reciprocal links as 'strong ties' and non-reciprocal links as 'weak ties'. Further studies (Friedkin, 1980) have confirmed this result—unsurprisingly, perhaps, a relationship that is mutual is stronger than one that is not. In addition, Granovetter (1977) noted that relationships become stronger if people share many different activities and interests; this is called the *multiplexity* of a tie. The concept of weak and strong (Granovetter, 1977) is defined from a structural, socio-centric viewpoint. However, the emotional closeness of a relationship is one of the best indicators of the *strength* of the social tie it forms (Marsden and Campbell, 1984; Granovetter, 1977). Since we have information on both the reciprocity and the multiplexity of the relationships (see also Chapter 4), we build on these two ideas to create a measure of the intensity of the links.

When relationships happen in a single (directed) network their reciprocity is characterised in a binary way, that is, links are either reciprocal (strong) or they are not (weak). On the other hand, when there are multiple networks (layers) reciprocity can occur at least at three levels; a link can be reciprocated in the same layer ($S$), in a different layer ($O$), or not reciprocated at all ($N$). From a social perspective these three types of behaviours are rather different, since a reciprocal link from the same network ($S$) is signalling a relationship that is not only mutual, but also agreed in its nature. Hence, we consider that links reciprocated at the same layer ($S$) have a higher value (intensity, strength) than those reciprocated in any other layer ($O$). Similarly, we also consider that the latter ($O$) have a higher value than those not reciprocated at all ($N$).

The previous ordering of $S, O$ and $N$ can be naturally extended to settings in which relationships may be formed out of more than one of these types of links—as it is the case in our data. All we have to do is to agree on how to compare any two pairs of these combinations. For example, we all would agree that a relationship based on four (as in our positive networks) $S$ links has a higher value than one based on a single, non-reciprocated

link ($N$). To extend this idea we choose a very simple decision algorithm: *Take any two sets with elements* $\in \{S, O, N\}$. *Then, the one with more S s is assigned the highest value. If a draw happens then the one with more Os has a higher value. If a draw still happens then the one with more Ns has a higher value—in case of a draw in all categories assign them the same value*.

If we apply the former rule to a single network, we recover the notion of *strength* from Granovetter (1977), where only two types of links can happen, $S$ (reciprocal) or $N$ (non-reciprocal), and $S$ is considered stronger. Adding an extra layer induces six different possibilities, and the above described algorithm results in the following (unique) ordering: $\{S,S\} > \{S,N\} > \{S\} > \{O\} > \{N,N\} > \{N\}$. Since we have two negative networks (DN and DW), we can use this ordering as a proxy for the intensity of the (negative) relationship between any two individuals. Similarly, considering four layers (the number of positive networks in our data) results in a (unique) sequence of twenty ordered strengths: $\{S,S,S,S\} > \{S,S,S,N\} > \cdots > \{N,N\} > \{N\}$. These ordered sets of strengths can be used to measure the intensity of the relationships—which we choose to decrease linearly for convenience (see section 2.1.3).

### 5.2.2 Model fitting

The number of alters with whom an ego has a relationship of maximum strength ($\{S,S\}$ or $\{S,S,S,S\}$) can now be assigned to his or her $\ell_1$, and so on until the number of relationships with strength $\{N\}$ (assumed to have the lowest cost) is attached to $\ell_r$—see section 2.1 to refresh the notation. So, at this point, we have all the information needed to fit the model as we did in Chapter 2—see section 2.2.1. However, in this chapter we will proceed in a slightly different way. The reason behind this variation is that we want to further explore the existence of a particular value of the parameter $\mu$ that characterises populations—the model *per se* is a model of individuals, not communities.

Recall that the value of $\mu$ is determined by the value of $\mathcal{S}/\mathcal{L}$ according to (see Chapter 2, equation 2.23)

$$\frac{s_1 - \mathcal{S}/\mathcal{L}}{s_1 - s_r} = f(\mu) \equiv e^{\mu} \frac{(r-1)e^{r\mu} - re^{(r-1)\mu} + 1}{(r-1)(e^{r\mu} - 1)(e^{\mu} - 1)},$$

were $s_1$ is the cost associated with $\ell_1$ (the most expensive), $s_r$ the cost associated with $\ell_r$ (the least expensive), and $r$ is the number of considered layers. The former expression leads to a linear relationship between $\mathcal{S}$ and $\mathcal{L}$ given by $\mathcal{S} = (s_1 - f(\mu)(s_1 - s_r))\mathcal{L} \equiv g(\mu)\mathcal{L}$. For the analysis shown in this chapter we choose, without loss of generality, a linear decrease in the costs with, $s_1 = 1$, $s_r = 0.1$, and $r = 4$, and estimate $\mathcal{S}$ and $\mathcal{L}$ for each individual as $\mathcal{S} \equiv S = \sum_{k=1}^{r} s_k \ell_k$ and $\mathcal{L} \equiv L = \sum_{k=1}^{r} \ell_k$ respectively —which are indeed the maximum likelihood estimators.

The slope of the linear regression, let's say $x$, is used to estimate $\mu$ by numerically solving the equation $g(\mu) = x$. The 99% confidence interval for the slope is computed using Bca Bootstrap (Bishara and Hittner, 2012; DiCiccio and Efron, 1996) ($n_{samples} = 10^6$), and this interval is used to compute the 99% confidence interval for the estimated $\mu$. Importantly, this estimation is based on information from the entire population. Therefore, if the linear regression produces significant results, the estimate would represent a characteristic value of $\mu$ for that particular population.

Notice that the actual number of layers in which we divided the positive ($r = 20$) and the negative ($r = 6$) relationships is not considered here—we consider $r = 4$. The reason is that the value of $\mu$ depends somewhat arbitrarily on the number of categories (layers) in which we split the relationships—see also Chapter 3. To facilitate the comparison with the empirical results observed for *Dunbar's circles* we choose $r = 4$ to estimate the parameter. Note, however, that the observed value of $r = 4$ for the empirical data is not arbitrary, as it seems to be the optimised value for large datasets (Mac Carron et al., 2016; Dunbar et al., 2015).

### 5.2.3 Results

In Figs. 5.2A and 5.2B we show the scatter plots of the pairs $(L, S)$ for the positive and the negative relationships. As we can see, in both cases the values are clustered around straight lines, with $R^2 = 0.77$ for the positive relationships and $R^2 = 0.73$ for the negative ones, in agreement with the model—see section 5.2.2. The slopes of these lines determine the characteristic value of $\mu$ for both types of relationships in the school population. The positive relationships turn out to be centred around a value of $\mu^+ = 0.67$ ($[0.60, 0.75]_{99\%}$) and the negative ones around $\mu^- = 1.05$ ($[0.88, 1.46]_{99\%}$).

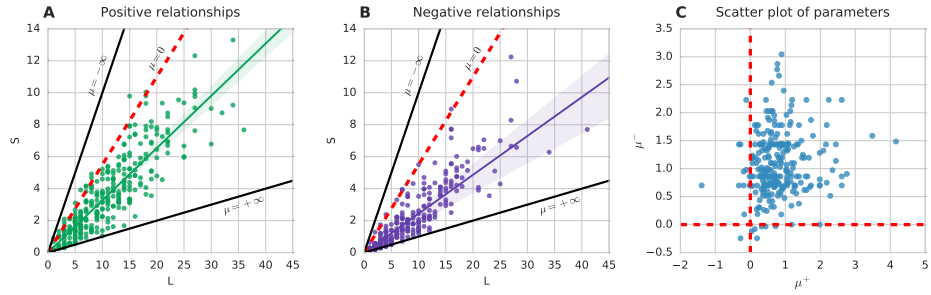


**Figure 5.2: Parameter estimates for positive and negative relationships (I). A,** Linear regression $S \sim L$ for the positive relationships ($n = 300$, the individuals with no relationships have been excluded). The fitted line ($R^2 = 0.77$) has a slope of $0.32$ ($[0.31, 0.35]_{99\%}$), resulting in an estimated value of $\mu^+ = 0.67$ ($[0.60, 0.75]_{99\%}$) —see Methods. The green, shadowed region corresponds to the $99\%$ confidence interval for the slope. An outlier with $L = 51, S = 13.5$ has been excluded in the plot but taken into consideration in the fitting. **B,** Linear regression $S \sim L$ for the negative relationships ($n = 284$). The fitted line ($R^2 = 0.73$) has a slope of $0.24$ ($[0.19, 0.28]_{99\%}$), which results in an estimated value of $\mu^- = 1.05$ ($[0.88, 1.46]_{99\%}$) —see Methods. The purple,shadowed region corresponds to the $99\%$ confidence interval for the slope. An outlier with $L = 85, S = 12.6$ has been excluded in the plot but taken into consideration in the fitting. **C,** Scatter plot of pairs of parameters. The figure shows the pairs $(\mu^+, \mu^-)$ for the 268 cases for which we can estimate both $\mu^+$ and $\mu^-$ for the same individual —see Methods . The Pearson correlation coefficient is small ($r = 0.14$) and, although $p = 0.03$, the $99\%$ confidence interval ($[-0.01, 0.28]_{99\%}$) crosses zero.

Notice that the confidence intervals of the estimates for both types of relationships do not overlap, so the hypothesis that both values are indeed the same should be rejected.

The values of the estimated parameters are close to the typically observed scaling of circles (Zhou et al., 2005; Dunbar, 2018) $\sim 3$, which would correspond to $\mu \approx 1.01$. The positive networks, however, exhibit a slightly lower value, 0.67, which would indicate a higher tendency to stablish strong relationships over acquaintances. In any case, both types of networks exhibit a preferred, positive scaling, which translates into personal networks typically organised with disproportionally more weak rela-

tionships than strong ones(Hill and Dunbar, 2003; Dunbar, 2016; Tamarit et al., 2018).

Positive and negative relationships seem to be characterised by particular (and different) values of the parameters, but there also exists variability across individuals—notice the dispersion of points in Figs. 5.2A and 5.2B. Next, we analyse if there is any connection between the parameters estimates of a given individual in the different networks ($\mu^+$ and $\mu^-$). In Fig. 5.2C we show the scatter plots for the cases in which we can estimate both $\mu^+$ and $\mu^-$ for the same individual[1]. Although there exists a weak correlation ($r = 0.14, p = 0.03$), the 99% confidence interval ($[-0.01, 0.28]_{99\%}$) includes the zero, so the the hypothesis that there exists no correlation can not be rejected —and in any case it is weak. In agreement with the fact that the out-degree distributions are not correlated (see Table 5.1), this result endorses that the internal organisation of positive and negative personal networks follow independent (but similar) patterns for every individual.

## 5.3 Further evidence: an additional experiment

So far we have presented results from a single sociometric study conducted in a school. We have focused on analysing the structure of personal networks of positive and negative relationships, and found that the similarities between them are considerable. More importantly, perhaps, we have shown that our model of the social atom (Tamarit et al., 2018) also applies to antagonistic relationships. Notice that the implications of this result are profound, since we present (at least) *prima facie* evidence that an equivalent pattern to *Dunbar's circles* also exists for negative relationships.

We acknowledge, nevertheless, that the study we have presented has limitations that may weaken the conclusions we can draw from it. Firstly, the intensity of the links had to be inferred from indirect measures such as multiplexity and reciprocity (see section 5.2.1), and, although these measures are reasonable proxies (Marsden and Campbell, 1984; Fried-

[1]The individuals' parameters are estimated as explained in section 5.2.2 but using simply the corresponding value $S/L$ of the individual—not the estimated slope of the regression. We excluded values for which either $L = 0$ or $|\mu| > 10$ —which are considered divergences. The confidence interval for the Pearson correlation coefficient is also computed used Bca Bootstrap ($n_{samples} = 10^6$).

kin, 1980; Granovetter, 1977), it is uncertain to what extent this particular choice may impact the results. Additionally, some of the questions indicated a higher level of proximity (for example SP) so, according to our model and the underlying theory, should incur in a higher cost. Secondly, the number of questions about positive and negative relationships was not balanced, so the results for both networks are hardly comparable. Most of these limitations are due to the fact that the experiment was designed having other research questions in mind—see also Chapter 4. To overcome this issue and assess the robustness of the (bold) results we present in this chapter, we performed a second study designed to measure the intensities in a more clean and balanced manner.

### 5.3.1 Experimental design

The new study was performed in December 2018 (13-21) in the same school we described in Chapter 4. This time, the teachers were instructed to independently carry out the data collection using *Conectaula* (see Appendix C.2). The pool of participants included 432 individuals (179 males) from grades 5-11 (ages ranging 10-17), but one of the courses (grade 11) ended up not doing the study. Eventually, we collected data from 343 students (148 males). The questionnaire included several questions organised in three main sections: social information, educational attainment, and use of technologies—it took about 30 minutes to be completed. This study is part of a set of experiments in which we explore the formation and diffusion of social norms. Here, we will briefly describe the main results regarding the organisation of antipathetic and sympathetic personal networks. Unfortunately, the file the school uploaded with the personal information of the students had a format error. As a consequence, the identifiers of the participants do not match the ones from our previous study— and we cannot treat this as a longitudinal study.

The new questionnaire was designed having several *desiderata* into account. Our goal was to get information about the entire personal network of the students in a weighted manner, so that no external assignment of intensities was in order—see section 5.2.1. Ideally, students would select any other peer in the school and “rate” his or her relationship with that person

in a Likert scale. Our software, however, does not provide that feature [2], so we opted for a simplified, direct set of questions divided in two parallel blocks of positive and negative relationships[3]:

The questions regarding positive relationships were as follows (see Appendix D.1 for the original version in Spanish):

> ♥ Who are your friends at school?
>
> ♥♥ Considering your friends: With whom do you have a closer relationship?
>
> ♥♥♥ Finally, among your closest friends: who would you say are your best friends? (We are referring to those people with whom you are ”flesh and bone”).

Negative relationships were asked in the following way:

> ☠ Which schoolmates you do not quite like or do not have a good relationship with?
>
> ☠☠ Considering people you do not quite like: who do you dislike or do you usually have problems with?
>
> ☠☠☠ Lastly, considering people you dislike: is there any person with whom you have a particularly bad or problematic relationship?

As can be observed, in both cases the structure of the questions is inclusive, reflecting how the social circles were defined in section 2.1.3. First we ask about the relationships (positive/negative) of lesser intensity and progressively increase the level of proximity. Therefore, it is to be expected that if a person is marked in a category of higher intensity (i.e. ♥♥♥ ), he or she has also been marked in the categories of lower intensity (i.e. ♥♥, and ♥ ).

[2]We have collaborated in the design of a questionnaire for the company *BraveUp* which will include this option. See Chapter 6, section 6.3.1 for details.

[3]Each question was displayed on a different page. The students had to click “next” (“back”) to proceed between questions.

### 5.3.2 Results

In Fig. 5.3 we see how the intersection patterns of the different networks reflect the inclusive nature of the questions. In the positive networks (Fig. 5.3B), 89% of the most intense relationships (♥♥♥) were also selected as medium (♥♥) and low (♥), and 95% of the medium ones (♥♥) were included also as low (♥). The results regarding negative relationships (Fig. 5.3B) show that 62% of the most intense (negative) relationships were reported also in the lower categories, and 76% of the medium ones were reported as low. Compared to the results obtained for sympathetic relationships (Fig. 5.3B), this result indicates that the inclusive nature of the questions was worse understood. In addition, in Fig. 5.3C we can see how a small proportion (1.9%) of links were reported as both positive and negative, indicating the presence of some noise in the data—but lower than in the previous study.

Assigning a weight to the relationships is straight forward thanks to the new set of questions. The intensity of a (directed) link is simply taken to be the highest level reported. For consistency, we will refer to the different levels as layers, and to its inclusion as circles—see Chapter 2. The average number of alters (and its standard deviation) in the positive layers was $\ell_1^+ =$ 4.44 (5.25), $\ell_2^+ = 3.73$ (4.07), and $\ell_3^+ = 10.23$ (7.69). Notice that the most intense relationships show again an average value $\sim 5$, and the overall size of the personal networks is 18.53 (10.80), close to 15. Additionally, $\ell_2^+$ is the least populated layer reflecting that relationships tend to group in either the first layer (support clique) or the third (the rest of the sympathy group).

The average values for the negative relationships are $\ell_1^- = 0.91$ (1.66), $\ell_2^- = 1.44$ (2.61), and $\ell_3^- = 4.52$ (7.41), thus, on average, the total number of negative relationships is 6.86 (08.49), a lower value than in our previous study, 9.04—see section 5.1.2. Actually, the network DN had itself an average degree of 5.97, so it seems that the refinement of the questions has lead to a higher resolution in the most intense relationships, not the less intense ones—perhaps, the first item (k) was already direct enough to elicit strong relationships.

In a nutshell, in section 5.2.3 we obtained one main result: positive and negative relationships were organised around distinct, uncorrelated values of the parameter ($\mu > 0$). That is, the organisation of antipathetic personal

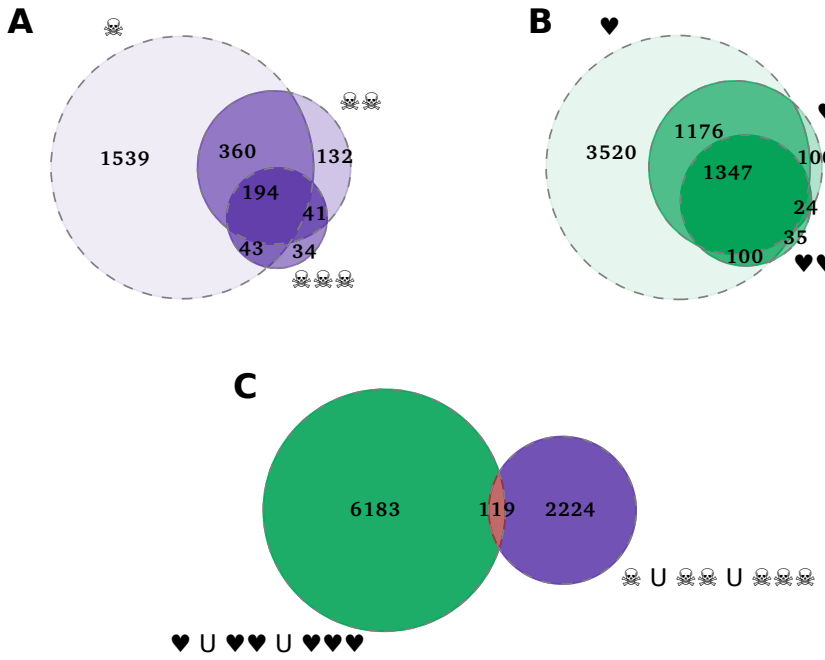


**Figure 5.3: Network overlap (II).** All figures are Venn diagrams of the number of edges common to the corresponding overlapping networks. **A,** Overlapping of negative networks. **B,** Overlapping of positive networks. **C,** Non-overlap of positive and negative networks.

networks mirrored that of the sympathetic ones. The results from the second study confirm this fact. Both types of relationships fit remarkably well ($R^2_+ = 0.82$ and $R^2_- = 0.85$) to straight lines with distinct values of the parameters ($\mu^+ = 0.38, \mu^- = 0.96$)—see caption in Fig. 5.4 for details. Furthermore, Fig. 5.4C reveals, as it did in section 5.2.3, that the pairs $(\mu^+, \mu^-)$ are not correlated; hence, both networks are organised independently.

## 5.4 Discussion

In this chapter we have presented results on the organisation of positive and negative personal networks. The data we used was obtained in two separate studies (with different sets of questions) performed in the same

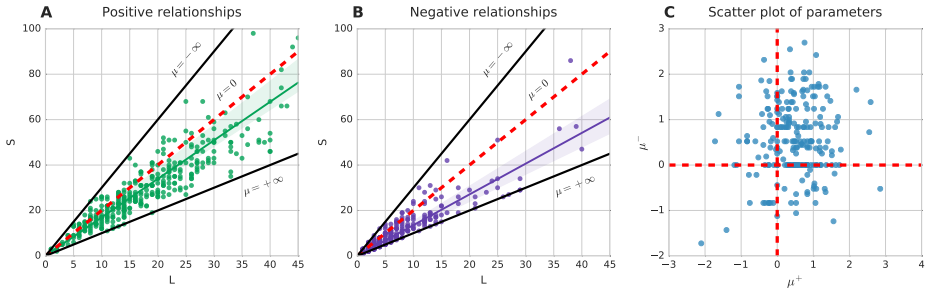


**Figure 5.4: Parameter estimates for positive and negative relationships (II).** This figure is equivalent to Fig. 5.2 but with data from a second study—see section 5.3 and 5.2.2 for details. **A,** Linear regression $S \sim L$ for the positive relationships ($n = 342$). The data are grouped around a straight line ($R^2 = 0.82$) with estimated value of $\mu^+ = 0.38$ ($[0.09, 0.50]_{99\%}$) —see section 5.2.2. The green, shadowed region corresponds to the 99% confidence interval for the slope. **B,** Linear regression $S \sim L$ for the negative relationships ($n = 312$). The fitted line ($R^2 = 0.85$) results in an estimated value of $\mu^- = 0.96$ ($[0.62, 1.44]_{99\%}$). The purple,shadowed region corresponds to the 99% confidence interval for the slope. **C,** Scatter plot of pairs of parameters. The figure shows the pairs $(\mu^+, \mu^-)$ for the 226 cases for which we can estimate both $\mu^+$ and $\mu^-$ for the same individual. The Pearson correlation coefficient is very small ($r = 0.07$) and the 99% confidence interval ($[-0.12, 0.28]_{99\%}$) broadly crosses zero—so there is no correlation.

school—sample sizes $\sim 300$. In both cases, the average number of positive relationships converged to $\sim 15$, the typical size of *sympathy groups*, and the number of most intimate ones was compatible with the typical size of the *support networks*(Dunbar, 2018) $\sim 5$.

It is remarkable that these numbers arise in a setting in which the universe was restricted to schoolmates, without considering family members and other possible relationships from outside the school. However, ours is not the only setting in which a restrictive social environment exhibits numbers in agreement with these social circles—see also Chapters 2 and 3. A good example is provided by on-line social networks (OSN) such as Facebook or Twitter, in which this precise structure has also been found (Dunbar et al., 2015). In this case, it is likewise unlikely that all social

relationships of the individuals occur within the boundaries of such platforms.

Both the school and the OSN can be regarded as closed, social environments in which an individual establishes relationships in a very concentrated social environment. The fact that the structure of (positive) personal networks in such settings resembles that of an entire, open social environment suggests that this pattern of relationships, the circles and their characteristic sizes (or their scaling), act as a sort of "template" that is reproduced at different scales, in different environments(Fuchs et al., 2014; Saramäki et al., 2014).

More surprising is the finding that personal networks of negative relationships are organised similarly. In other words, that an equivalent pattern to *Dunbar's circles* also exists for negative relationships. However, the size of the negative networks was significantly lower in both studies, and the central value of $\mu^-$ was higher than $\mu^+$. These two facts taken together suggest that the amount of energy we devote to negative relationships is somewhat lower than the one we dedicate to positive ones. Nevertheless, it is a bit far-fetched to ensure that the intensities of the bonds, as we have measured them, are also comparable in their costs, so the only thing we can affirm is that the size of negative personal networks is smaller than the corresponding for positive (Card, 2010).

Our results further suggest that, from the ego's viewpoint, positive and negative networks are intrinsically different, working as separate, but self-consistent, social environments. As we have seen, their degree distributions were not correlated, and both exhibited different, but self-consistent scaling patterns. Thus, from the individuals' perspective, positive and negative relationships seem to be idiosyncratically different. In the light of the model described in the introduction (Tamarit et al., 2018), these results have a precise interpretation. If we assume that individuals devote a certain amount of resource to each of the different social environments, then, the internal organization of such networks would still be governed by Eq. 2.17. That is, in each of these contexts, a given amount of resource has to be allocated among the different relationships as if that particular context was the only one available.

A good example of this would be precisely the scenario on which this (and the previous) chapter focuses: a school. Although students may cer-

tainly have relationships outside the centre, the school's social ecosystem functions as an independent entity in which they spend a given amount of time and are *forced* to interact socially with a more or less stable set of individuals. These are the individuals with whom they share most common interests (the homophily effect (McPherson et al., 2001)) and hence are the individuals they feel most emotionally engaged with.

Nevertheless, if we aggregate all possible social contexts, and their associated costs, we would recover an identical situation where the cost of a relationship is the combination of the ones in the different contexts, and the total limitation of resource is given by the overall capacity of the individual. Indeed, the resulting personal networks would be organised similarly. Furthermore, if the actual equilibrium between resource ($\mathcal{S}$) and size of the personal network ($\mathcal{L}$) occurs around a value of $\mathcal{L} = 150$, with estimated parameter $\mu \sim 1$, then the expected numbers in an hypothetical distribution of alters into four layers would be very similar to the so called Dunbar's circles(Zhou et al., 2005): 5, 15, 50, 150. Therefore, the model gives a plausible explanation for the ubiquity of this type of structure and connects it to an overall limitation on humans' relationships.

The reason why there appears to be a discretisation in the structure of egocentric networks of this kind is uncertain. Indeed, the model allows for any number of layers (or even a continuum, see Chapter 3) and there is no a priori reason to choose one over the other. The dual interpretation of personal networks, that is, whether they have a precise discrete structure or they are a continuum (or, perhaps, both), is an interesting question to be addressed. To shed light on this issue, any closed, social environment in which one can measure the intensity of the relationships of the individuals can be used to test the hypothesis that we indeed use a sort of discrete, social template to manage the complexities of social interaction.

## 5.5 Conclusions

The structure of personal networks of antipathetic relationships mirrors that of the positive ones. Both types of relationships are well described by the social atom model (Tamarit et al., 2018), and each of them seems to be characterised by a different (population-level) positive estimate of the parameter. Interestingly, there exists no correlation between the parame-

ter estimates of different networks, so individuals handle them as separate entities—or social environments.

The average number of negative relationships reported is consistently lower than the number of sympathetic ones. The latter tends to be stable around the typical size of *sympathy groups* (15), and, remarkably, the number of most intense positive relationships was also consistent (in two different settings) with the standard figure for *support groups*, 5.

We argue that the composition of all kinds of personal networks (online, offline, workplace, positive, negative, etc.) seems to be governed by a sort of (psychological) social template that humans adapt to different contexts, with different cognitive demands. The resource allocation within contexts, however, is equally governed by the model presented in this thesis—although the model is indifferent to the precise sizes of the networks.

# 6

# Conclusions and future work

> "It seems that if one is working from the point of view of getting beauty in one's equations, and if one has really a sound insight, one is on a sure line of progress."
>
> *Paul Dirac*
> The evolution of the physicists picture of nature (1963)

This thesis set out to contribute to the realm of social physics, with a special focus on human social networks. In particular, we developed a model of how humans handle social relationships (based on the Social Brain Hypothesis) which has proven to be strikingly accurate and with high predictive power. Building on that seminal theory, we extended our research to cover a continuum description of layers, the structure of personal networks of negative relationships, and the role that negative social relationships have in the overall structure of the social networks. Here we summarise in some detail those main results and outline some further lines of research that open as a consequence of this work.

## 6.1 The social atom

In Chapter 2 we introduced a model that explains the organisation of personal networks as a resource allocation problem. The problem is that of splitting a given amount of resource ($\mathcal{S}$) among a number ($\mathcal{L}$) of relationships that incur in different costs. The allocation of resources determines the proximity, or emotional closeness, of these relationships, which are organised according to the maximum entropy principle. Eventually, the organisation of personal networks depends on a single parameter, $\mu$, which characterises two distinct types of behaviours depending on the ratio $\mathcal{S}/\mathcal{L}$.

When $\mu > 0$ ($\mathcal{S}/\mathcal{L}$ low) the model reproduces pervasive experimental evidence showing that humans organise relationships in a series of hierarchical circles (with characteristic sizes) of increasing size but decreasing intensity, or proximity—we call this the *standard* regime. These social circles ("Dunbar's circles") typically exhibit a more or less constant scaling ratio $\sim 3$, and represent an internal structure to the so call "Dunbar's number". On the other hand, when $\mu < 0$ ($\mathcal{S}/\mathcal{L}$ large) we have that few strong relationships are greatly favoured instead of a larger number of acquaintances—we call this the *inverse* regime. This new type of organisation was predicted by the model and confirmed empirically using data from four different communities of immigrants (Tamarit et al., 2018).

Two different empirical pieces of evidence, namely "Dunbar's number" and "Dunbar's circles", are intimately related to the SBH. However, it was unclear how both facts related to each other. The hierarchical organisation of personal relationships (Dunbar's circles) has, a priori, nothing to do with the existence of an upper limit to the number of these relationships (Dunbar's number). Furthermore, the existence of a constant scaling remained a conundrum (Zhou et al., 2005). Our model provides a precise, mathematical interpretation of how these phenomena emerge from the roots of the SBH. More precisely, as we described in Chapter 2: "when individuals handle a fixed number of relationships (on average) (Hill and Dunbar, 2003; Saramäki et al., 2014; Wang et al., 2016), which are not equally costly (Oswald et al., 2004; Sutcliffe et al., 2012), and they have a constrained capacity (on average) to manage them (Dunbar, 1993; Miritello et al., 2013), then the most likely organisation of these relationships (dic-

tated by the maximum entropy principle) exhibits a constant scaling (Zhou et al., 2005; Hamilton et al., 2007; Dunbar et al., 2015)".

Importantly, the internal organisation of personal networks seems to depend entirely on the ego (and the availability of relationships), and not on the structure of the (emergent) social system. It is a local property, explained by a (cognitive) constraint that applies to all individuals independently. Therefore, it is appropriate to talk of our model as a representation of a social atom, not only because it reproduces a structure of layers and *energies* that could resemble physical particles, but primarily because it describes the cornerstone of any social system: how individuals handle their relationships.

### 6.1.1 Continuous interpretation

As we have seen, the typical structure of the personal networks consists of a discrete set of hierarchically inclusive layers with specific sizes (Zhou et al., 2005). Consequently, the model we first developed in (Tamarit et al., 2018) considered a discrete set of categories (layers). In Chapter 3 we presented an alternative version of this model in which layers were no longer needed and relationships were classified on a continuous scale. The two regimes found in the discrete version also exist in its continuous variant. Remarkably, since the continuous version was built upon the discrete one, we could estimate how the constant scaling of $\sim 3$ ($\mu \approx 1$) translated in this new framework, resulting in a prediction for its (unique) parameter of $\eta \approx 6$—a rough estimation. We confirmed the prediction $\eta \approx 6$ in three different datasets from phone records (Saramäki et al., 2014), face-to-face contacts (Isella et al., 2011), and interactions in Facebook (Arnaboldi et al., 2012).

In other words, as the discrete layers collapse in a continuum, the hierarchical nature gives rise to a universal scaling parameter that does not depend on a particular choice of layers—however, it must be calibrated with a minimum and a maximum for the intensities. Since both versions of the model rely on the same principles, and the parameter estimates are consistent with each other, it follows that the model must be capturing a key feature of how humans allocate social resource—according to the maximum entropy principle.

The continuous interpretation of the social atom presented in Chapter 3 produced additional exciting results. We showed that the estimate of $\eta$ for each individual captures, with a single real number, the so-called social signatures (Saramäki et al., 2014) found in human communications. Moreover, we confirmed that the structure of online relationships in Facebook mirrored the offline world (Arnaboldi et al., 2012; Dunbar et al., 2015). In addition, the distribution of the parameter estimates in this large dataset from Facebook (Arnaboldi et al., 2012) exhibited a long tail of individuals with disproportionally large networks. This result further endorses an earlier statement (Tamarit et al., 2018) that online social networks shall favour the standard regime. Nevertheless, we also found a tiny fraction of individuals (0.3%) with networks in the inverse scheme ($\eta < 0$).

### 6.1.2 The structure of negative personal networks

A significant part of Chapters 4 and 5 aimed to contribute to the growing body of knowledge on negative social relationships (Card, 2010). Remarkably, our experimental results show that the model of social atom (Tamarit et al., 2018) also describes the organisation of antipathetic personal networks. Even though their size is significantly smaller, negative networks also exhibit a hierarchical substructure. Individuals, nonetheless, treat both types of networks separately: There is no correlation either in the number of reported positive and negative links or the parameter estimates ($\mu^+$ and $\mu^-$)—and, unsurprisingly, negative and positive relationships are mutually exclusive.

Our data show that the number of sympathetic relationships tends to be stable around the typical size of *sympathy groups* (15), and, that the number of most intense positive relationships is also consistent with the standard figure for *support groups*, 5. Notice that these particular numbers are ubiquitous in the literature (Dunbar, 1998; Zhou et al., 2005; Dunbar et al., 2015) even though they emerge in somewhat different social contexts. It seems therefore that this specific pattern of organisation acts as a sort of template that helps us to deal with the complexity of social interaction; a structure that we reproduce and adapt to the different contexts in which we interact socially.

Since the model is agnostic towards a discrete or a continuous organisation of the networks (see Chapter 3), the explanation to the ubiquity of characteristic, distinct sizes must be found elsewhere. Nevertheless, if we fix the number of layers and the size of the networks, setting a particular number of alters in any layer would very much determine the organisation of the others. It is particularly interesting that the first layer (support group) may indeed act as a seed to the pattern of the whole structure (Dunbar, 1993; Zhou et al., 2005). Notice that when humans are born, we depend, for quite a few years, on the care of a primary group for our survival. It is therefore reasonable to conjecture that this primary group imprints a sort of model that we use to deal with relationships later on in our lives—in fact, a similar mechanism of social inheritance has been able to explain the structure of other animals' networks (Ilany and Akcay, 2016).

### 6.1.3 Further applications of the model and future work

The models we presented in Chapters 2 and 3 were completely general. The abundant regularities reported in the structure of personal networks (Dunbar, 2018) motivated them, but their principles apply to any situation in which someone has to (more or less freely) assign a limited resource among many options. Here we present just a couple of examples of potential applications of the model, but, given its generality, it may well serve for other (perhaps unexpected) purposes—some of which we are currently exploring or will address in the future.

Firstly, let us notice that the quotient $\mathcal{S}/\mathcal{L}$ seems to be very similar across genera of primates (including humans) (Dunbar, 1993). Besides, although their typical group sizes differ significantly, the same scaling is also present in groups of non-human primates (Dunbar et al., 2018). Hence, we are confident that our model could apply to other complex social species, starting with primates.

Back to humans, organising our networks is not the only situation in which we have to allocate a fixed amount of any resource among differently costly options. A good example is how we distribute our time in familiar locations. In a recent study, Alessandretti et al. (2018) found evidence that the number of places we visit and the way we allocate our time among them are conserved quantities at any point; a picture that clearly resembles what

is found in the organisation of personal networks (Tamarit et al., 2018). Moreover, the same study reports a significant correlation between the total number of places an individual visits and the size of his or her network. It is therefore plausible that the model we presented in Chapter 2 may also lie behind this phenomenon.

A last example worth mentioning is the allocation of time in different tasks within a given context. For instance, let us consider the edition of articles in Wikipedia. A given editor has a practically infinite number of articles to choose from. Naturally, he or she must focus on a reduced set of them. Within this limited set, he or she dedicates different amounts of time to various articles, from correcting a typo, to enter a discussion on a controversial topic. The analogy with our model is apparent if we consider the different articles as the "alters", and the time (or any other measure like the number of edited words) as the *intensity* of the edition.

## 6.2 Atomic (social) ensembles

Beyond the limited resource allocation scenario, having a social atom model that is consistent with (and even anticipates) experimental observations on personal networks allows us to start thinking on the next level of structure in human relationships: social networks. In chapter 4 we delved into this problem for the first time and presented results from a novel experiment carried out in a school—with software designed by the research team. The most important features we observed are:

### 6.2.1 Homophily and gender effects

Our data confirms the presence of relevant gender effects in the composition and the structure of social networks (Shrum et al., 1988; Dijkstra et al., 2007; Roberts et al., 2008; Card, 2010; Berger and Dijkstra, 2013; Stehlé et al., 2013; Laniado et al., 2016). Importantly, these effects are not necessarily symmetrical. Whereas the out-degree distributions of positive relationships showed strong homophily effects, those of negative relationships presented no effects for boys, and a weak *over rejection* of girls towards boys. We also found a similar result in the reciprocity of the relationships. Boys and girls tend to be more reciprocal in positive relationships if the

other person is also a boy or a girl, respectively. Interestingly, this phenomenon is more pronounced in girls, with boys showing no predilection towards any particular gender in the networks of strongest relationships (IPN, IPN*, and SP). Once again, the effects in negative networks are much weaker, and only significant for girls—who tend not to reciprocate bad relationships from other girls, and to *over reciprocate* those coming from boys.

### 6.2.2 Interplay between positive and negative networks

One of the most striking results of this thesis came from exploring the interplay between positive and negative networks—Chapter 4. Using state-of-the-art machine learning techniques (Therneau and Atkinson, 1997; Liaw and Wiener, 2002; Dimitriadou et al., 2011) we found that most of the information that determines the existence of links (and therefore the overall structure of the networks) is contained in the way in which the various personal networks are intertwined.

When the information given was the number of alters (in and out edges) in a positive network (UPN), and the number of common acquaintances, the algorithms reached an accuracy of 92% predicting the existence of a (directed) link in the same network. More surprisingly, if the same information was provided, but this time from the negative relationships, the algorithms were still able to predict the existence of a positive, directed link with an accuracy of 86%. Interestingly, the results are (practically) symmetrical with respect to the *sign* of the relationship. Our results may confirm the underlying hypothesis of theories such as the *Social Balance Theory* (Cartwright and Harary, 1956) or the *Status Theory* (Leskovec et al., 2010b), namely that the structures of both types of networks are highly interdependent.

As we have seen, local information about the overlap of personal networks contains an enormous predictive power on the overall structure of a social network. Hence the importance of studying personal networks (Perry et al., 2018): personal networks are not mere subsets of social networks; social networks are ensembles of personal networks.

### 6.2.3 Future work

#### Machine Learning to deal with missing data

One potential application of the results summarised in section 6.2.2 is to help researchers to deal with missing information in sociometric surveys. Indeed, when inferring network measures in a given context, not having complete information may have a major impact on the results (Robins et al., 2004; Kossinets, 2006; Huisman, 2009). Importantly, if the individuals not completing the study can still be nominated by the respondents, our results show that we could reconstruct the networks of these people with high accuracy ($\sim 90\%$)—based solely on the answers given by the respondents.

Notice that, even though this technique might be beneficial for researchers, it also raises some ethical concerns. Indeed, it may well be the case that the non-respondents may have freely decided not to give their data and, nonetheless, the research team would be able to recreate them. A similar situation has been reported in online settings, the so-called *shadow profile hypothesis* (Garcia, 2017), and should also be taken into account when gathering data in off-line, more traditional contexts.

#### The social fluid

This thesis has focused on studying and modelling the way humans handle relationships, but the final goal is to understand the collective behaviour of social systems. The way we humans organise our networks is very stable (Saramäki et al., 2014), deeply rooted in our psychology (Fuchs et al., 2014), and ultimately linked to our brain capacity (Dunbar, 1993). Therefore, any model attempting to characterise global properties of the emergent networks must be (at least) consistent with this constraint of its constituents (Tamarit et al., 2018). Once we have a precise, mathematical description of the latter, the social atom, we can start thinking of building models of social collectives, that is, ensembles of particles.

Let us begin by the simplest scenario; let us build our first *toy*-society. The inhabitants in this *toy*-society inherit a common template given by the model presented in Chapter 2—for simplicity, we stick to the discrete version. This template consists of *social holes*, organised in a series of $r$ layers

with different costs, that must be filled in to achieve balance. Notice that the templates can be controlled by fixing the ratio $\mathcal{S}/\mathcal{L}$ of the population and the number of layers. Then, if a network is not adequately filled, we consider that a sort of *dissonance* (Heider, 1946; Festinger, 1957) acts as potential energy forcing[1] the individuals to try and complete their layers—as physical atoms do when their charges are not balanced.

Notice that our *toy*-society is purely individualistic. A relationship is satisfying (fills in a hole) as long as the person who experiences it believes it so. Reciprocity does (a priori) not matter at all. Each of the inhabitants in our *toy*-society can have a relationship $r_i$ of level $1, 2, \ldots, r$ with any other neighbour. Likewise, that particular neighbour is free to have any relationship ($r_j$) with him or her—or no relationship at all. Consequently, each relationship in the emergent network is characterised by a pair $(r_i, r_j)$. If we assume symmetry, so that the overall network is indifferent to the particular direction of the links, then $(r_i, r_j) \equiv (r_j, r_i)$. In that case, and excluding no-relations ($r_i = 0, r_j = 0$), we have a total of $N_l = (r)(r+3)/2$ possible types of relationships, each of them characterised by a (symmetrical) *energy* $E_{ij}$.

The main insight of the models we want to build is that each of the $N_l$ links may have a different energy, which may affect the overall composition of the social network. This energy determines the stability of the ties and, therefore, the probability that we find them in systems in equilibrium. This approach is connected to the so-called exponential random graph models (ERGM) (Holland and Leinhardt, 1981; Snijders, 2011), which, as Park and Newman (2004) showed, play the role of the Boltzmann distribution in classical statistical mechanics.

Eventually, the whole process reduces to find a suitable graph Hamiltonian for the system (Park and Newman, 2004). The Hamiltonian $H(G)$ determines the probability of observing a particular graph ($G$) (within the ensemble of all possible graphs) as $P(G) = \dfrac{e^{-H(G)}}{Z}$, where $Z$ is the normalisation constant (or *partition function*). In our *toy*-society, a simple version of the Hamiltonian could be the sum of all the energies of the edges in the network. Once we have a suitable Hamiltonian, the partition function

[1] Let us note that the term 'force' is explicitly used in (Heider, 1946) to state how unbalanced situations tend to balance—see also section 1.2

$Z = \sum_G e^{-H(G)}$ encodes the information needed to find the expected values of the parameters (i.e. the different energies $E_{ij}$) given empirical data.

With an appropriate model and suitable data, we can obtain the empirical energies, thus fully characterising the global system (in equilibrium). We can draw predictions about the evolution of the system, expected values for macroscopic variables (such as the reciprocity), and explore how the system would react under different circumstances (such as an increase of its size).

Notice that the relationships in our *toy*-society can be of any *sign* (positive or negative). The set of layers is not restricted to relationships of any kind. However, given the results found in Chapters 4 and 5, we expect that the pairs $(r_i, r_j)$ have the same sign—that is, that someone you consider your *friend* does not have a conflictive relationship with you. Importantly, this situation would be directly reflected in the Hamiltonian, and the energies of such crossed-signs relationships should be (empirically) infinite—reflecting impossible effective states of the system.

The model we have described[2] is just an example of the sort of models that can be built taking as a social unit our model of the social atom. It can be extended with other variables, such as triads and other long-range interactions, or include gendered nodes, to name a few examples. Most importantly, it offers a vision of social collectives that departs, conceptually, from the classic notion of a social network. The mathematical description of such models is indeed closer to a physical system such as a fluid (Park and Newman, 2004) than to the static viewpoint of networks.

We are well aware that the classic theory of networks contemplates temporal evolution (Holme and Saramäki, 2012), the possibility of interactions in multiple layers (Kivelä et al., 2014), and so many other variations and generalisations (Snijders, 2011; Newman, 2018)—see also section 1.2. However, this does not mean that it is the most appropriate paradigm to understand social collectives. Take for example the case of a physical fluid. If we take a (high-resolution) picture of a liquid (or a gas) at any time, we would see a set of particles occupying a given space. If we then take a second picture, we would see that these particles have moved, and now

[2] This model is the cornerstone of the Master's Thesis in Mathematical Engineering (UC3M) by Diego Escribano, which is expected to be defended in June 2019 and was co-supervised by the author of this thesis.

hold a different spot. In our quest to understanding this system, we could have decided, in the first picture, that any two particles were *connected* if they happened to be at less than a given distance. Then, the second and subsequent pictures could be used to understand the evolution of the so-constructed networks. Clearly, this method may help us gain insights into the system, but it is not the best way to understand a fluid.

We believe that social systems might be in a similar scenario—albeit at a much slower time scale. Even though each *snapshot* we take might well be represented as a (social) network (Clauset and Eagle, 2012), trying to encapsulate the whole system as a set of nodes and edges might be a bit too far-fetched—the difficulty of recreating inherently dynamic processes via static *snapshots* has, in fact, hindered the development of social physics (Bernard and Killworth, 1979). Just as the particles in a fluid are governed by physical and chemical forces (interactions), social systems seem to be guided by complex psychological patterns (Fuchs et al., 2014; Tamarit et al., 2018) and other social needs (Cartwright and Harary, 1956; Leskovec et al., 2010b). Moreover, the interactions among its constituents (us, humans) occur in a multidimensional space not limited to the physical notion of time and space—indeed, a relationship might be affected by the mental state of one of its members with no intervention whatsoever of the other. Hence, even though networks might be a useful representation of the state of the system at any moment, its true nature seems to be much more subtle and complex. We propose that the right way to understand such systems is as ensembles of personal networks (or social atoms, see Chapter 4) that interact in a multidimensional (social) space, just as physical particles interact in the standard physical dimensions.

## 6.3 Data collection and experiments

This thesis started more as a theoretical endeavour than an experimental one. However, the lack of available data, particularly on negative relationships, encouraged us to perform our own experiments. In the process, we developed experimental software (*Conectaula*, see Appendix C.2 for details) as a by-product of this thesis. The software allowed us to gather high-quality data on both the personal and the social networks of the participants, keeping their identity safe and anonymous.

*Conectaula* is currently being used for a longitudinal study in two different schools. This study is designed to observe the co-evolution of personal and social networks (positive and negative), together with the diffusion and establishment of social norms—with particular emphasis on gender effects. Additionally, other research groups have shown interest in using the software, for example, to analyse the integration of LGBT+ students in UK classrooms.

### 6.3.1 Fighting Bullying with *BraveUp*: future work

One of the most exciting things about the experimental work is that it is inherently connected to reality. The data we collected and analysed in Chapters 4 and 5 belong to real students, for whom their social life is a significant concern—mainly since they are teenagers. Therefore, if our analyses may help the students or the educational institutions, it is really worth pursuing that goal.

One potential application of these studies is to detect and prevent bullying or other social conflicts. For example, during the analysis of the data we presented in this thesis we identified one student with a particularly unusual set of answers. She (or he) reported barely any positive relationships, most of them were not even reciprocal, and she was unhappy about most of her schoolmates—who did not like her back. We reported this situation to the school immediately, but that student had already left the school.

Our experience dealing with experimental settings in schools and network data facilitated the beginning of a collaboration with the company BraveUp[3] , which fights to eradicate bullying from schools. The collaboration includes the design of questionnaires and experimental protocols to be used to gather data with their software—somewhat more sophisticated than *Conectaula*. On the one hand, the data will be used as a necessary companion to the theoretical models of social collectives to be developed (see the previous section). On the other hand, we are optimistic that the use of machine learning techniques may help us anticipate and detect students in a situation of potential risk. The questionnaires and protocols have al-

[3] "BraveUp: plataforma para la mejora de la convivencia escolar", last accessed 25 February 2019, `https://braveup.eu/`.

ready been designed, and we expect to gather longitudinal data on the order of $10^4$ children starting on the second semester of 2019.

# A

# Appendix A

## A.1 Background information on data sources

The community of Bulgarians in Roses (Mestres et al., 2012) is quite recent (average time of residence: 3.5 years). They typically arrived in Catalonia either on their own (to "try their luck"), following migratory family chains (some relatives established first and served as connections), or following a "migratory work chain" (using co-ethnic contacts to join a particular company recently installed in Roses). The initial settlements may also be followed by friends and other acquaintances. In terms of education profiles, they either are well educated or people or have little or no education.

Although the Sikh community is quite numerous, it is also the smallest of the ones analysed in Barcelona (Molina et al., 2015; Molina and Pelissier, 2010). Their religion, Sikhism, is a key aspect of their social lives: 15% of their contacts were made in their religious center. From a social perspective, a Sikh can be differentiated by a series of items with symbolic connotations (the "five Ks"): long and cared-for hair (*Kesh*), a wooden comb for the hair (*Kangha*), an iron dagger (*Kirpan*), short cotton trousers (*Kachera*), and an iron bracelet (*Kara*). Their businesses have a

strong ethnic character. They are predominantly rural males with low levels of education, and a strong feeling of ethnic identity which is promoted by the use of the Punjabi dialect (Molina et al., 2015; Molina and Pelissier, 2010).

Despite being one of the largest groups of immigrants in Catalonia, the Chinese community is also one of the more dispersed (Molina et al., 2015; Molina and Pelissier, 2010). The participants in the study worked mainly in family businesses (restaurants and bazaars). These create structured collectives including all close family members (parents and children) alongside other extended family members. They maintain the use of the Chinese language and encourage its use among children. However, most of them are bilingual, speaking both the dialect of their mother's tongue (unintelligible to other Chinese speakers) plus the official Putonghua.

The former status of Philippines as a Spanish colony has favoured migratory fluxes to Spain for a long time. In 2007, the Filipino community in Barcelona was especially concentrated in the neighbourhood of "Ciutat Vella", and was made of young urban females with intermediate or high levels of education, working in domestic service, and with strong religious (catholic) ties (Molina et al., 2015; Molina and Pelissier, 2010).

## A.2 Supplementary Figures for Chapter 2

Here we show a comprehensive set of figures complementing the ones presented in Chapter 2. In Fig. A.1 we display all the results corresponding to the community of students taking into account four layers, as in the main text. In Fig. A.2 we present the same set but considering five instead of four layers, that is, including the answers: "1- I recognize this person but we never talked" as the weakest type of relationship — see section 2.2.2 for details. Lastly, Figs. A.3 to A.6 show the results for all individuals in the different communities of immigrants.

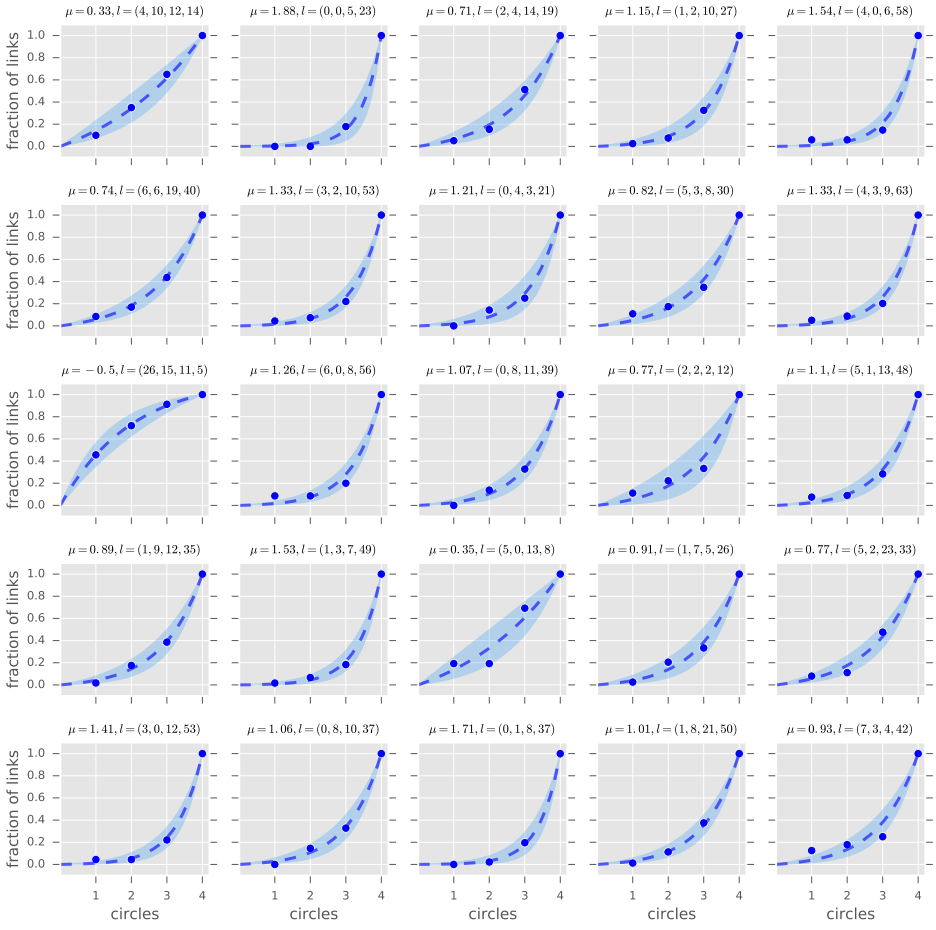


**Figure A.1: Complete set of figures for the fittings in the Students community (case considering four layers 1/4).**

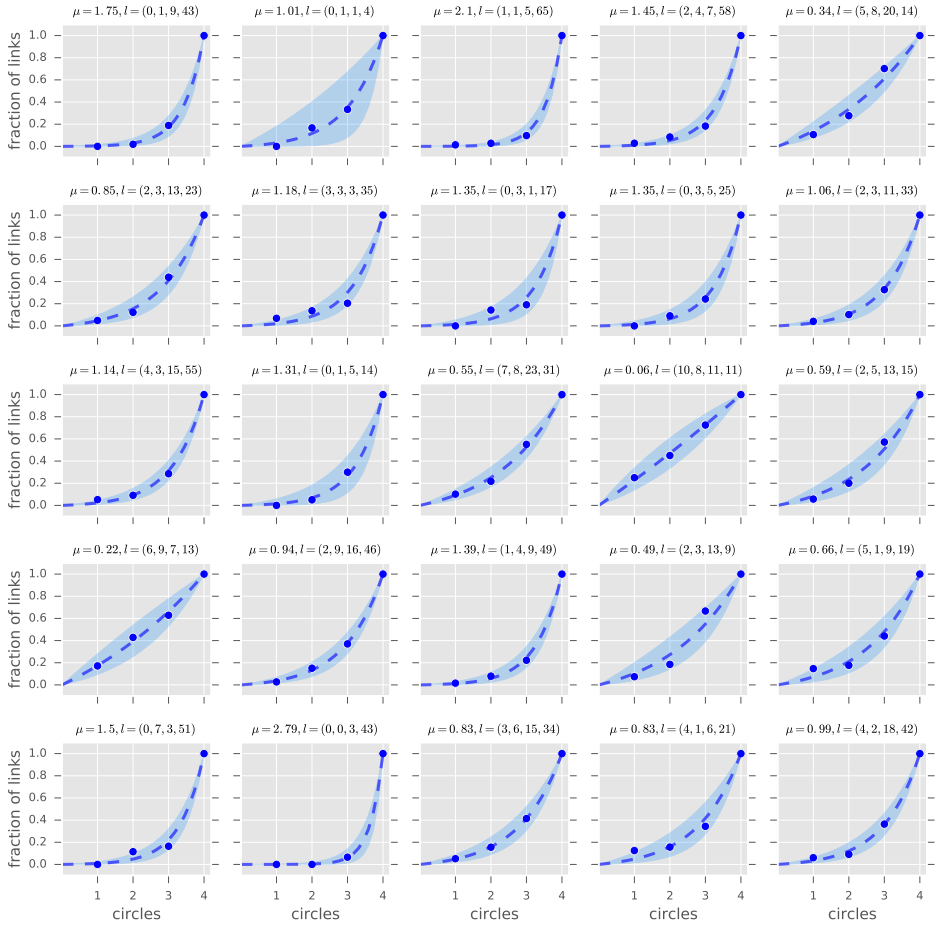


**Figure A.1: Complete set of figures for the fittings in the Students community (case considering four layers 2/4).**

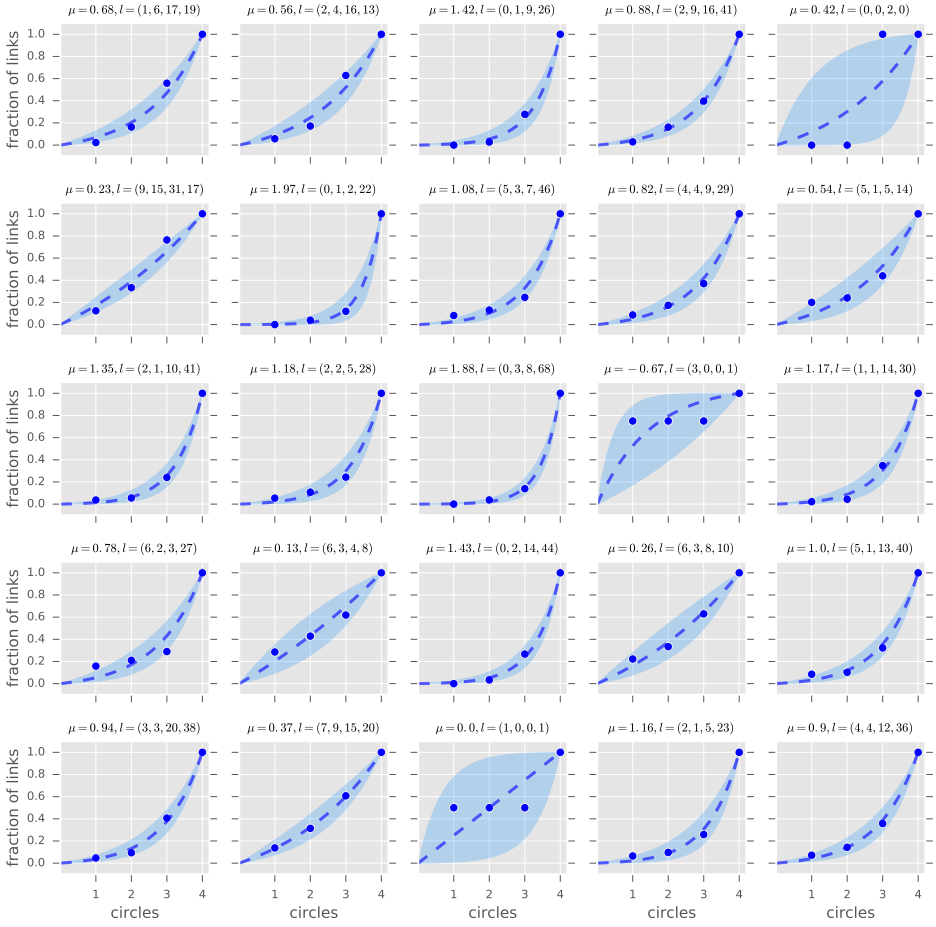


**Figure A.1: Complete set of figures for the fittings in the Students community (case considering four layers 3/4).**

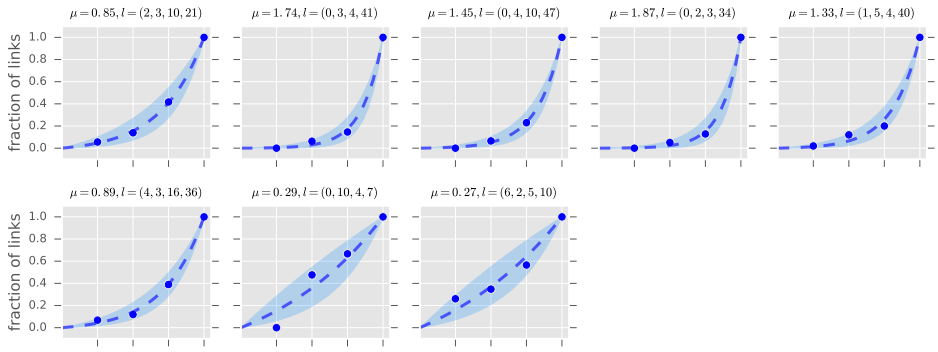


**Figure A.1: Complete set of figures for the fittings in the Students community (case considering four layers 4/4).**

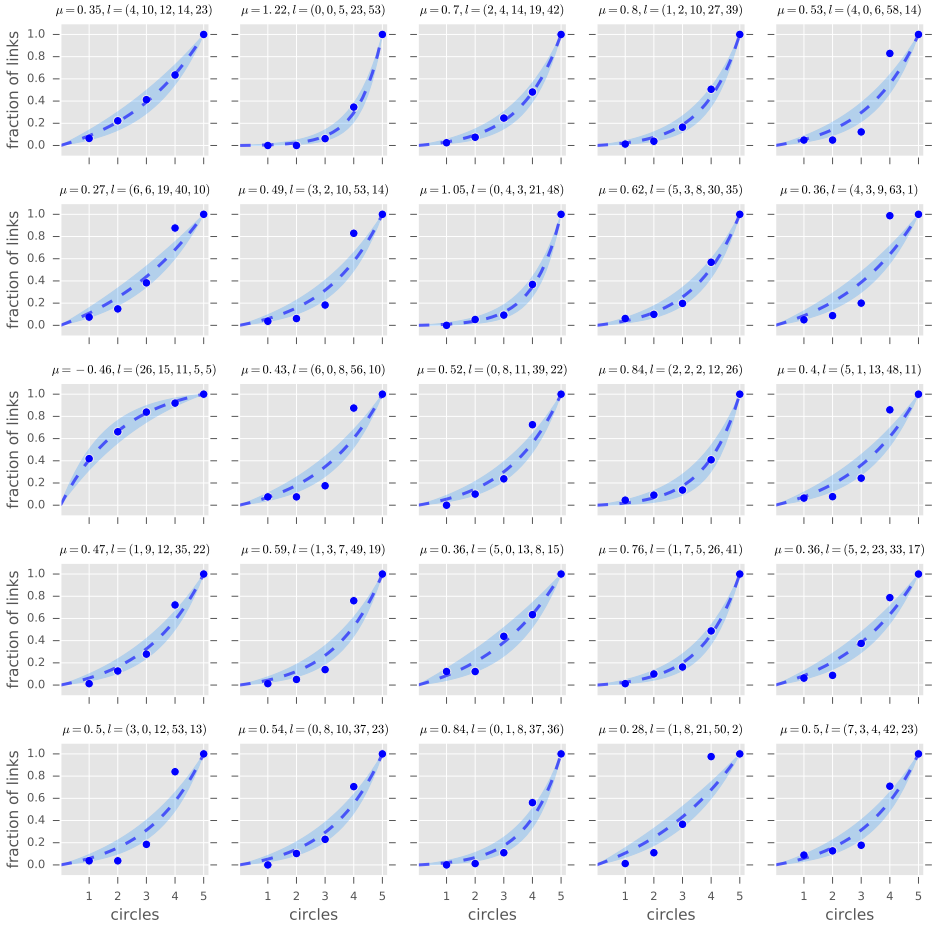


**Figure A.2: Complete set of figures for the fittings in the Students community (case considering five layers 1/4).**

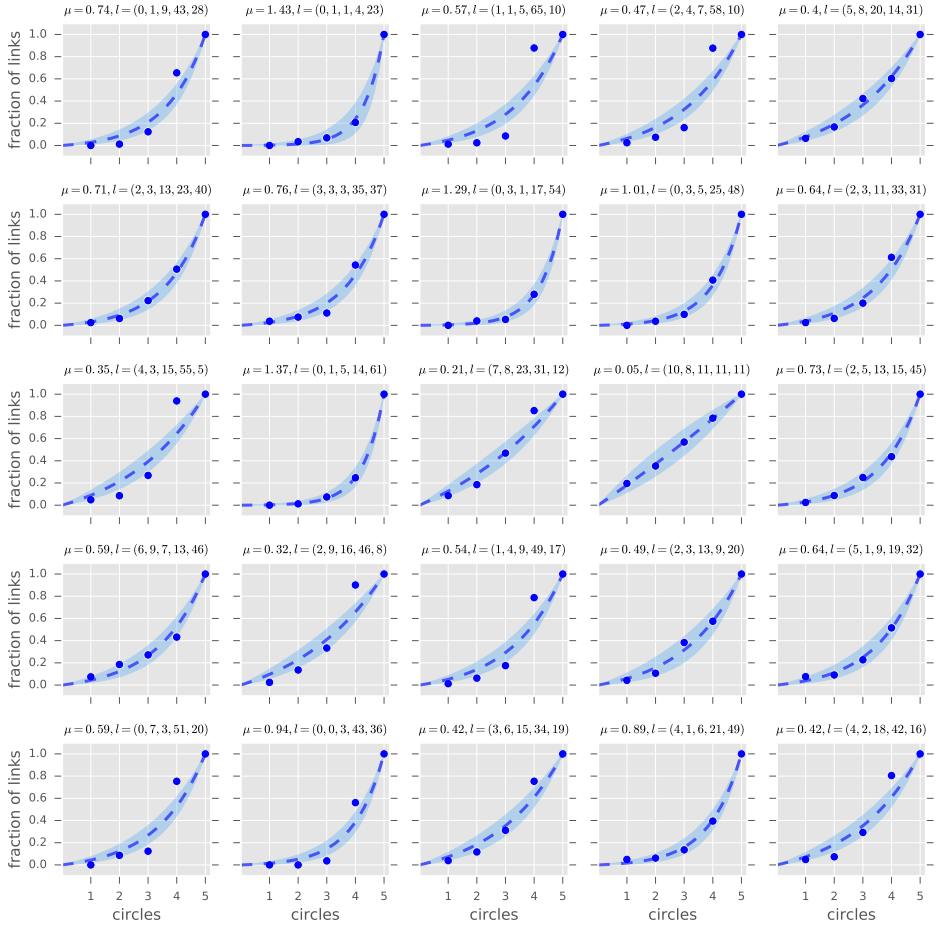


**Figure A.2: Complete set of figures for the fittings in the Students community (case considering five layers 2/4).**

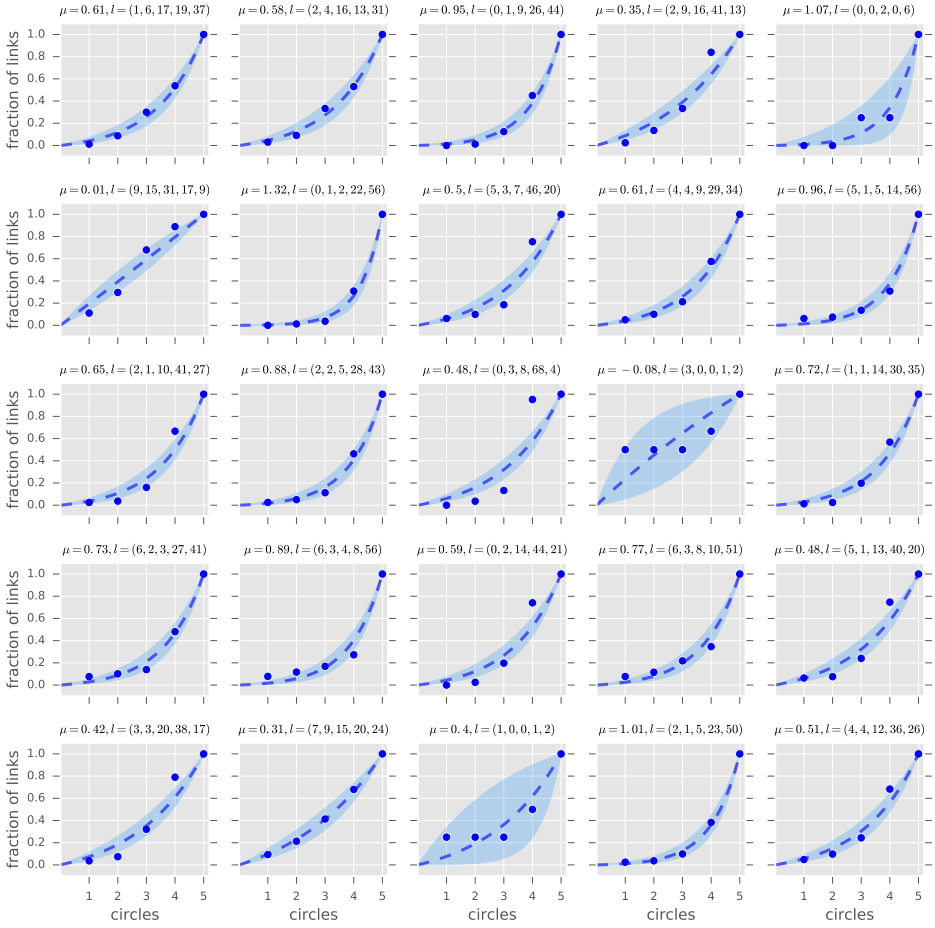


**Figure A.2: Complete set of figures for the fittings in the Students community (case considering five layers 3/4).**

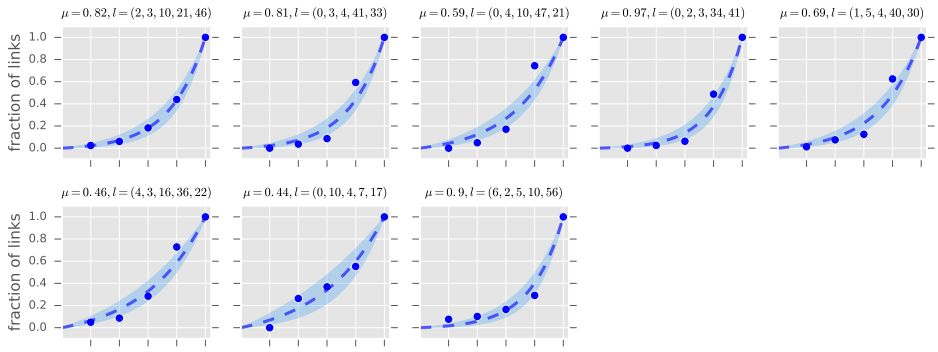


**Figure A.2: Complete set of figures for the fittings in the Students community (case considering five layers 4/4).**

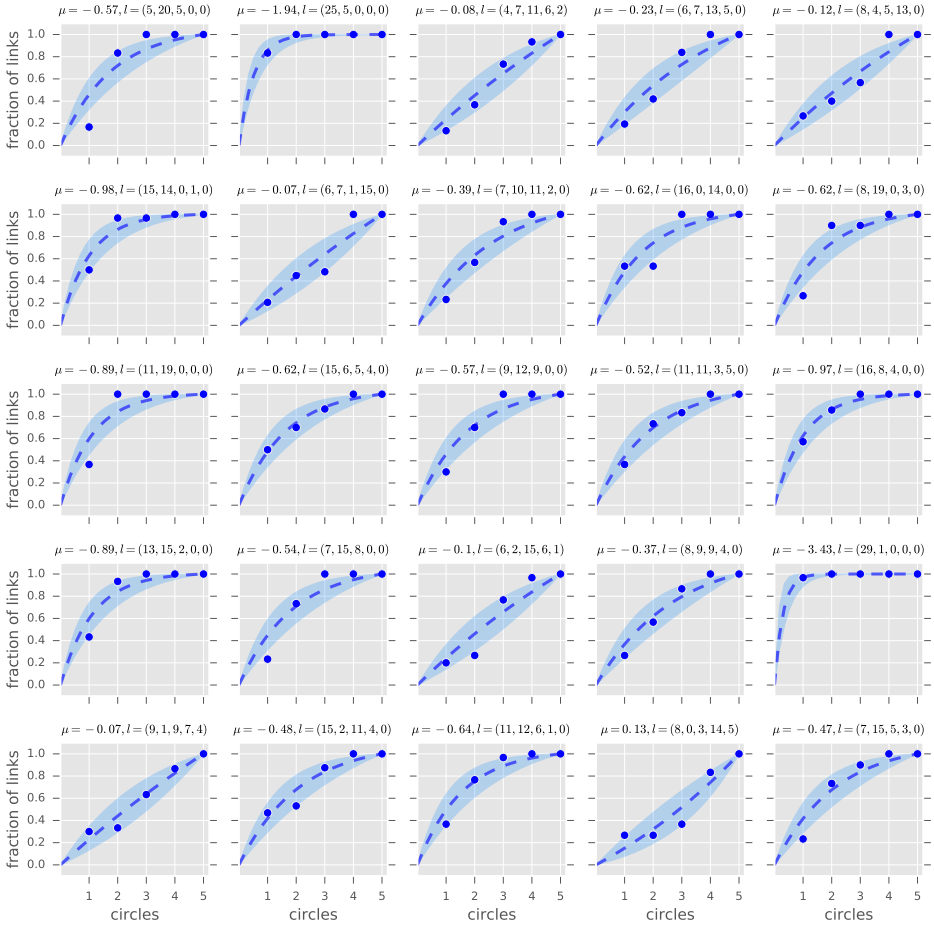


**Figure A.3: Complete set of figures for the fittings in the Bulgarian community**

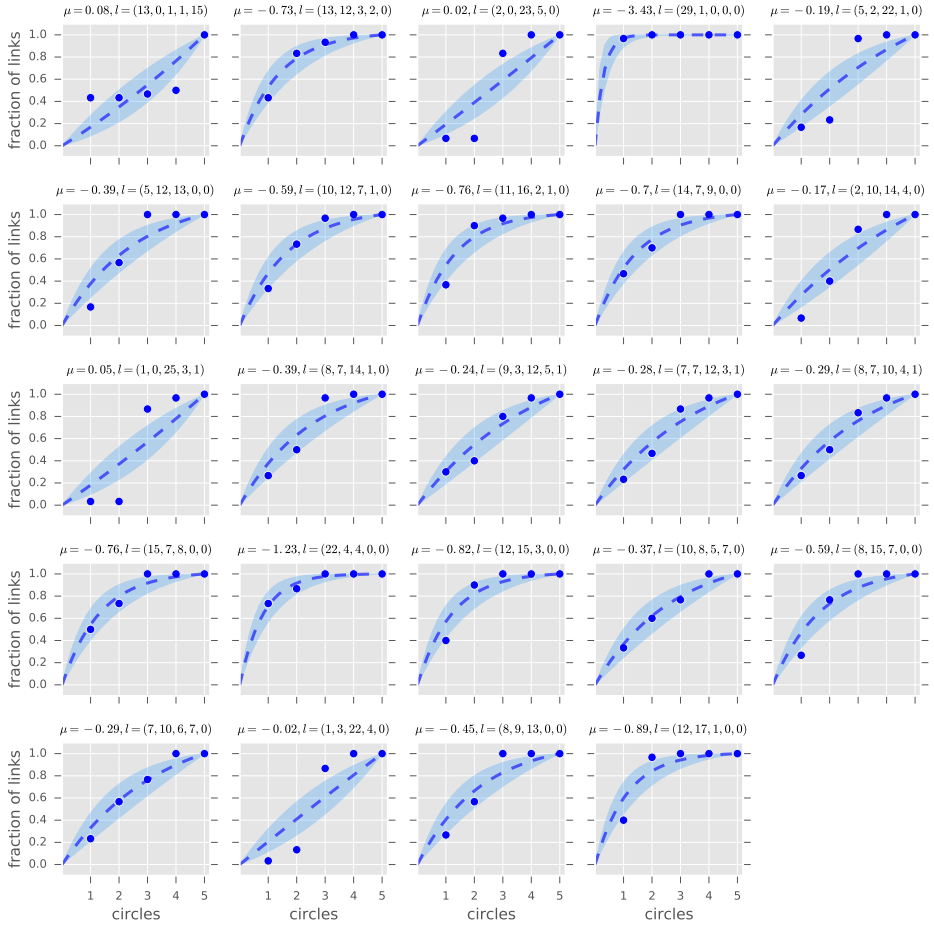


**Figure A.4: Complete set of figures for the fittings in the Sikh community**

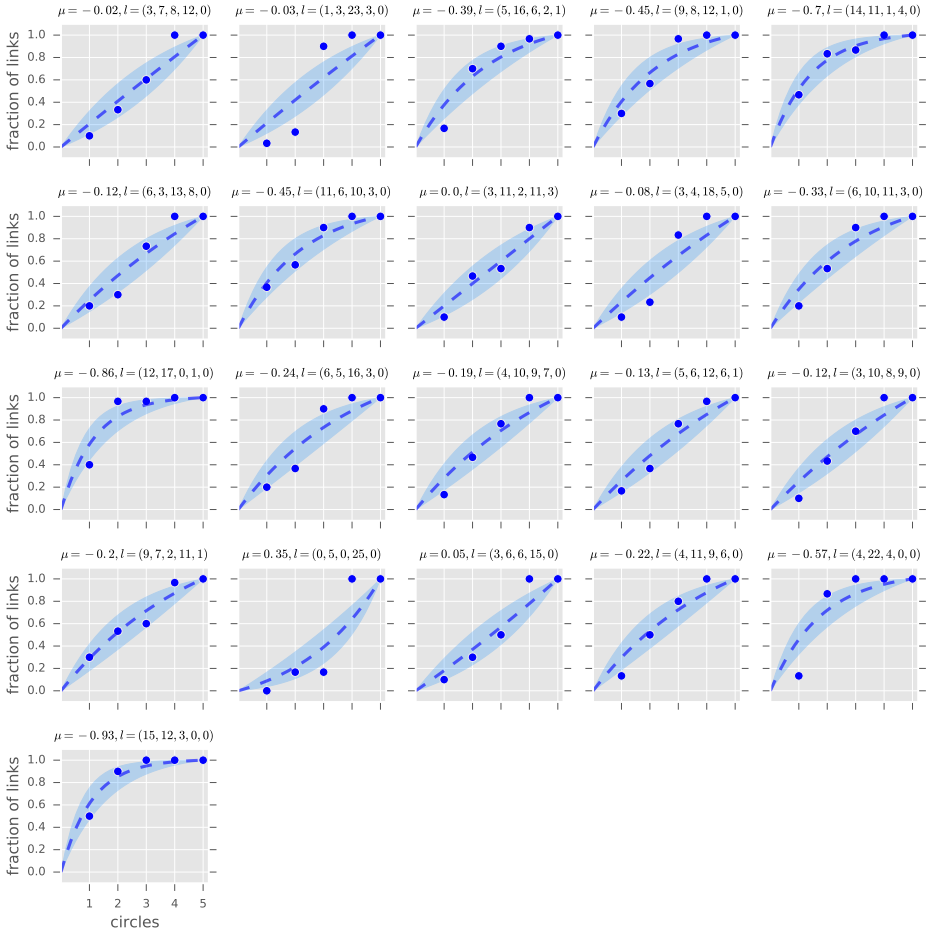


**Figure A.5: Complete set of figures for the fittings in the Chinese community**

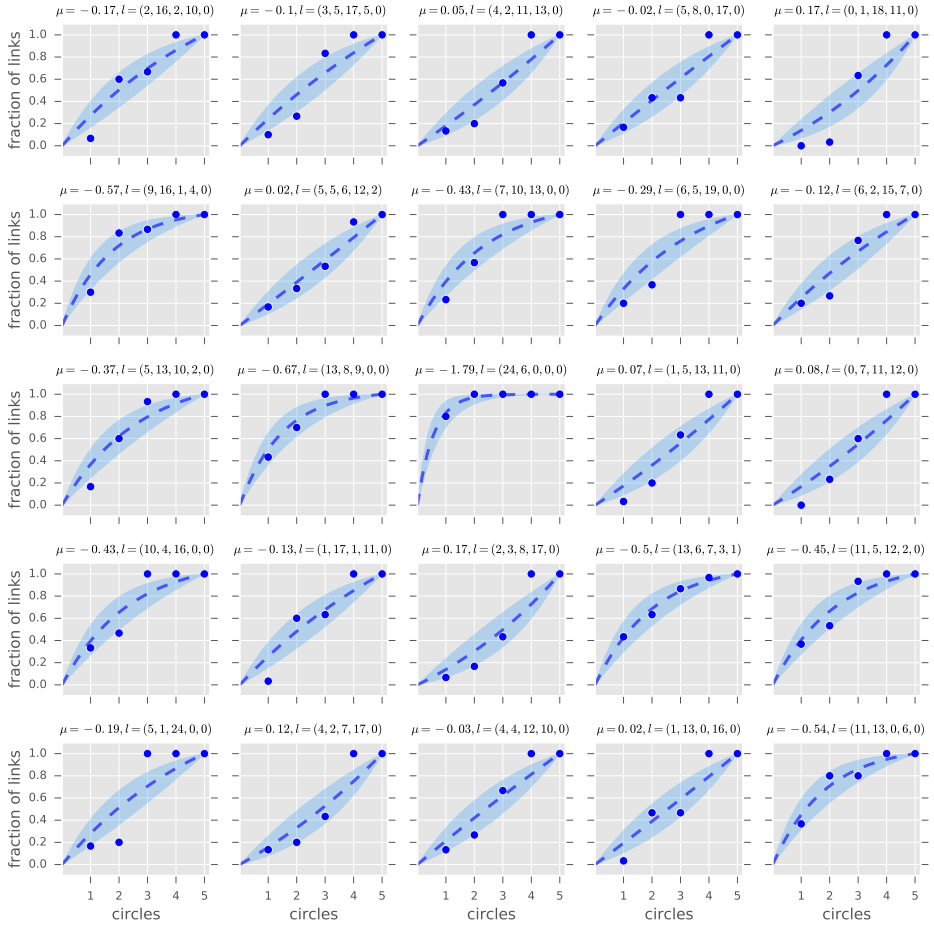


**Figure A.6: Complete set of figures for the fittings in the Filipino community**

# B

# Appendix B

## B.1 Supplementary figures for Chapter 3

### B.1.1 Mobile phones dataset: comprehensive set of figures

Here we show a comprehensive set of figures complementing the ones presented in Chapter 3, section 3.2.2, where we analysed data from mobile phone calls (Saramäki et al., 2014)—see the corresponding section for details and interpretation of the figures. In Fig. B.1 we display all the results corresponding to the first time window ($T1$), in Fig. B.2 the results corresponding to the second time window ($T2$), in Fig. B.3 those corresponding to the third time window ($T3$), and in Fig. B.2 the results corresponding to the full 18 months of the study ($T1 \cup T2 \cup T3$).

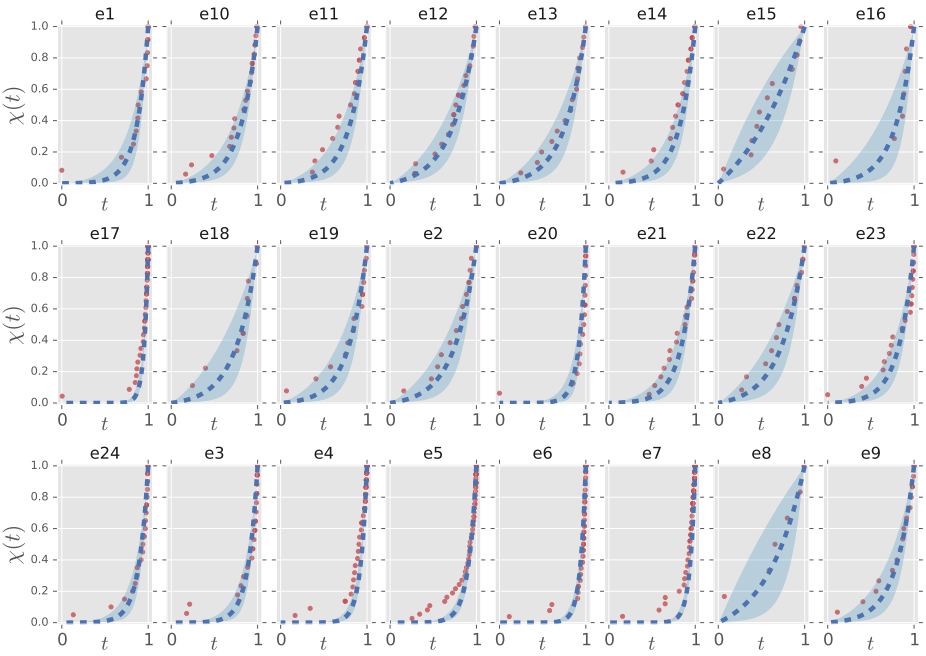


**Figure B.1: Complete set of figures for the fittings in $T1$.**

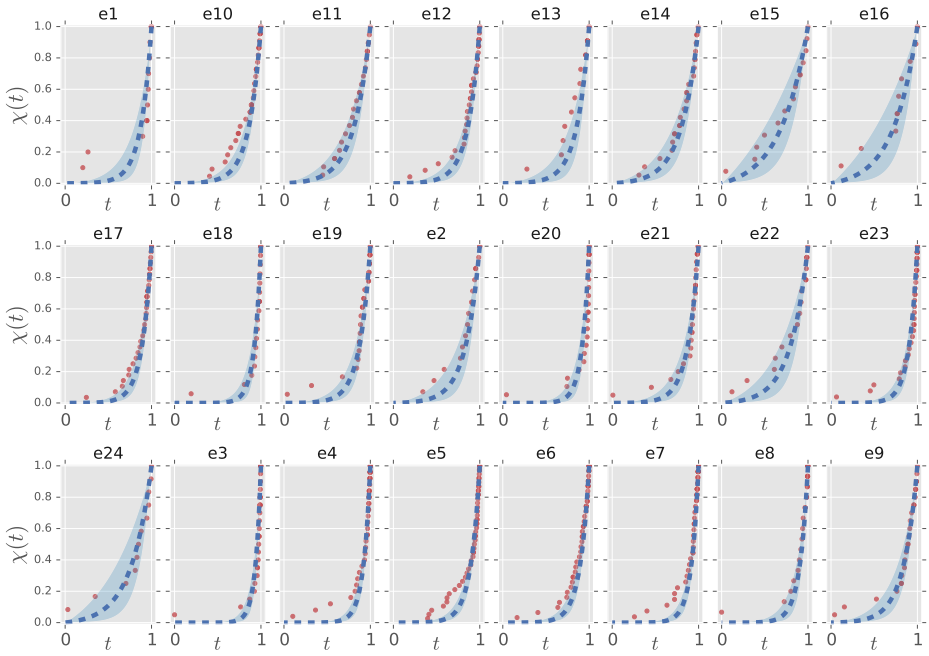


**Figure B.2: Complete set of figures for the fittings in $T2$.**

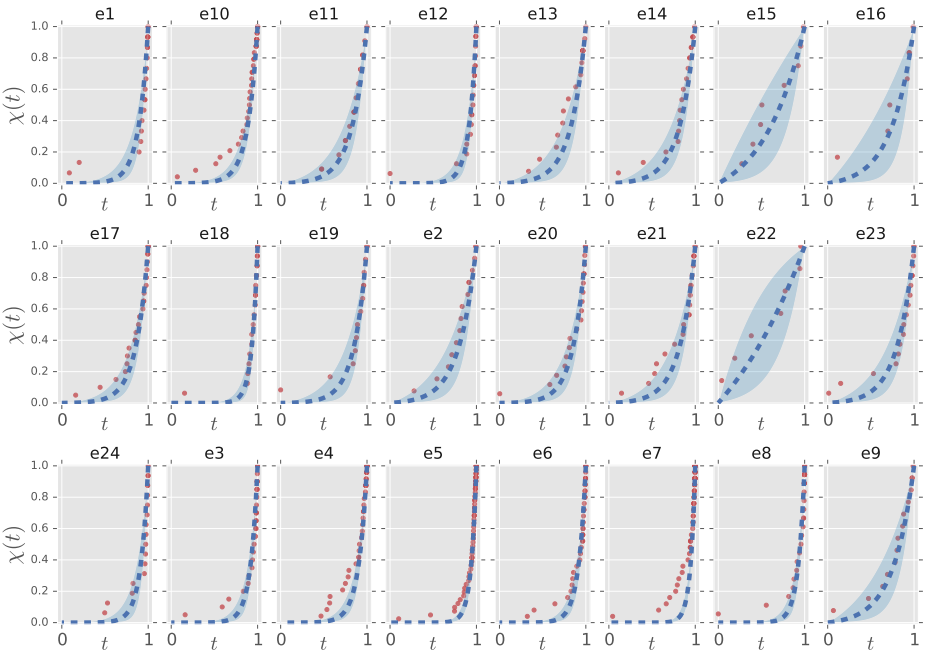


**Figure B.3: Complete set of figures for the fittings in $T3$.**

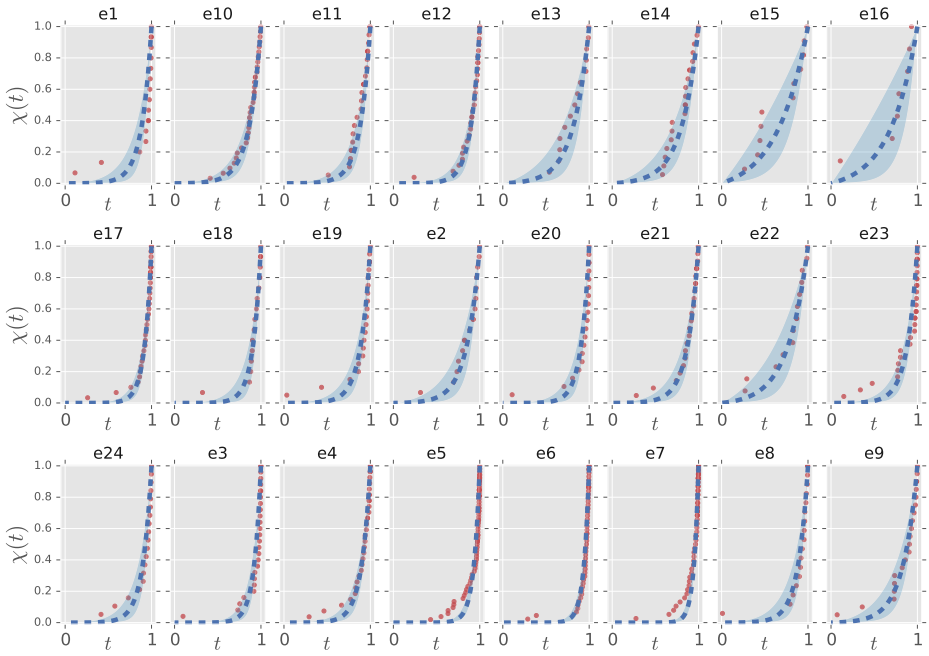


**Figure B.4: Complete set of figures for the fittings in $T1 \cup T2 \cup T3$.**

### B.1.2 Aternative estimation of $s_{min}$ and $s_{max}$: face-to-face contacts dataset

Here we show an equivalent figure to the one we showed in section 3.2.3, but considering the sum of the maximum time spent with any alter on each day as $s_{max}$, and the sum of the minima as $s_{min}$. The individual fittings are slightly worse (Fig. B.5b), and the distribution of the parameter estimates (Fig. B.5a) is centred around a higher value ($\eta \approx 14$) than in the figure shown in the main text (Fig. 3.3a, $\eta \approx 6$). Moreover, filtering out individuals with less than five alters leaves us in this case with a sample of $n = 74$—as opposed to $n = 95$.

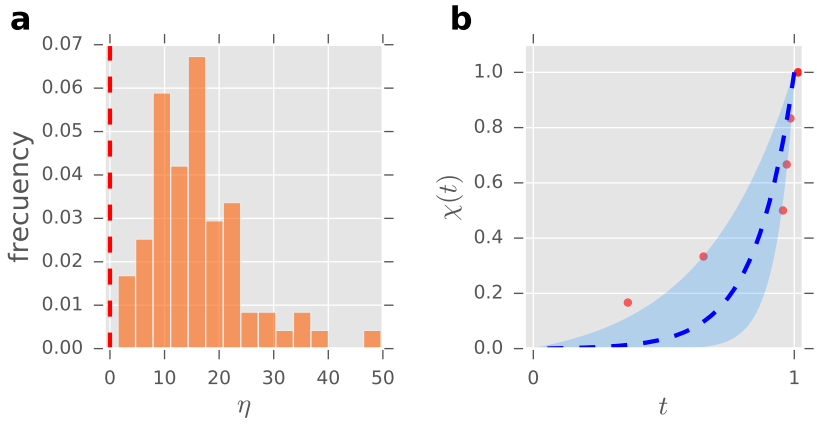


**Figure B.5: Summary of the results for the face-to-face contacts dataset. a,** Distribution of the parameter estimates for the face-to-face contacts dataset ($n = 74$). The red, dashed line marks the change of regime $\eta = 0$; $mean = 16.01$, $median = 14.81$, $mode = 14.33$, $std = 8.57$ **b,** Example of fitting for an individual exhibiting the standard regime (chosen at random from those with $3 < \eta < 9$). Solid dots represent experimental data, blue dashed lines represent the graph of equation (3.4) with the corresponding estimated parameter, and shaded regions show the 95% confidence interval for that estimate (see section 3.2.1). Estimated $\eta = 8.54$, 95% confidence interval $(4.67, 15.29)$, $\tilde{L} = 11$.

### B.1.3 Examples of fittings: face-to-face contacts dataset

Here we show 24 examples of fittings (chosen at random using the same seed as in Fig. 3.3) for individuals in the face-to-face contacts dataset—sampled from the entire population.

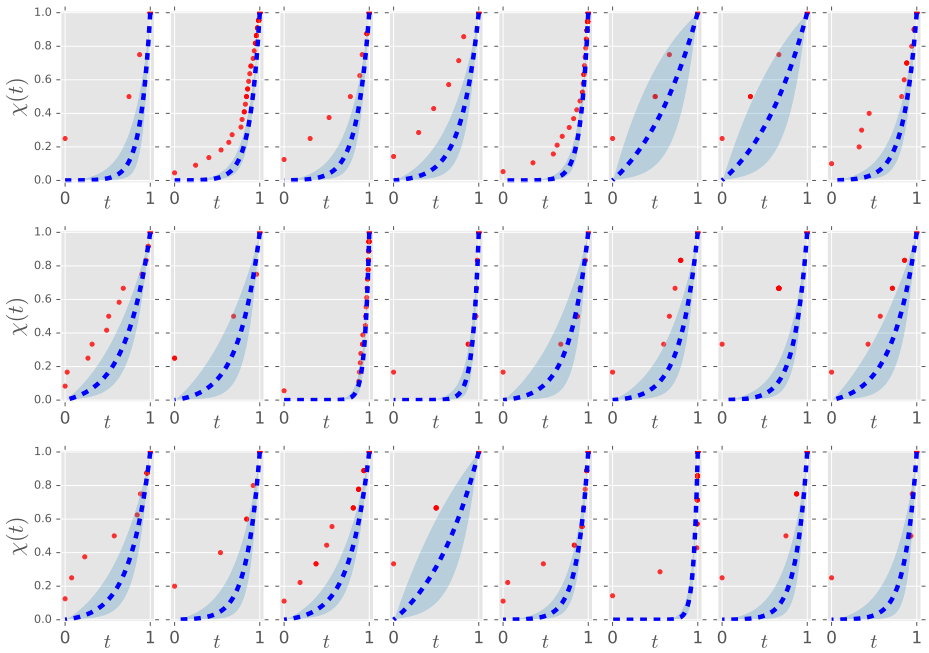


**Figure B.6: Examples of fittings for the face-to-face contacts dataset.**

### B.1.4 Examples of fittings: Facebook dataset

Here we show 24 examples of fittings (chosen at random using the same seed as in Fig. 3.4) for individuals in the Facebook dataset—sampled from the entire population.

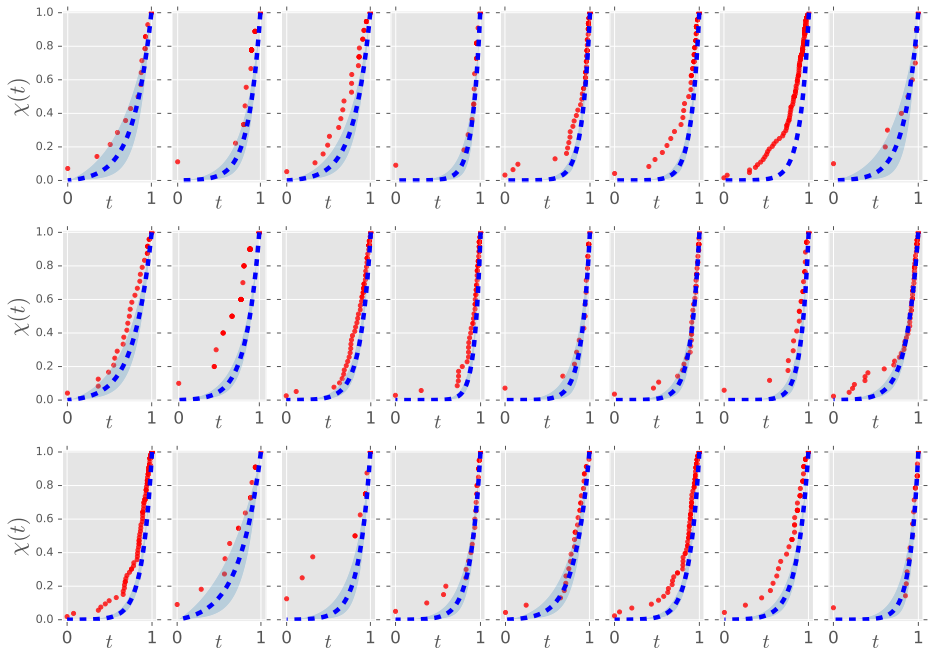


**Figure B.7: Examples of fittings for Facebook dataset.**

C

# Appendix C

## C.1 Social networks questionnaire: Spanish version

- Si tuvieras un problema personal e importante, ¿con qué compañeros y/o compañeras estarías dispuesto/a a compartirlo? (SP)
- Si hay personas que no querrías bajo ningún concepto que se tuvieran que marchar del colegio márcalas, en caso contrario marca la opción "Ninguno". (DL)
- Si pudieras elegir a tus compañeros y compañeras de mesa en el comedor (independientemente del tamaño actual de las mesas), ¿a quiénes escogerías? (LT)
- Si hay personas con las que preferirías no tener que compartir ninguna actividad márcalas. Marca "Ninguno" si no tienes inconveniente en compartir actividades con nadie en particular. (DN)
- Si tienes que hacer un trabajo en el colegio, ¿a quién o quiénes elegirías de compañeros/as? Marca "Ninguno" si prefieres trabajar solo/a. (WW)

- Marca los compañeros/as con los que preferirías no tener que hacer un trabajo en el colegio (independientemente de cómo te lleves con ellos/as). Marca "Ninguno" si no tienes inconveniente en trabajar con nadie en particular. (DW)

## C.2 Experimental software: Conectaula

For the collection of the data we use in Chapters 4 and 5 we developed[1] our own software: *Conectaula*. This software allows for a secure, anonymous, and fast data collection in large social settings. The application consists of three different types of *Users* with the following (brief) description:

- *Admin* (Researcher): This user can create new *Admin* and *Docente* (Teacher) users. Besides, it is the only one able to create *Estudios* (Studies) which he or she links to a specific *Docente*, belonging to a specific *Centro* (School). The *Admin* is the only user that can see the (anonymous) answers of the participants of a study.

- *Docente* (Teacher): This user is created by an *Admin* and is the maximum responsible for the studies within the participating school. His role is to enter the data from the participants by uploading an Excel (or csv) file to the app. Besides, he or she has the rights to "activate" and "deactivate" a given study, that is, to grant access to the participants to enter the platform. All personal data is codified in the Data Base (see Fig. C.1 for a schematic representation of the structure of the database). Once the data of the participants have been uploaded, he or she can send an automatic email to the participants (*Alumnos*) with their credentials to enter the platform. Importantly, this user doesn't have permissions to see either the questions or the answers of a study.

[1] The first fully operative desktop version of the app was designed and developed in `Python` (`Tkinter`) by the author of this thesis. The online version (PHP) was developed afterwards by Juan Zamora and Nieves Maestro: `https://lapizmente.com/` (last accessed 29 January 2019). We are deeply thankful for their professionalism and support throughout all the process.

- *Alumno* (Student): This user is the target participant. He can only access a study (to answer the questions) if both he has correct credentials and the study is activated.

The main feature of the app (indeed, the one that encouraged us to develop it in the first place) is the way it handles questions about social relationships. It has integrated a particular type of question (type *Alumnos*) whose possible answers are the very same participants of the study (excluding in each case the one who is answering), organised in drop-down buttons with the same structure of classes and groups as in the school—that is, class X, group Y. Importantly, although the personal information of the participants is never accessible to the researchers, the participants can see the actual names of their peers on the screen, and click on as many of them as they want.

We have prepared a demo questionnaire that can be accessed (as a student) with the following credentials[2]:

- URL: `https://gisc.uc3m.es/~ConectAula/`
- NÚMERO DE IDENTIFICACIÓN: 1710
- CONTRASEÑA: w62MkiYt

As of January, 29, 2019, *Conectaula* has been used to collect over a thousand surveys in two different schools. The data collected is currently being used for several different research projects—see(Robertson et al., 2019) for an example.

## C.3 Description of network measures

In this section, we briefly describe the network measures used in Chapter 4. Even though most of these measures are standard (Newman, 2018) we include all of them for completeness. All numerical analyses are performed with `Python` and the package `Networkx`.

[2]Please, when reaching the last page (13) just close the tab so that the demo remains active for other users.

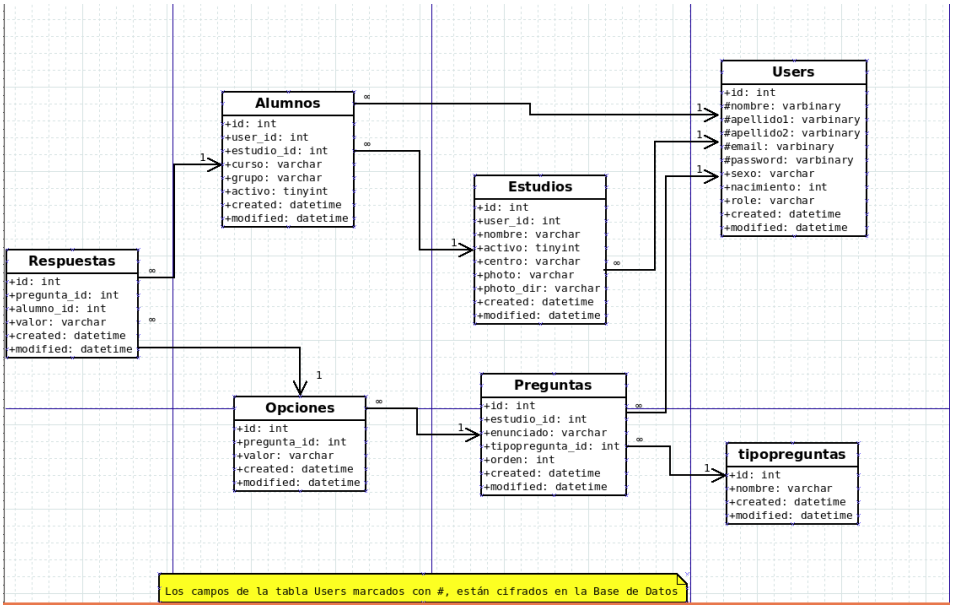


**Figure C.1: Entity-relationship diagram of the database of Conectaula.** The figure depicts a schematic representation of the relationships among the different data (objects) stored in the database. The tables represent "entities", and its contents are the different "attributes" these entities may have. The lines connecting the different entities define how they are related, and the numbers within them represent the "cardinality" of this relationship, that is, the number of entities associated with each other. The fields marked with # are codified in the database.

### C.3.1 Average degree

The *degree* of a node is simply the number of links that this node either sends (*out-degree*) or receives (*in-degree*). The average of this quantity over all nodes in a network is the *average degree*. Notice that, while the average of *in-degrees* and *out-degrees* must be the same (all links sent are received), their standard deviation may differ. To illustrate this point let us use an extreme example. Imagine a network in which every individual sends out three links. Then, the standard deviation of the *out-degrees* would be, obviously, zero. On average, every individual in our imaginary network would receive three links, but these links can actually be

distributed in infinitely many ways, so the standard deviation is not necessarily zero.

### C.3.2 Reciprocity

The *reciprocity* of a given node is the fraction of links coming out that node that also come back to it. The average over all nodes in a network is the *average reciprocity*.

### C.3.3 Assortativity

The *assortativity coefficient* is a measure of the tendency of the nodes in a network to be linked with nodes with the same attribute as theirs. It gets the value 1 when nodes only link with other nodes with the same attribute and $-1$ when they only link to nodes with a different attribute. In Chapter 4, these attributes are either gender, class, or grade. We use the *assortativity coefficient*, $r$, and its error, $\sigma_r$, as they were defined in (Newman, 2003) (equations (2) and (4) respectively). The definition of $r$ is somewhat involved, so we omit it in here—the interested reader is referred to either (Newman, 2003) or (Newman, 2018) for a detailed explanation. The error $\sigma_r$ is what we use as a measure of the expected standard deviation on the value of $r$, and it is computed as

$$\sigma_r = \sqrt{\sum_{i=1}^{M} (r_i - r)^2},$$

where $M$ is the total number of edges in the network and $r_i$ is the value of $r$ when the link $i$ is removed from the network.

### C.3.4 Connected components

In an undirected network, a *connected component* is a maximal subset of nodes such that every two nodes in the set are connected by at least one path. In a directed network, a *weakly connected component* is a maximal subset of nodes such that, if we consider its links as undirected, then it is a connected component. On the other hand, a *strongly connected component*

is a maximal subset of nodes such that, for every two nodes $i, j$ in the set, there exists a (directed) path from $i$ to $j$ and also from $j$ to $i$.

# D

# Appendix D

## D.1 Social networks questionnaire (II): Spanish version

♥ Quiénes son tus amigos/as dentro del colegio?

♥♥ Considerando a tus amigos/as: Con quiénes tienes una relación más cercana?

♥♥♥ Por último, de entre tus amigos más cercanos: quiénes dirías que son tus mejores amigos/as? (Nos referimos a aquellas personas con las que eres ”uña y carne”).

☠ Qué compañeros/as no te caen del todo bien o no tienes buena relación con ellos?

☠☠ Considerando la gente que no te cae del todo bien: quiénes te caen mal o sueles tener problemas con ellos/as?

☠☠☠ Por último, considerando las personas que te caen mal: hay alguna con la que tengas una relación especialmente mala o problemática?

# Bibliography


Acedo-Carmona, C. and A. Gomila (2016). A critical review of dunbars social brain hypothesis. *Revis Intern de Socio 74*, e037.

Aiello, L. C. and P. Wheeler (1995). The expensive-tissue hypothesis: The brain and the digestive system in human and primate evolution. *Current Anthropology 36*(2), 199–221.

Alani, H., M. Szomszor, C. Cattuto, W. Van den Broeck, G. Correndo, and A. Barrat (2009). Live social semantics. In *International Semantic Web Conference*, pp. 698–714. Springer.

Alessandretti, L., P. Sapiezynski, V. Sekara, S. Lehmann, and A. Baronchelli (2018). Evidence for a conserved quantity in human mobility. *Nature Human Behaviour*, 1.

Almaatouq, A., L. Radaelli, A. Pentland, and E. Shmueli (2016). Are you your friends friend? poor perception of friendship ties limits the ability to promote behavioral change. *PloS one 11*(3), e0151588.

Anderssen, E., K. Dyrstad, F. Westad, and H. Martens (2006). Reducing over-optimism in variable selection by cross-model validation. *Chemometrics and Intelligent Laboratory Systems 84*(1), 69 – 74. Selected papers presented at the 9th Scandinavian Symposium on Chemometrics Reykjavik, Iceland 2125 August 2005.

Antonioni, A., S. Bullock, and M. Tomassini (2014). Reds: an energy-constrained spatial social network model. In *Artificial Life Conference Proceedings 14*, pp. 368–375. MIT Press.

Arnaboldi, V., M. Conti, A. Passarella, and F. Pezzoni (2012). Analysis of ego network structure in online social networks. In *Privacy, security, risk and trust (PASSAT), 2012 international conference on and 2012 international confernece on social computing (SocialCom)*, pp. 31–40. IEEE.

Arnaboldi, V., M. Conti, A. Passarella, and F. Pezzoni (2013). Ego networks in twitter: an experimental analysis. In *INFOCOM, 2013 Proceedings IEEE*, pp. 3459–3464. IEEE.

Arnaboldi, V., A. Guazzini, and A. Passarella (2013). Egocentric online social networks: Analysis of key features and prediction of tie strength in facebook. *Computer Communications 36*(10-11), 1130–1144.

Asimov, I. (1951). *Foundation*. Spectra.

Ball, P. (2002). The physical modelling of society: a historical perspective. *Physica A: Statistical Mechanics and its Applications 314*(1-4), 1–14.

Barthélemy, M. (2011). Spatial networks. *Physics Reports 499*(1-3), 1–101.

Berger, C. and J. K. Dijkstra (2013). Competition, envy, or snobbism? how popularity and friendships shape antipathy networks of adolescents. *Journal of Research on Adolescence 23*(3), 586–595.

Bernard, H. R. and P. D. Killworth (1973). On the social structure of an ocean-going research vessel and other important things. *Social Science Research 2*(2), 145–184.

Bernard, H. R. and P. D. Killworth (1979). Why are there no social physics? *Journal of the Steward Anthropological Society 11*(1), 33–58.

Bishara, A. J. and J. B. Hittner (2012). Testing the significance of a correlation with nonnormal data: comparison of pearson, spearman, transformation, and resampling approaches. *Psychological methods 17*(3), 399.

Boguná, M., R. Pastor-Satorras, A. Díaz-Guilera, and A. Arenas (2004). Models of social networks based on social distance attachment. *Physical review E 70*(5), 056122.

Buchanan, M. (2008). *The social atom: Why the rich get richer, cheaters get caught, and your neighbor usually looks like you*. Bloomsbury Publishing USA.

Burton-Chellew, M. N. and R. I. Dunbar (2014). Hamiltons rule predicts anticipated social support in humans. *Behavioral ecology 26*(1), 130–137.

Buys, C. J. and K. L. Larson (1979). Human sympathy groups. *Psychological Reports 45*(2), 547–553.

Card, N. A. (2010). Antipathetic relationships in child and adolescent development: A meta-analytic review and recommendations for an emerging area of study. *Developmental Psychology 46*(2), 516.

Carrington, P. J., J. Scott, and S. Wasserman (2005). Models and methods in social network analysis.

Cartwright, D. and F. Harary (1956). Structural balance: a generalization of heider's theory. *Psychological review 63*(5), 277.

Casari, M. and C. Tagliapietra (2018). Group size in social-ecological systems. *Proceedings of the National Academy of Sciences 115*(11), 2728–2733.

Castellano, C., S. Fortunato, and V. Loreto (2009). Statistical physics of social dynamics. *Reviews of modern physics 81*(2), 591.

Caticha, A. and A. Giffin (2006). Updating probabilities. In *AIP Conference Proceedings*, Volume 872, pp. 31–42. AIP.

Cattuto, C., W. Van den Broeck, A. Barrat, V. Colizza, J.-F. Pinton, and A. Vespignani (2010). Dynamics of person-to-person interactions from distributed rfid sensor networks. *PloS one 5*(7), e11596.

Clauset, A. and N. Eagle (2012). Persistence and periodicity in a dynamic proximity network. *arXiv preprint arXiv:1211.7343*.

Conte, R., N. Gilbert, G. Bonelli, C. Cioffi-Revilla, G. Deffuant, J. Kertesz, V. Loreto, S. Moat, J.-P. Nadal, A. Sanchez, et al. (2012). Manifesto of computational social science. *The European Physical Journal Special Topics 214*(1), 325–346.

Curry, O., S. G. Roberts, and R. I. Dunbar (2013). Altruism in social networks: Evidence for a kinship premium. *British Journal of Psychology 104*(2), 283–295.

DeCasien, A. R., S. A. Williams, and J. P. Higham (2017). Primate brain size is predicted by diet but not sociality. *Nature ecology & evolution 1*(5), 0112.

DiCiccio, T. J. and B. Efron (1996). Bootstrap confidence intervals. *Statistical science*, 189–212.

Dijkstra, J. K., S. Lindenberg, and R. Veenstra (2007). Same-gender and cross-gender peer acceptance and peer rejection and their relation to bullying and helping among preadolescents: Comparing predictions from gender-homophily and goal-framing approaches. *Developmental psychology 43*(6), 1377.

Dimitriadou, E., K. Hornik, F. Leisch, D. Meyer, and A. Weingessel (2011). e1071: Misc Functions of the Department of Statistics (e1071), TU Wien. R package version 1.5-25.

Dunbar, R. I. (1992). Neocortex size as a constraint on group size in primates. *Journal of human evolution 22*(6), 469–493.

Dunbar, R. I. (1993). Coevolution of neocortical size, group size and language in humans. *Behavioral and brain sciences 16*(4), 681–694.

Dunbar, R. I. (1998, 01). The social brain hypothesis. *Evolutionary Anthropology 6*, 178–190.

Dunbar, R. I. (2014). The social brain psychological underpinnings and implications for the structure of organizations. *Current Directions in Psychological Science 23*(2), 109–114.

Dunbar, R. I. (2015). Social networks and their implications for community living for people with a learning disability. *International Journal of Developmental Disabilities 61*(2), 101–106.

Dunbar, R. I. (2016). Do online social media cut through the constraints that limit the size of offline social networks? *Open Science 3*(1), 150292.

Dunbar, R. I. (2018). The anatomy of friendship. *Trends in cognitive sciences 22*(1), 32–51.

Dunbar, R. I., V. Arnaboldi, M. Conti, and A. Passarella (2015). The structure of online social networks mirrors those in the offline world. *Social Networks 43*, 39–47.

Dunbar, R. I., N. Duncan, and D. Nettle (1995). Size and structure of freely forming conversational groups. *Human nature 6*(1), 67–78.

Dunbar, R. I., P. Mac Carron, and S. Shultz (2018). Primate social group sizes exhibit a regular scaling pattern with natural attractors. *Biology letters 14*(1).

Dunbar, R. I. and S. Shultz (2017). Why are there so many explanations for primate brain evolution? *Philosophical Transactions of the Royal Society B: Biological Sciences 372*(1727).

Dunbar, R. I. and R. Sosis (2018). Optimising human community sizes. *Evolution and Human Behavior 39*(1), 106–111.

Dunbar, R. I. and M. Spoors (1995). Social networks, support cliques, and kinship. *Human Nature 6*(3), 273–290.

Ester, M., H.-P. Kriegel, J. Sander, X. Xu, et al. (1996). A density-based algorithm for discovering clusters in large spatial databases with noise. In *Kdd*, Volume 96, pp. 226–231.

Feng, D., R. Altmeyer, D. Stafford, N. A. Christakis, and H. H. Zhou (2018). Testing for balance in social networks. *arXiv preprint arXiv:1808.05260*.

Festinger, L. (1957). *A theory of cognitive dissonance*, Volume 2. Stanford university press.

Freeman, L. C. (1978). Segregation in social networks. *Sociological Methods & Research 6*(4), 411–429.

Friedkin, N. (1980). A test of structural features of granovetter's strength of weak ties theory. *Social networks 2*(4), 411–422.

Friedman, H. S. and S. E. Taylor (2012). Social support: A review.

Fuchs, B., D. Sornette, and S. Thurner (2014). Fractal multi-level organisation of human groups in a virtual world. *Scientific reports 4*, 6526.

Garcia, D. (2017). Leaking privacy and shadow profiles in online social networks. *Science advances 3*(8), e1701172.

Gavrilets, S. and A. Vose (2006). The dynamics of machiavellian intelligence. *Proceedings of the National Academy of Sciences 103*(45), 16823–16828.

Gonçalves, B., N. Perra, and A. Vespignani (2011). Modeling users' activity on twitter networks: Validation of dunbar's number. *PloS one 6*(8), e22656.

Goyal, S. (2012). *Connections: an introduction to the economics of networks*. Princeton University Press.

Granovetter, M. S. (1977). The strength of weak ties. In *Social networks*, pp. 347–367. Elsevier.

Haerter, J. O., B. Jamtveit, and J. Mathiesen (2012). Communication dynamics in finite capacity social networks. *Physical review letters 109*(16), 168701.

Hall, J. A. (2018). How many hours does it take to make a friend? *Journal of Social and Personal Relationships*, 0265407518761225.

Hamilton, M. J., B. T. Milne, R. S. Walker, O. Burger, and J. H. Brown (2007). The complex structure of hunter–gatherer social networks. *Proceedings of the Royal Society B: Biological Sciences 274*(1622), 2195.

Harré, M. S. and M. Prokopenko (2016). The social brain: scale-invariant layering of erdős–rényi networks in small-scale human societies. *Journal of The Royal Society Interface 13*(118), 20160044.

Hastie, T., R. Tibshirani, and J. Friedman (2001). *The Elements of Statistical Learning*. Springer Series in Statistics. New York, NY, USA: Springer New York Inc.

Heider, F. (1946). Attitudes and cognitive organization. *The Journal of psychology 21*(1), 107–112.

Hill, R. A. and R. I. Dunbar (2003). Social network size in humans. *Human nature 14*(1), 53–72.

Holland, P. W. and S. Leinhardt (1981). An exponential family of probability distributions for directed graphs. *Journal of the american Statistical association 76*(373), 33–50.

Holme, P. and J. Saramäki (2012). Temporal networks. *Physics reports 519*(3), 97–125.

Holovatch, Y., R. Kenna, and S. Thurner (2017). Complex systems: physics beyond physics. *European Journal of Physics 38*(2), 023002.

Huisman, M. (2009). Imputation of missing network data: some simple procedures. *Journal of Social Structure 10*(1), 1–29.

Huitsing, G., M. A. Van Duijn, T. A. Snijders, P. Wang, M. Sainio, C. Salmivalli, and R. Veenstra (2012). Univariate and multivariate models of positive and negative networks: Liking, disliking, and bully–victim relationships. *Social Networks 34*(4), 645–657.

Humphrey, N. K. (1976). The social function of intellect. In *Growing points in ethology*, pp. 303–317. Cambridge University Press.

Ilany, A. and E. Akcay (2016). Social inheritance can explain the structure of animal social networks. *Nature communications 7*, 12084.

Isella, L., J. Stehl, A. Barrat, C. Cattuto, J. Pinton, and W. Van den Broeck (2011). What's in a crowd? analysis of face-to-face behavioral networks. *Journal of Theoretical Biology 271*(1), 166–180.

Jackson, M. O. (2010). *Social and economic networks*. Princeton university press.

Jaynes, E. T. (2003). *Probability theory: The logic of science*. Cambridge University Press.

Jin, E. M., M. Girvan, and M. E. Newman (2001). Structure of growing social networks. *Physical review E 64*(4), 046132.

Jo, H.-H., Y. Murase, J. Török, J. Kertész, and K. Kaski (2018). Stylized facts in social networks: Community-based static modeling. *Physica A: Statistical Mechanics and its Applications 500*, 23–39.

Kahn, R. L. and T. Antonucci (1980). *Convoys Over the Life Course: Attachment Roles and Social Support*, Volume 3, pp. 253 267.

Kanai, R., B. Bahrami, R. Roylance, and G. Rees (2012). Online social network size is reflected in human brain structure. *Proc. R. Soc. B 279*(1732), 1327–1334.

Kawachi, I. and L. F. Berkman (2001). Social ties and mental health. *Journal of Urban health 78*(3), 458–467.

Kirkley, A., G. T. Cantwell, and M. Newman (2019). Balance in signed networks. *Physical Review E 99*(1), 012320.

Kivelä, M., A. Arenas, M. Barthelemy, J. P. Gleeson, Y. Moreno, and M. A. Porter (2014). Multilayer networks. *Journal of complex networks 2*(3), 203–271.

Klimek, P., M. Diakonova, V. M. Eguíluz, M. San Miguel, and S. Thurner (2016). Dynamical origins of the community structure of an online multi-layer society. *New journal of Physics 18*(8), 083045.

Kossinets, G. (2006). Effects of missing data in social networks. *Social networks 28*(3), 247–268.

Kwak, S., W.-t. Joo, Y. Youm, and J. Chey (2018). Social brain volume is associated with in-degree social network size among older adults. *Proc. R. Soc. B 285*(1871), 20172708.

Laniado, D., Y. Volkovich, K. Kappler, and A. Kaltenbrunner (2016). Gender homophily in online dyadic and triadic relationships. *EPJ Data Science 5*(1), 19.

Lazarsfeld, P. F. (1961). Notes on the history of quantification in sociology–trends, sources and problems. *Isis 52*(2), 277–333.

Lazer, D., A. Pentland, L. Adamic, S. Aral, A.-L. Barabási, D. Brewer, N. Christakis, N. Contractor, J. Fowler, M. Gutmann, T. Jebara, G. King, M. Macy, D. Roy, and M. Van Alstyne (2009). Computational social science. *Science 323*(5915), 721–723.

Lehmann, J., P. Lee, and R. Dunbar (2014). Unravelling the evolutionary function of communities. *Lucy to language: the benchmark papers*, 245–276.

Leskovec, J., D. Huttenlocher, and J. Kleinberg (2010a). Predicting positive and negative links in online social networks. In *Proceedings of the 19th international conference on World wide web*, pp. 641–650. ACM.

Leskovec, J., D. Huttenlocher, and J. Kleinberg (2010b). Signed networks in social media. In *Proceedings of the SIGCHI Conference on Human Factors in Computing Systems*, CHI '10, New York, NY, USA, pp. 1361–1370. ACM.

Lewis, P. A., R. Rezaie, R. Brown, N. Roberts, and R. I. Dunbar (2011). Ventromedial prefrontal volume predicts understanding of others and social network size. *Neuroimage 57*(4), 1624–1629.

Liaw, A. and M. Wiener (2002). Classification and Regression by randomForest. *R News 2*(3), 18–22.

Liben-Nowell, D. and J. Kleinberg (2007). The link-prediction problem for social networks. *journal of the Association for Information Science and Technology 58*(7), 1019–1031.

Lin, J. (1991). Divergence measures based on the shannon entropy. *IEEE Transactions on Information theory 37*(1), 145–151.

Lubbers, M. J., J. L. Molina, and H. Valenzuela-García (2019). When networks speak volumes: Variation in the size of broader acquaintanceship networks. *Social Networks 56*, 55–69.

Mac Carron, P., K. Kaski, and R. Dunbar (2016). Calling dunbar's numbers. *Social Networks 47*, 151–155.

Marsden, P. V. and K. E. Campbell (1984). Measuring tie strength. *Social forces 63*(2), 482–501.

Mastrandrea, R., J. Fournet, and A. Barrat (2015). Contact patterns in a high school: a comparison between data collected using wearable sensors, contact diaries and friendship surveys. *PloS one 10*(9), e0136497.

McPherson, M., L. Smith-Lovin, and J. M. Cook (2001). Birds of a feather: Homophily in social networks. *Annual review of sociology 27*(1), 415–444.

Mestres, S. G., J. L. Molina, S. Hoeksma, and M. Lubbers (2012). Bulgarian migrants in spain: Social networks, patterns of transnationality, community dynamics and cultural change in catalonia (northeastern spain) 1. *Southeastern Europe 36*(2), 208–236.

Milgram, S. (1967). The small world problem. *Psychology today 2*(1), 60–67.

Miritello, G., E. Moro, R. Lara, R. Martínez-López, J. Belchamber, S. G. Roberts, and R. I. Dunbar (2013). Time as a limited resource: Communication strategy in mobile phone networks. *Social Networks 35*(1), 89–95.

Molina, J. L. and F. Pelissier (2010). Les xarxes socials de sikhs, xinesos i filipins a barcelona.

Molina, J. L., S. Petermann, and A. Herz (2015). Defining and measuring transnational social structures. *Field Methods 27*(3), 223–243.

Moreno, J. (1934). Who shall survive? foundations of sociometry, group psychotherapy, and sociodrama. beacon, ny: Beacon house.

Moreno, J. (1947). Organization of the social atom. *Sociometry 10*(3), 287–293.

Murase, Y., J. Török, H.-H. Jo, K. Kaski, and J. Kertész (2014). Multilayer weighted social network model. *Physical Review E 90*(5), 052810.

Newman, M. (2018). *Networks*. Oxford university press.

Newman, M. E. (2003). Mixing patterns in networks. *Physical Review E 67*(2), 026126.

Omodei, E., M. E. Brashears, and A. Arenas (2017). A mechanistic model of human recall of social network structure and relationship affect. *Scientific reports 7*(1), 17133.

Oswald, D. L., E. M. Clark, and C. M. Kelly (2004). Friendship maintenance: An analysis of individual and dyad behaviors. *Journal of Social and clinical psychology 23*(3), 413–441.

Park, J. and M. E. Newman (2004). Statistical mechanics of networks. *Physical Review E 70*(6), 066117.

Perry, B. L., B. A. Pescosolido, and S. P. Borgatti (2018). *Egocentric network analysis: Foundations, methods, and models*, Volume 44. Cambridge University Press.

Pollet, T. V., S. G. Roberts, and R. I. Dunbar (2011). Extraverts have larger social network layers. *Journal of Individual Differences*.

Pollet, T. V., S. G. Roberts, and R. I. Dunbar (2013). Going that extra mile: individuals travel further to maintain face-to-face contact with highly related kin than with less related kin. *PloS one 8*(1), e53929.

Powell, J., P. A. Lewis, N. Roberts, M. García-Fiñana, and R. I. Dunbar (2012). Orbital prefrontal cortex volume predicts social network size: an imaging study of individual differences in humans. *Proceedings of the Royal Society of London B: Biological Sciences 279*(1736), 2157–2162.

Rambaran, J. A., J. K. Dijkstra, A. Munniksma, and A. H. Cillessen (2015). The development of adolescents friendships and antipathies: A longitudinal multivariate network test of balance theory. *Social Networks 43*, 162–176.

Ravasz, E. and A.-L. Barabási (2003). Hierarchical organization in complex networks. *Physical review E 67*(2), 026112.

Roberts, S. B. and R. I. Dunbar (2015). Managing relationship decay. *Human Nature 26*(4), 426–450.

Roberts, S. G. and R. I. Dunbar (2011a). Communication in social networks: Effects of kinship, network size, and emotional closeness. *Personal Relationships 18*(3), 439–452.

Roberts, S. G. and R. I. Dunbar (2011b). The costs of family and friends: an 18-month longitudinal study of relationship maintenance and decay. *Evolution and Human Behavior 32*(3), 186–197.

Roberts, S. G., R. I. Dunbar, T. V. Pollet, and T. Kuppens (2009). Exploring variation in active network size: Constraints and ego characteristics. *Social Networks 31*(2), 138–146.

Roberts, S. G., R. Wilson, P. Fedurek, and R. Dunbar (2008). Individual differences and personal social network size and structure. *Personality and individual differences 44*(4), 954–964.

Robertson, C., I. Tamarit, A. Masjid, and R. I. Dunbar (in preparation, 2019). Processing embedded complement clauses may support social cognition.

Robins, G., P. Pattison, and J. Woolcock (2004). Missing data in networks: exponential random graph ($p^*$) models for networks with non-respondents. *Social Networks 26*(3), 257–283.

Roth, G. and U. Dicke (2012). Evolution of the brain and intelligence in primates. In *Progress in brain research*, Volume 195, pp. 413–430. Elsevier.

Saramäki, J., E. A. Leicht, E. López, S. G. Roberts, F. Reed-Tsochas, and R. I. Dunbar (2014). Persistence of social signatures in human communication. *Proceedings of the National Academy of Sciences 111*(3), 942–947.

Shrum, W., N. H. Cheek Jr, and S. MacD (1988). Friendship in school: Gender and racial homophily. *Sociology of Education*, 227–239.

Sivia, D. and J. Skilling (2006). *Data Analysis: A Bayesian Tutorial*. Oxford science publications. OUP Oxford.

Snijders, T. A. (2011). Statistical models for social networks. *Annual Review of Sociology 37*, 131–153.

Sparrowe, R. T., R. C. Liden, S. J. Wayne, and M. L. Kraimer (2001). Social networks and the performance of individuals and groups. *Academy of management journal 44*(2), 316–325.

Stauffer, D. (2013). A biased review of sociophysics. *Journal of Statistical Physics 151*(1-2), 9–20.

Stehlé, J., F. Charbonnier, T. Picard, C. Cattuto, and A. Barrat (2013). Gender homophily from spatial behavior in a primary school: a sociometric study. *Social Networks 35*(4), 604–613.

Stiller, J. and R. I. Dunbar (2007). Perspective-taking and memory capacity predict social network size. *Social Networks 29*(1), 93–104.

Sutcliffe, A., R. Dunbar, J. Binder, and H. Arrow (2012). Relationships and the social brain: integrating psychological and evolutionary perspectives. *British journal of psychology 103*(2), 149–168.

Takano, M. (2018). Two types of social grooming methods depending on the trade-off between the number and strength of social relationships. *Royal Society Open Science 5*(8), 180148.

Tamarit, I., J. A. Cuesta, R. I. M. Dunbar, and A. Sánchez (2018). Cognitive resource allocation determines the organization of personal networks. *Proceedings of the National Academy of Sciences 115*(33), 8316–8321.

Therneau, T. M. and E. J. Atkinson (1997, 01). An introduction to recursive partitioning using the rpart routines. Technical report, Mayo Foundation.

Toivonen, R., L. Kovanen, M. Kivelä, J.-P. Onnela, J. Saramäki, and K. Kaski (2009). A comparative study of social network models: Network evolution models and nodal attribute models. *Social Networks 31*(4), 240–254.

Valente, T. W. (2010). *Social networks and health: Models, methods, and applications*, Volume 1. Oxford University Press New York.

Van den Broeck, W., C. Cattuto, A. Barrat, M. Szomszor, G. Correndo, and H. Alani (2010). The live social semantics application: a platform for integrating face-to-face presence with on-line social networking. In *Pervasive Computing and Communications Workshops (PERCOM Workshops), 2010 8th IEEE International Conference on*, pp. 226–231. IEEE.

Varma, S. and R. Simon (2006, Feb). Bias in error estimation when using cross-validation for model selection. *BMC Bioinformatics 7*, 91–91. 1471-2105-7-91[PII].

Vega-Redondo, F. (2007). *Complex social networks*. Number 44. Cambridge University Press.

Vigil, J. M. (2007). Asymmetries in the friendship preferences and social styles of men and women. *Human Nature 18*(2), 143–161.

Waal, F. d. (1982). Chimpanzee politics: Sex and power among apes. *London, UK: Jonathan Cape 10*, 393142.

Wang, H. and M. Song (2011). Ckmeans. 1d. dp: optimal k-means clustering in one dimension by dynamic programming. *The R journal 3*(2), 29.

Wang, Q., J. Gao, T. Zhou, Z. Hu, and H. Tian (2016). Critical size of ego communication networks. *EPL (Europhysics Letters) 114*(5), 58004.

Wasserman, S. and K. Faust (1994). *Social network analysis: Methods and applications*, Volume 8. Cambridge university press.

Watts, D. J., P. S. Dodds, and M. E. Newman (2002). Identity and search in social networks. *science 296*(5571), 1302–1305.

Watts, D. J. and S. H. Strogatz (1998). Collective dynamics of small-worldnetworks. *nature 393*(6684), 440.

Whiten, A. and R. Byrne (1988). *The Machiavellian intelligence hypotheses*. United Kingdom: Oxford University Press.

Zhang, J., M. S. Ackerman, and L. Adamic (2007). Expertise networks in online communities: structure and algorithms. In *Proceedings of the 16th international conference on World Wide Web*, pp. 221–230. ACM.

Zhou, W.-X., D. Sornette, R. A. Hill, and R. I. Dunbar (2005). Discrete hierarchical organization of social group sizes. *Proceedings of the Royal Society of London B: Biological Sciences 272*(1561), 439–444.